Functional genomics of BAHD acyltransferases in different varieties of the wine grape, *Vitis vinifera*

by

Brent Wiens, B.Sc.

A Thesis

submitted to the Department of Biological Sciences

in partial fulfillment of the requirements

for the degree of

Master of Science

February, 2012

Brock University

St. Catharines, Ontario

Abstract

The characteristic "foxy" aroma of *Vitis labrusca* Concord grapes is due in large part to methyl anthranilate, a volatile ester formed by the enzyme anthraniloyl-CoA:methanol anthraniloyltransferase (VlAMAT) of the superfamily of BAHD acyltransferases. The publication of the genome of the closely related wine grape *Vitis vinifera*, which does not accumulate methyl anthranilate, permitted the searching for any putative *VlAMAT*-like genes, with the result of 5 highly homologous candidates being found, with one candidate sharing 95% identity to *VlAMAT*. Probing the gene expression of 18 different cultivars of *V. vinifera* ripe berries by RT-PCR showed that many varieties do indeed express *VlAMAT*-like genes. Subsequent cloning of the full-length open reading frame of one of these genes from cDNA prepared from the cultivar Sauvignon Blanc permitted preliminary biochemical characterization of the enzyme after heterologous expression in *E. coli*. It was determined that this alcohol acyltransferase (named *VvsbAAT1*) catalyzes the formation of *cis*-3-hexenyl acetate, a "green-leaf" volatile. Although the cloned gene from Sauvignon Blanc had 95% identity at the amino acid level to VlAMAT, it displayed an altered substrate specificity and expression pattern. These results highlight the difficulty in predicting substrate specificity and function of enzymes through the basis of sequence homology, which is a common finding in the study of BAHD acyltransferases. Also, the determination of function of *VvsbAAT1* and other BAHD acyltransferases in *V. vinifera* could be used as a genetic marker for certain aroma characteristics in grape breeding programs.

Acknowledgements

Firstly, I would like to thank Dr. Vincenzo De Luca for his guidance, insight, and endless well of knowledge throughout the course of this project. His commitment to my success, mentorship, and patience are the reasons this work was possible. Also, I would like to thank the members of my supervisory committee, Dr. Adonis Skandalis and Dr. Sandra Peters, for their support, helpful suggestions, and guidance throughout my project.

Second, I would like to thank Dr. John Paroschy (Château des Charmes Winery, Niagara-on-the-Lake), Dr. Helen Fisher (University of Guelph Rittenhouse Research Station, Vineland), and Wes Lowrey (Five Rows Craft Wines, Niagara-on-the-Lake), for kindly providing the grape samples necessary for the project. Also, Dr. Inglis and Dr. Pickering of the CCOVI department for providing access to the GC, and Linda Tremblay for teaching me how to use it. Thanks to Dr. Brindle for allowing access to the GC-MS.

Thirdly, peer support is an important aspect of science, not only for interesting discussion of the subject area but also for technical aspects of doing bench science. Dylan Levac, Fang Yu, Kim Ghosh, Sayaka Masada-Atsumi, Antje Thamm, Elizabeth Edmunds, Matt Czerwinski, and Vonny Salim all supported me in one way or another of these aspects throughout my time in the De Luca Lab.

Most importantly, I would like to thank my wife Jessica, whose never-ending support, patience, motivation (and perhaps foolhardiness) prompted me to pursue my education, and who truly is the yin to my yang. Finally, I have to thank my children Olivia and Wesley, for providing me the necessary balance to keep all things in life in perspective.

Table of Contents

List of Tables

List of Figures

Chapter 1. Introduction and Literature Review

1.1 General Introduction

Secondary metabolism in plants generally refers to the production of metabolites that are not immediately necessary for survival, but contribute to the apparent long-term reproductive success of the plant. Many of these secondary metabolites can be modified through acylation, methylation, glycosylation or other decorations of the molecule to enhance or otherwise alter their biological properties. The superfamily of BAHD acyltransferases is a recently described group of coenzyme A-dependant acyltransferases that function in the acylation of a diverse array of secondary metabolites, such as anthocyanins, alkaloids, amides, and volatile organic molecules (D'Auria, 2006). A particular subfamily of BAHD acyltransferases is important in the production of aroma and taste compounds in ripening fruit and developing flowers. These acyltransferases catalyze the coenzyme A-dependant acylation of alcohols to form volatile esters that typically are characteristic of the perceived aroma and taste of the fruit. In general, these alcohol acyltransferases (AATs) are versatile and display a broad range of activities when supplied with different substrates *in vitro* (D'Auria, 2006). However, predicting their substrate specificity based on amino acid sequence similarity to known acyltransferases has proven to be difficult (Beekwilder et al., 2004), and it has been shown that similar enzymes can have different substrate specificities (Beekwilder et al., 2004; Burhenne et al., 2003) while phylogenetically distant enzymes will perform the same reaction (Beekwilder et al., 2004).

The wine grape, *Vitis vinifera*, is an economically important crop throughout the world, and has widely been regarded as the one of the first domesticated plants used by

humans in agriculture (Myles, 2011). The quality and variety of wines produced from *V. vinifera* depend on fermentation conditions but more importantly on the germplasm or genotype that the berries originate from (Dunlevy, Kalua, Keyzers, & Boss, 2009). Important characteristic compounds generated by the berries include terpenoids, tannins, anthocyanins, and esters which vary from one variety to the next.

Previous work in the closely related *Vitis labrusca* Concord grape identified and characterized a BAHD acyltransferase, anthraniloyl-CoA:methanol anthraniloyltransferase (VlAMAT), responsible for the characteristic "foxy" aroma compound found in Concord berries, methyl anthranilate (Wang & De Luca, 2005). This enzyme was shown to be versatile in its substrate specificity and could catalyze the formation of a range of volatile esters *in vitro*, but due to the endogenous substrates available, Concord berries preferentially accumulated methyl anthranilate *in vivo*.

1.2 Discovery of the BAHD acyltransferases

The superfamily of BAHD acyltransferases is involved in a large diversity of acyl-CoA dependent reactions of secondary metabolites and was named according to the first 4 plant genes to be biochemically characterized (B. St-Pierre, Laflamme, Alarco, & De Luca, 1998). BEAT (acetyl-CoA: benzyl alcohol acetyltransferase) catalyzes the formation of benzyl acetate, and was isolated from the flower petals of *Clarkia breweri* (N. Dudareva, Raguso, Wang, Ross, & Pichersky, 1998). AHCT (anthocyanin *O*-hydroxycinnamoyltransferase) from *Gentiana triflora* transfers caffeoyl-CoA to the 5-*O*-glucoside of the anthocyanin delphinidin (Fujiwara et al., 1997). HCBT (hydroxycinnamoyl/benzoyl-CoA: anthranilate *N*-hydroxycinnamoyl/benzoyltransferase)

acylates at a nitrogen group to generate an amide in contrast to the esters formed by the oxygen (*O*-) acylating members above. HCBT was purified from fungal-elicited cultures of carnation (*Dianthus caryophyllus*), and catalyzes the formation of *N*-benzoylanthranilate, a precursor of certain phytoalexins synthesized in response to fungal infection (Yang, Reinhard, Schiltz, & Matern, 1997). DAT (deacetylvindoline *O*-acetyltransferase) catalyzes the final reaction in the biosynthesis of the important anti-cancer alkaloid, vindoline. This enzyme was isolated and characterized from the Madagascar periwinkle, *Catharanthus roseus* (St-Pierre et al., 1998).

These first 4 BAHD acyltransferases are a good representation of the variety of reactions performed by all BAHD acyltransferases described thus far. These enzymes either *O*- or *N*-acylate substrates to form esters or amides, respectively, with *O*-acylation being the most frequently described reaction. Of all the reactions described to date, the two most common are the acylation of alcohols, typically short-chain aliphatic or aromatic alcohols to form volatile esters which contribute to the characteristic aroma of fruits such as grapes, bananas, strawberries, apples, and melon; while the other most common reaction involves acylation of anthocyanins and flavonoids, usually with malonyl or hydroxycinnamoyl groups (Yu, Gou, & Liu, 2009). Other BAHD acyltransferases acylate alkaloids (such as DAT), amides (polyamines such as spermidine and agmatine were shown to be conjugated both by AtSDT (spermidine sinapoyl CoA acyltransferase) and AtACT (agmatine coumaroyl-CoA transferase), respectively, in *Arabidopsis thaliana* (Muroi et al., 2009; Luo et al., 2009)), and terpenoids (e.g. DBTNBT (*N*-debenzoyl-2'-deoxytaxol *N*-benzoyltransferase) in the synthesis of Taxol (Walker, Long, & Croteau, 2002)).

1.3 Physical properties of BAHD acyltransferases: crystal structures, three-dimensional modelling and sequence elements conferring substrate specificity

BAHD acyltransferases contain an average of 449 amino acids in their open reading frames, have molecular weights around 48-55 kDa, occur and function as monomers, and are cytosolic. Exceptions to this are described by Lucchetta et al. (Lucchetta et al., 2007), who used gel filtration to suggest that the native enzyme from *Cucumis melo* functions as a 196 kDa tetramer *in vivo*, while sodium dodecyl sulfate-polyacrylamide gel electrophoresis (SDS-PAGE) showed that the size of the enzyme was 51 kDa. Two main consensus motifs define the BAHD family of acyltransferases that include the catalytic HXXXD motif located towards the centre of the molecule and the DFGWG with unknown function located near the carboxy terminus. Subfamilies of BAHD acyltransferases may have additional motifs that play a role in their unique functions, such as the conserved YFGNC motif shared by most of the malonyl- and hydroxycinnamoyltransferases that acylate glycosylated anthocyanins (D'Auria, 2006).

1.3.1 Crystal structure of some BAHD acyltransferases

Vinorine synthase (RsVs) from *Rauvolfia serpentina*, acetylates 16-epi-vellosimine to form vinorine (an intermediate in the monoterpene indole alkaloid pathway to ajmaline), and was the first member of the BAHD family of acyltransferases to be crystallized and described (Ma, Koepke, Panjikar, Fritzsch, & Stöckigt, 2005). Phylogenetic analysis places this enzyme in Clade II, along with other acyltransferases involved in alkaloid biosynthesis as well as numerous other alcohol acyltransferases that often utilize acetyl-Coenzyme A as the acyl donor. The solved x-ray crystal structure of RsVs describes a monomer composed of two approximately equal-sized domains with a

solvent channel running between them. The HXXXD motif is found in the solvent channel, with the catalytically active His residue occupying the direct centre, and is accessible from both sides of the channel. This model together with previously published biochemical and mutagenesis data (Bayer, Ma, & Stöckigt, 2004), led to a proposed reaction mechanism for RsVs that may be generalized to all the BAHD acyltransferases (Ma et al., 2005; St-Pierre & De Luca, 2000). The His residue (of the HXXXD motif) acts as a general base, which abstracts a proton from the hydroxyl or amide group of the acceptor substrate, creating an activated nucleophilic oxygen or nitrogen group, respectively. This group in turn attacks the carbonyl carbon of the acyl donor (i.e. of the acyl-CoA substrate), forming a high-energy tetrahedral intermediate. Nearby residues may lower the energy of this intermediate via hydrogen bonding, and subsequently breakdown the complex to complete the acyl transfer reaction with release of the ester or amide product and free CoA-SH (Ma et al., 2005; St-Pierre & De Luca, 2000).

Recently, a Clade I family anthocyanidin 3-*O*-glucoside-6''-*O*-malonyltransferase from *Dendranthema morifolia* (Dm3MaT3), was co-crystallized with its bound acyl donor, malonyl-CoA, to permit detailed substrate-binding characterization (Unno et al., 2007). In support of the previously proposed reaction mechanism for RsVs, His-170 of Dm3MaT3 (of the HXXXD motif) was found proximal to the carbonyl carbon of the bound malonyl-CoA, while the DFGWG motif was located in a position too far to away interact with malonyl-CoA. Interestingly, His-170 was in turn hydrogen-bonded to the side chain carboxamide of Asn-319 of the YFGNC motif. In fact, an alignment of biochemically characterized BAHD acyltransferases show that 86 of 88 sequences have this conserved asparagine residue, suggesting its importance in the function of these

enzymes (Appendix I, Figure S1). The malonyl-CoA molecule was found to interact with a total of 17 residues in the enzyme; 3 of which are capable of forming hydrogen bonds (H-bonds) to the malonyl (acyl) moiety while the other 14 amino acids form either H-bonding or hydrophobic interactions with the Coenzyme A portion. This portion of the molecule with the acyl-CoA binding pocket was termed the "front face" of the protein model, while the "back face" represented the acyl acceptor binding pocket, which in this case was an anthocyanin-binding pocket formed by another 14 amino acid residues. The connection of the acyl-CoA binding and acyl donor binding pocket via the active-site channel is similar to that proposed for RsVs, and other acyl-CoA dependant enzymes such as the bacterial dihydrolipoyl transacetylase from *Azotobacter vinelandii* ((Mattevi et al., 1993), Protein Database files 1EAD and 1EAB) and the mouse carnitine acetyltransferase (Jogl & Tong, 2003), Protein Database files 1NDB and 1NDI). However, further comparison with RsVs showed that when the Dm3MaT3 three-dimensional model was superimposed over RsVs, the front faces (acyl-CoA binding sites) fit quite nicely, while the back faces that bind the acyl acceptor were not easily superimposed. It is not surprising that BAHD acyltransferases have maintained their acyl-CoA binding pocket throughout evolution, while the acyl acceptor binding pocket that accommodates the wide variety of acceptor molecules of BAHD acyltransferases has been diversified by selection pressure.

The clade I family of anthocyanin acyltransferases can be functionally divided into two groups: those that utilize aliphatic acyl-CoA donors (i.e. malonyl-CoA) and those that utilize aromatic hydroxycinnamoyl-CoA donors (i.e. coumaroyl-CoAs). The study by Unno et al. suggested that in Dm3MaT3, Arg-178 interacted specifically with the

carboxyl oxygen of the malonyl moiety, and this residue was conserved in an alignment with other malonyl (i.e. aliphatic) acyltransferases. Conversely, this arginine residue was substituted with phenylalanine in hydroxycinnamoyl (i.e. aromatic) acyltransferases, where it was suggested that aromatic ring stacking between the phenylalanine side chain and hydroxycinnamoyl moieties could stabilize the interaction. These observations suggest that residue 178 may be essential in determining substrate specificity between aliphatic or aromatic acyl donors in clade I anthocyanin acyltransferases. Indeed, a broadened alignment of all Clade I anthocyanin acyltransferases characterized to date further substantiates this hypothesis, since all enzymes that utilize hydroxycinnamoyl-CoAs as acyl donors have phenylalanine at this position, while those utilizing malonyl-CoAs have arginine, isoleucine, valine, serine or threonine at this position (Figure 1.1). However, two clade III anthocyanin 3-*p*-coumaroyltransferases (Ih3AT1 and Ih3AT2 from the monocot *Iris hollandica*), and one clade I agmatine-*N*-coumaroyltransferase from *A. thaliana* (AtACT) have an alanine residue at this position. These results suggest that while the phenylalanine residue may play such a role in substrate specificity in clade I anthocyanin acyltransferases, it is not an essential one in all hydroxycinnamoyl-CoA: anthocyanin aromatic acyltransferases, since other sequence elements must contribute to the similar functionality in these other three enzymes.

1.4 Phylogeny of all the BAHD acyltransferases characterized to date

Novel and interesting BAHD acyltransferases continue to be described at an increasing rate. Since the description of this superfamily in 1997, 46 members were characterized by 2006 (D'Auria, 2006). In about half that amount of time, the number of

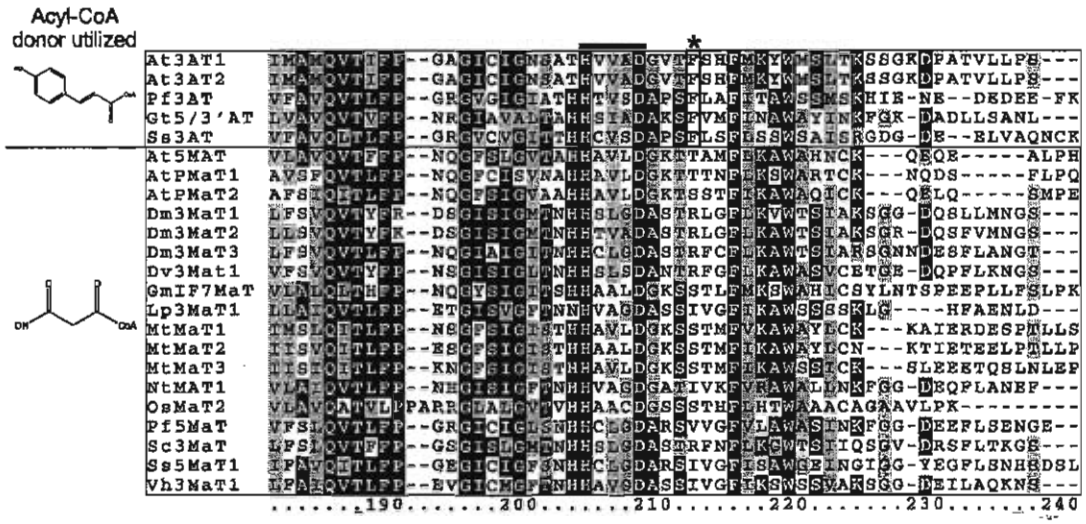

Figure 1.1: Partial multiple sequence alignment of all clade I anthocyanin acyltransferases that utilize either hydroxycinnamoyl-CoA or malonyl-CoA as acyl donors. The HXXXD motif conserved among all BAHD acyltransferases is marked with black line and the conserved phenylalanine residue (boxed) among clade I anthocyanin hydroxycinnamoyl transferases is marked with an asterisk.

biochemically characterized acyltransferases has nearly doubled. A phylogenetic tree constructed with 88 biochemically characterized enzymes forms roughly five clades (see Materials and Methods, section 2.3), as others have previously published (Figure 1.2).

Clade I contains 24 members, 23 of which are involved in the acylation (either malonylation or hydroxycinnamoylation) of glycosylated anthocyanins, while the last member, agmatine coumaroyltransferase from *A. thaliana*, *N*-acylates agmatine with a coumaroyl group. Clade II has 16 biochemically characterized members, the majority of which (15 members) perform acetylation reactions involved in fruit and flower scent formation (11 members) or alkaloid biosynthesis (4 members). The last member, Ss5MaT2 (*Salvia splendens* anthocyanin 5-O-glucoside-4'''-O-malonyltransferase), is functionally more related to the clade I anthocyanin acyltransferases and may represent a case of convergent evolution (Suzuki et al., 2004).

As a group, the 27 members of clade III are the most diverse in terms of function and acyl-CoA donors utilized. Fourteen members are involved in scent formation in fruit, flower, or wound responses and can variously generate aromatic and/or aliphatic esters. Two members of this clade form hydroxycinnamic acid amides by the acylation of spermidine in *A. thaliana*. 5 members are involved in the biosynthesis of Taxol (a structurally diverse diterpenoid) and use acetyl-, benzoyl-, and β-phenylalanoyl-CoAs as substrates (Walker et al., 2002). Other members of this clade are involved in acylation of suberin and anthocyanins (2 members each, each using hydroxycinnamoyl-CoAs), and quinolizidine alkaloids (2 members from *Lupinus* that can use tigloyl-CoA). Clade IV acyltransferases (20 members) are mostly hydroxycinnamoyl transferases, involved in the modification of phenylpropanoids in the lignin biosynthetic pathway, or other

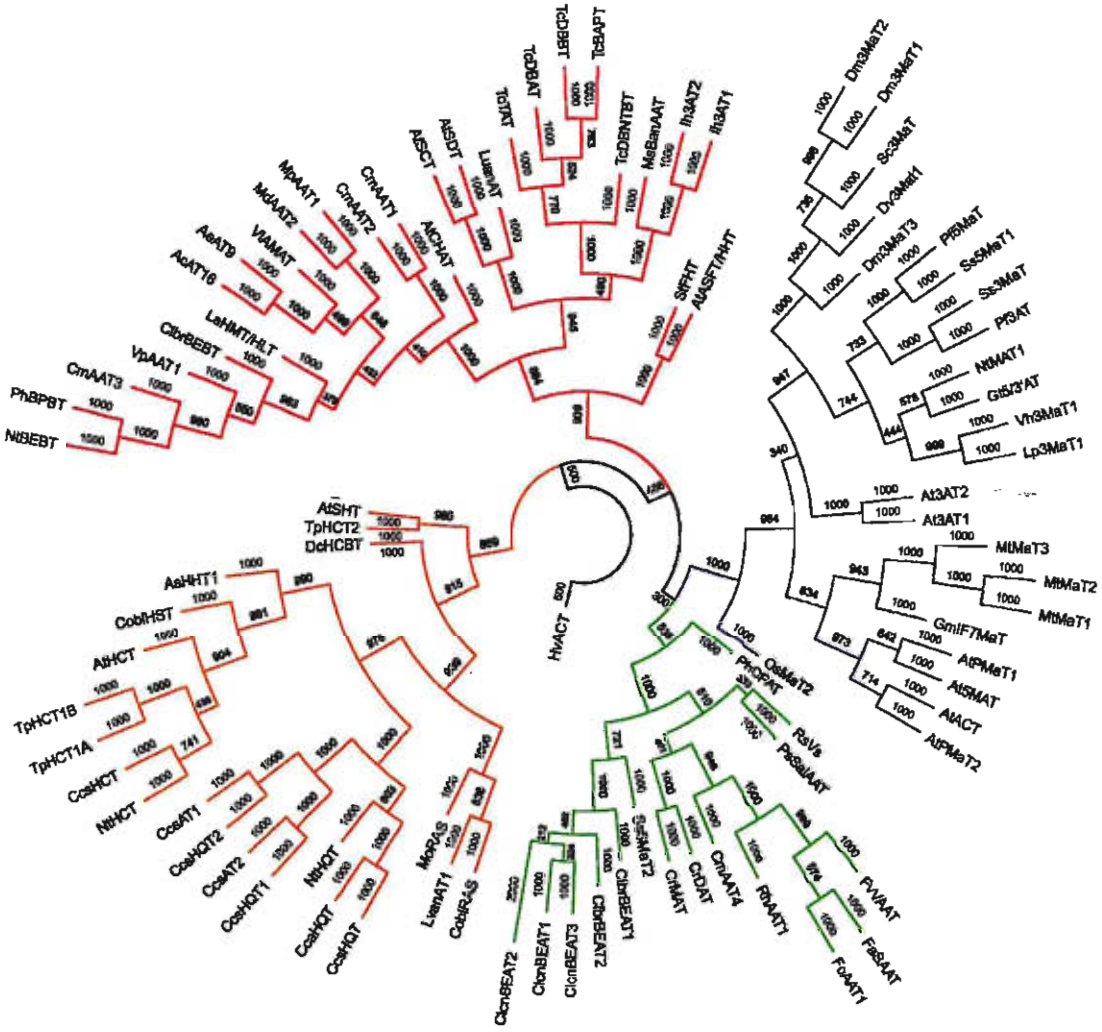

Figure 1.2: Unrooted phylogenetic tree of 88 biochemically characterized BAHD acyltransferases. Coloured branches indicate different clades: blue, clade I; green, clade II; red, clade III, orange, clade IV; black, clade V and others. Members and GenBank accession numbers are as follows: AcAT16 (*Actinidia chinensis* AT16, HO772640), AeAT9 (*Actinidia eriantha* AT9, HO772637), AsHHT1 (*Avena sativa* HHT1, BAC78633), At3AT1 (*Arabidopsis thaliana* 3AT1, AEE27636), At3AT2 (*Arabidopsis thaliana* 3AT2, AEE27579), At5MaT (*Arabidopsis thaliana* 5MaT, NP_189600), AtACT (*Arabidopsis thaliana* ACT, Q9FNP9), AtASFT/HHT (*Arabidopsis thaliana* ASFT/HHT, NP_851111/AED94628), AtCHAT (*Arabidopsis thaliana* CHAT, AAN09797), AtHCT (*Arabidopsis thaliana* HCT, NP_199704), AtPMaT1 (*Arabidopsis thaliana* PMaT1, AED94391), AtPMaT2 (*Arabidopsis thaliana* PMaT2, AEE77599), AtSCT (*Arabidopsis thaliana* SCT, AAP81804), AtSDT (*Arabidopsis thaliana* SDT, AEC07460), AtSHT (*Arabidopsis thaliana* SHT, AEC06845), CcaHQT (*Cynara cardunculus* var. *altilis* HQT, ABK79690), CcsAT1 (*Cynara cardunculus* var. *scolymus* AT1, ADL62854), CcsAT2 (*Cynara cardunculus* var. *scolymus* AT2, ADL62855), CcsHCT (*Cynara cardunculus*

var. *scolymus* HCT, AAZ80046), CcsHQT (*Cynara cardunculus* var. *scolymus* HQT, ABK79689), CcsHQT1 (*Cynara cardunculus* var. *scolymus* HQT1, CAM84302), CcsHQT2 (*Cynara cardunculus* var. *scolymus* HQT2, ACJ23164), ClbrBEAT (*Clarkia breweri* BEAT, AAC18062), ClbrBEAT2 (*Clarkia breweri* BEAT2, AAF04787), ClbrBEBT (*Clarkia breweri* BEBT, AAN09796), ClcnBEAT1 (*Clarkia concinna* BEAT1, AAF04782), ClcnBEAT2 (*Clarkia concinna* BEAT2, AAF04783), ClcnBEAT3 (*Clarkia concinna* BEAT3, AAF04784), CmAAT1 (*Cucumis melo* AAT1, CAA94432), CmAAT2 (*Cucumis melo* AAT2, AAL77060), CmAAT3 (*Cucumis melo* AAT3, AAW51125), CmAAT4 (*Cucumis melo* AAT4, AAW51126), CoblHST (*Coleus blumei* HST, CBI83579), CoblRAS (*Coleus blumei* RAS, CAK55166), CrDAT (*Catharanthus roseus* DAT, AAC99311), CrMAT (*Catharanthus roseus* MAT, AAO13736), DcHCBT (*Dianthus caryophyllus* HCBT, CAB11466), Dm3MaT1 (*Dendranthema x morifolium* 3MaT1, AAQ63615), Dm3MaT2 (*Dendranthema x morifolium* 3MaT2, AAQ63616), Dm3MaT3 (*Dendranthema x morifolium* 3MaT3, BAF50706), Dv3MaT1 (*Dahlia variabilis* 3MaT1, Q8GSN8), FaSAAT (*Fragaria ananassa* SAAT, AAG13130), FcAAT1 (*Fragaria chiloensis* AAT1, ACT82247), FvVAAT (*Fragaria vesca* VAAT, CAC09062), GmIF7MaT (*Glycine max* IF7MaT, BAF73620), Gt5/3'AT (*Gentiana triflora* 5/3'AT, Q9ZWR8), HvACT (*Hordeum vulgare* ACT, AAO73071), Ih3AT1 (*Iris hollandica* AT1, BAE72676), Ih3AT2 (*Iris hollandica* AT2, BAE94328), LaHMT/HLT (*Lupinus albus* HMT/HLT, BAD89275), Lp3MaT1 (*Lamium purpureum* 3MaT1, AAS77404), LuanAT (*Lupinus angustifolius* AT, BAJ49867), LvanAT1 (*Lavandula angustifolia* AT1, ABI48360), MdAAT2 (*Malus domestica* AAT2, AAS79797), MoRAS (*Melissa officinalis* RAS, CBW35684), MpAAT1 (*Malus pumila* AAT1, AAU14879), MsBanAAT (*Musa sapientum* BanAAT, CAC09063), MtMaT1 (*Medicago truncatula* MaT1, ABY91220), MtMaT2 (*Medicago truncatula* MaT2, ABY91222), MtMaT3 (*Medicago truncatula* MaT3, ABY91221), NtBEBT (*Nicotiana tabacum* BEBT, CAA64636), NtHCT (*Nicotiana tabacum* HCT, CAD47830), NtHQT (*Nicotiana tabacum* HQT, CAE46932), NtMAT1 (*Nicotiana tabacum* MAT1, BAD93691), OsMaT2 (*Oryza sativa* MaT2, NP001046855), Pf3AT (*Perilla frutescens* 3AT, BAA93475), Pf5MaT (*Perilla frutescens* 5MaT, AAL50565), PhBPBT (*Petunia* x *hybrida* BPBT, AAU06226), PhCFAT (*Petunia* x *hybrida* CFAT, ABG75942), PsSalAAT (*Papaver somniferum* SalAAT, AAK73661), RhAAT1 (*Rosa hybrida* AAT1, AAW31948), RsVS (*Rauwolfia serpentina* VS, CAD89104), Sc3MaT (*Pericallis cruenta* 3MaT, AAO38058), Ss3MaT (*Salvia splendens* 3MaT, AAR28757), Ss5MaT1 (*Salvia splendens* 5MaT1, AAL50566), Ss5MaT2 (*Salvia splendens* 5MaT2, AAR26385), StFHT (*Solanum tuberosum* FHT, ACS70946), TcBAPT (*Taxus cuspidata* BAPT, AAL92459), TcDBAT (*Taxus cuspidata* DBAT, AAF27621), TcDBBT (*Taxus cuspidata* DBBT, Q9FPW3), TcDBTNBT (*Taxus cuspidata* DBTNBT, Q8LL69), TcTAT (*Taxus cuspidata* TZT, AAF34254), TpHCT1A (*Trifolium pratense* HCT1A, ACI16630), TpHCT1B (*Trifolium pratense* HCT1B, ACI28534), TpHCT2 (*Trifolium pratense* HCT2, ACI16631), Vh3MAT1 (*Verbena hybrida* MAT1, AAS77402), VlAMAT (*Vitis labrusca* AMAT, AAW22989), VpAAT1 (*Vasconcellea pubescens* AAT1, ACT82248).

phenylpropanoids such as phaselic, chlorogenic and rosmarinic acid. Two different studies on rosmarinic acid synthases from *Coleus blumei* (CoblRAS) and *Lavandula angustifolia* (LvanAT1) exemplify the versatility of BAHD acyltransferases. Both enzymes displayed the highest activities in the formation of esters (hydroxyphenyllactate coumarates), but also transferred hydroxycinnamoyl moieties to form amides with previously untested acceptor substrates such as phenethylamine, tryptamine, tyramine, in the case of LvanAT1 and DL-phenylalanine, DL-tyrosine, and DL-dihydroxyphenylalanine in the case of CoblRAS. Although there may be no *in vivo* relevance to these novel compounds, the authors suggest that they may serve as interesting candidates for pharmacological studies (Landmann et al., 2011). Clade V contains just one member, the amide-forming agmatine coumaroyltransferase from barley (*Hordeum vulgare* ACT).

1.5 Fruit and floral scent related BAHD enzymes: the alcohol acyltransferases

1.5.1 Introduction

Over 20 BAHD acyltransferases that are important in fruit or floral scent production have been cloned and biochemically characterized. Phylogenetically, they all fall either into clades II or III, with clade II members exclusively utilizing aliphatic acyl donors (mostly acetyl-CoA), and clade III members mostly, but not exclusively, utilizing aromatic acyl donors (e.g. benzoyl-CoA). For instance, AtCHAT in clade III catalyzes the production of *cis*-3-hexenyl acetate, and cannot use benzoyl-CoA as a substrate (D'Auria, Pichersky, Schaub, Hansel, & Gershenzon, 2007).

These alcohol acyltransferases from clades II and III all catalyze the *O*-acylation of small alcohol molecules to form volatile esters. Common reactions include the

esterification of short- to medium-chain aliphatic or aromatic alcohols, such as ethanol, butanol, hexanol, benzyl alcohol, etc., with similarly sized CoA thioesters of their carboxylic acids (i.e. acetyl-CoA, butyryl-CoA, hexanoyl-CoA, benzoyl-CoA etc., see Figure 1.3). Only a few biosynthetic pathways synthesize most of these precursors, such as the lipoxygenase pathway that is involved in the breakdown of long-chain fatty acid molecules to produce some of the short- to medium-chain aliphatic alcohols. The catabolism of other amino acids such as valine, leucine or isoleucine produce other short-chain aliphatic molecules. The shikimate pathway can be attributed in the formation of some aromatic molecules from the amino acid *L*-phenylalanine, such as phenylpropanoids and benzenoids, and further reactions can modify them to form the alcohol or CoA thioester derivatives used in acylation reactions.

1.5.2 Biochemical pathways of plant volatile compounds

Plant volatile molecules can be divided into 4 broad categories: terpenoids, phenylpropanoid/benzenoids, fatty acid derivatives and amino acid-derived volatiles. In relation to the alcohol acyltransferases, they act mostly on the fatty acid/amino acid derived compounds and phenylpropanoid/benzenoid derivatives, and the least on some terpenoid-derived alcohols.

The phenylpropanoid/benzenoid derived volatiles originate from the amino acid phenylalanine (Phe). The first step in this pathway is the conversion of *L*-phenylalanine to *trans*-cinnamic acid by phenylalanine ammonia lyase (PAL). From here, hydroxycinnamic alcohols and thioesters can be formed through hydroxylations or esterifications, respectively. The synthesis of benzenoid compounds similarly requires

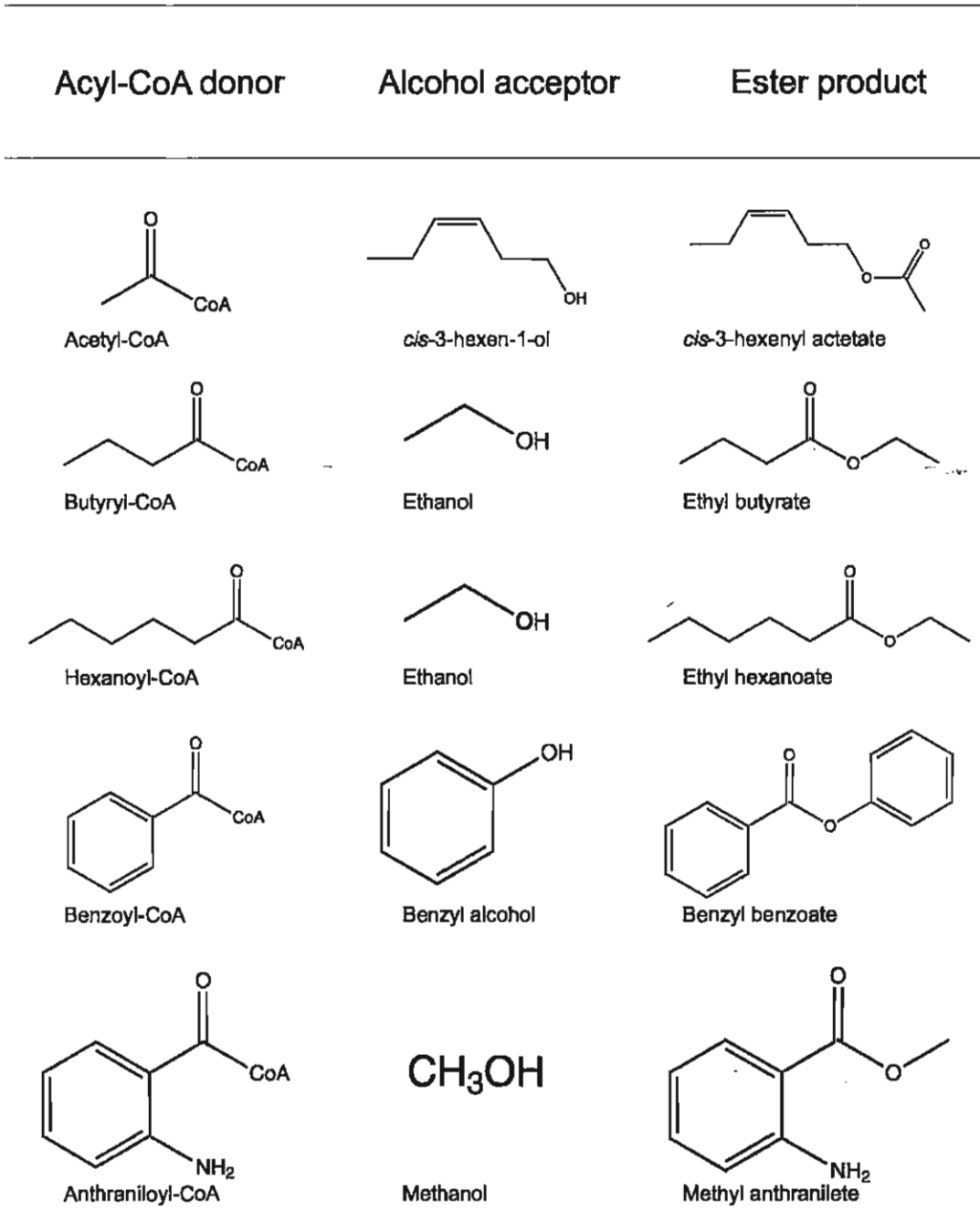

Figure 1.3: Structures of some substrates and products of alcohol acyltransferases.

trans-cinnamic acid as an initial precursor, and side-chain shortening can occur through either CoA-dependant or CoA-independent β-oxidation reactions. Recent studies in *Petunia* x *hybrida* using stable isotope-labelled precursors found that both pathways were being used to produce benzenoid compounds in flower petals (Boatright et al., 2004).

Fatty acid derived plant volatiles originate from the lipoxygenase pathway. The breakdown of the C18 unsaturated fatty acids linoleic and linolenic acids is initiated by lipoxygenase enzymes (termed 9-LOX or 13-LOX) which can dioxygenate the fatty acids at either the C9 or C13 positions (or sometimes both). The 9-hydroperoxypolyenic fatty acids can then be metabolized by hydroperoxide lyases (HPLs), while the 13-hydroperoxypolyenic fatty acids can be metabolized by either HPLs or allene oxide synthase (AOS). The action of either AOS of HPL is the first committed step on the pathway to form volatile molecules (Negre-Zakharov, Long, & Dudareva, 2009).

In the AOS pathway, the precursor 13-hydroperoxy linolenic acid is converted to methyl jasmonate in a series of enzymatic reactions, an important plant hormone involved in activation of plant defense responses and secondary metabolism pathways (Wasternack & Parthier, 1997). In both branches of the HPL pathway, the C18, 13- or 9-hydroperoxy fatty acids are converted to short-chain C6 or C9 aldehydes (with the resultant C12 or C9 fatty acids) by 13-HPL or 9-HPL, members of the CYP74 family of cytochrome P450 enzymes (Matsui et al., 1996). The aldehydes can be further modified by spontaneous or enzymatically-assisted isomerization, and also reduced to their alcohol forms by the enzyme alcohol dehydrogenase (ADH).

These C6 aldehydes (e.g. *trans*-2-hexenal, cis-3-hexenal), alcohols (*cis*-3-hexenol) and corresponding esters (*cis*-3-hexenyl acetate) endow fruit and vegetables with their characteristic "green leaf" aroma. These C6 volatiles are commonly released by damaged or wounded tissue in most green vegetative tissues studied thus far (D'Auria et al., 2007), but are also found in flowers and fruits (D'Auria et al., 2007). Not only important in perception to humans, they have also been shown to be essential as signalling molecules to plants and other organisms. For instance, infection of the bean plant (*Phaseolus vulgaris*) by the pathogenic bacterium *Pseudomonas syringae* caused the release of the volatiles cis-3-hexanol and trans-2-hexanal during the hypersensitive response. These compounds were also shown to have bactericidal properties, suggesting a role for them in plant defense (Croft, Juttner, & Slusarenko, 1993). In support of this, it was shown in *A. thaliana* that exposure to trans-2-hexenal, hexanol, or hexenyl acetate induced expression of LOX mRNA in a feedback mechanism (Bate & Rothstein, 1998), which activates synthesis of methyl jasmonate, a common elicitor of defense-related gene expression (Bate & Rothstein, 1998). Finally, "green-leaf" volatiles can act in an indirect defense response to herbivory by attracting predators or parasitoids of the herbivores causing the damage to the plant (D'Auria et al., 2007).

1.5.3 Fruit and floral volatiles made by BAHD acyltransferases

As mentioned previously, there are over 20 BAHD acyltransferases from plants in 11 different genera and 8 different orders that have been characterized to date as being involved in fruit or floral scent production, some of which have been already reviewed (D'Auria et al., 2007). In general, the expression, protein levels, and activity of these enzymes increases throughout the maturation of the fruit to peak at full maturity, and the

esters produced by these enzymes accumulate and contribute significantly to their final aroma profiles as perceived by humans. Often, the substrate specificity of the alcohol acyltransferases (AATs) *in vitro* is broad, both in regards to their acyl donor and acyl acceptor utilized, and thus may be responsible for producing more than one type of molecule *in vivo*; however this is most likely determined by the endogenous substrates that are made available by each plant species.

One of the first BAHD acyltransferases characterized was BEAT, acetyl-CoA:benzylalcohol acetyltransferase from *Clarkia breweri* flowers (ClbrBEAT1). ClbrBEAT1 was purified from flower petals, and a cDNA encoding it was expressed in *E. coli*. It was shown to catalyze the formation of benzyl acetate, a major constituent of the *C. breweri* aroma profile (Dudareva, D'Auria, Nam, Raguso, & Pichersky, 1998), when supplied with benzyl alcohol and acetyl-CoA. *ClbrBEAT1* transcripts were found exclusively in flower petals, and their expression correlated well with the appearance of enzyme activity as the flower bud matured. In a follow-up study, a homolog from the same species (*ClbrBEAT2*), along with 4 orthologs from a similar, unscented species (*Clarkia concinna*; *ClcnBEAT1*, *ClcnBEAT2*, *ClcnBEAT3*, *ClcnBEAT4*) were cloned and characterized. *ClbrBEAT2* was isolated from a line of *C. breweri* that showed low activity of benzyl acetate formation, and is probably an allele of *ClbrBEAT1*, since *C. breweri* was previously shown to have only one *BEAT* gene (Dudareva et al., 1998; Nam, Dudareva, & Pichersky, 1999) (98.4% identity between the two, 426/433 amino acids matched). Although similar levels of *ClbrBEAT1* and *ClbrBEAT2* mRNA transcripts accumulated in the two lines of *C. breweri* throughout the development of the flower (as measured by Northern blotting), Western blots and enzyme activity assays showed that

there was about twice the protein levels and associated enzymatic activity in the higher-activity line. The two alleles of ClbrBEAT had similar relative activities towards the different alcohol substrates tested, but interestingly ClbrBEAT2 (from the low activity line) had a slightly higher specific activity, and a K_m for benzylalcohol that was about half that of ClbrBEAT1. The results were interpreted to suggest that that smaller production of benzyl acetate in the low-activity line of *C. breweri* could be due to some differences in post-transcriptional regulation of the BEAT enzyme, such as low efficiency of protein synthesis or a higher rate of protein degradation (Nam et al., 1999). It could also be that the ClbrBEAT2 enzyme had a lower affinity towards its other substrate, acetyl-CoA, which was not measured, or perhaps there was an insufficient supply of benzylalcohol *in vivo* that would contribute to the lack of benzyl acetate formation in the low-producing line.

The four *BEAT*-like genes isolated from the unscented *C. concinna* species came from the combination of a genomic library screen and the amplification of cDNA sequences from flower petal mRNA. Three of the sequences obtained had 91-95% identity to the *C. breweri BEAT* sequences, while the fourth appeared to be a truncated form since the last one-third of its coding region was missing (Nam et al., 1999). When the three intact coding sequences were expressed in *E. coli* and the resultant proteins assayed, it was found they all had some activity with benzylalcohol. ClcnBEAT1 had a similar K_m towards benzylalcohol, while the value for ClcnBEAT2 was higher, and no accurate value could be measured for ClcnBEAT3 because it displayed very low activity for this substrate. However, all the BEAT-like enzymes had higher relative activities towards other substrates, especially the aliphatic alcohol heptanol (about 4-fold higher)

and cinnamyl alcohol (especially with ClcnBEAT3, about 8-fold higher). An analysis of mRNA and processing states by RT-PCR using intron-spanning oligonucleotides and subsequent Northern blotting showed that transcripts could only be detected for *ClcnBEAT*1 and *ClcnBEAT*3 and that in both cases, it was all or mostly unprocessed transcript. Only *ClcnBEAT*3 had any detectable levels of processed transcript (Nam et al., 1999).

This comparative study in *Clarkia* highlights two common findings in studies of floral and fruit-scent related BAHD alcohol acyltransferases: First, predicting substrate specificity on the basis of sequence similarity can be difficult, which is true for all BAHD acyltransferases. Most alcohol acyltransferases have a broad substrate specificity, which can be altered by only a few amino acid changes. Secondly, gene expression, protein levels and activity of these enzymes tend to increase during development to peak at maturity of the flower/fruit.

In petunia (*Petunia* x *hybrida*) flowers, scent is derived almost exclusively from benzenoid/phenylpropanoid volatiles (Boatright et al., 2004). Previous studies on petunia scent volatiles showed a daily rhythm of emission that peaked at midnight (Kolosova, Gorenstein, Kish, & Dudareva, 2001; Verdonk et al., 2003; Boatright et al., 2004) and scent-related genes, including *PhBPBT*, a BAHD acyltransferase responsible for benzylbenzoate production, showed an expression pattern that correlated well with this (Boatright et al., 2004). *PhCFAT* (*Petunia* x *hybrida* acetyl-CoA: coniferyl alcohol acetyltransferase), was later shown to follow this pattern as well. Coniferyl acetate is hypothesized to be the substrate of isoeugenol synthase (PhIGS1) in the production of isoeugenol, a major component of petunia scent. Heterologous expression of *PhCFAT*

and subsequent enzyme assays determined that PhCFAT had the highest acetyltransferase activity with coniferyl alcohol and acetyl-CoA, although it also had activity with several other alcohols, such as sinapyl alcohol, cinnamyl alcohol, octanol and geraniol (Dexter et al., 2007). Other acyl-CoA substrates were not tested. Interestingly, the relative substrate preferences of PhCFAT could be altered by a change in pH. At pH 6.0, activity was highest with coniferyl alcohol with strong activity towards sinapyl alcohol (70.6% relative to maximum), while other substrates tested all showed minimal conversion (12% or less relative to maximum). At pH 7.5, activity was still maximal with coniferyl alcohol, but the range of substrates expanded as well as their relative activities compared with coniferyl alcohol (octanol 54.2%, cinnamyl alcohol 41.6%, geraniol 40.4%, sinapyl alcohol 25.6% of maximum). *PhCFAT* transcripts were found only in flowers, specifically the limbs (i.e. the outer flower parts), and only during anthesis and post-anthesis. Also, gene expression of *PhCFAT* was 15-30 times higher at night than in daytime and this coincided with peak volatile emission.

The characterization and substrate preferences of fruit alcohol acyltransferases from cDNA-clones of wild strawberry (*Fragaria vesca*, FvVAAT), cultivated strawberry (*Fragaria* x *ananassa*, FaSAAT), and banana (*Musa sapientum*, MsBanAAT) (Beekwilder et al., 2004) were compared, based on a previous characterization of FaSAAT (Aharoni et al., 2000; Beekwilder et al., 2004). This study provided a good opportunity to compare substrate preferences of alcohol acyltransferases with high identity (FvVAAT and FaSAAT, 86% identical), especially due to the comprehensive list of substrates tested. The 28 acyl acceptor substrates tested included aliphatic and aromatic alcohols, benzenoid/phenylpropanoid alcohols, and terpenoid alcohols, and

were supplied to FaSAAT in combination with acetyl-CoA, butyryl-CoA, and hexanoyl-CoA. As had been reported previously (Aharoni et al., 2000), FaSAAT preferred C6 to C10 aliphatic alcohols (Beekwilder et al., 2004) when assayed with acetyl-CoA; however geraniol, which hadn't been tested previously, proved to be the most preferred acyl acceptor substrate. When assayed in combination with butyryl-CoA and hexanoyl-CoA, substrate preference for alcohols remained somewhat similar, in that C6 to C9 aliphatic alcohols and geraniol were preferred, however there was a significant increased preference towards 1- and 2-butanol, while activity with decanol significantly decreased (Beekwilder et al., 2004). The cloned acyltransferases from wild strawberry and banana were also tested with a range of alcohols, but only with acetyl-CoA as the acyl donor. Unlike FaSAAT, FvVAAT did not efficiently utilize C7 to C10 aliphatic alcohols; however there was an overlap for preference of C6 alcohols between the two. FvVAAT also had limited activity with shorter-chain alcohols as well as with benzyl and phenethyl alcohols, which differentiated it from FaSAAT. MsBanAAT had a similar substrate preference profile as FvVAAT. While its highest activity was with cinnamyl alcohol, it also efficiently utilized the terpenoid alcohols geraniol and nerol, as well as the aliphatic alcohols octanol and *trans*-2-hexenol. Surprisingly, MsBanAAT showed only minimal activity towards isoamyl alcohol and butanol, since these acetate esters are characteristic of banana aroma. Remarkably, a previous study had shown that total alcohol acyltransferase activity, as measured by supplying alcohol to either whole banana fruit or tissue discs in a sealed chamber, followed by headspace analysis by GC-MS showed a preference for C6 alcohols over C3 or C4 alcohols, similar to the results obtained with the recombinant MsBanAAT. This suggested that MsBanAAT was responsible for

production of banana aroma and that substrate supply must be the limiting factor in the final volatile ester profile produced in the fruit (Wyllie & Fellman, 2000). The fact that banana accumulates significant amounts of isoamyl alcohol and butanol during ripening (Nogueira, Fernandes, & Nascimento, 2003; Shiota, 1993) strongly supports this hypothesis.

A recent study of an alcohol acyltransferase (FcAAT1) isolated from the wild Chilean strawberry *Fragaria chiloensis*, a progenitor of the cultivated strawberry *Fragaria* x *ananassa* (González et al., 2009), showed that expression of the gene as measured by quantitative real time reverse transcription PCR (qRT-PCR), correlated well with ester production during ripening of the fruit, and was not expressed to any significant amount in other tissues of the plant (González et al., 2009). The addition of the gene expression, enzyme activity and volatile profile analysis throughout berry development in *Fragaria chiloensis* with the previous biochemical characterizations of AATs in *Fragaria* x *ananassa* and *Fragaria vesca* strawberry strongly suggest that alcohol acyltransferases may play a significant role in the final aroma and flavour profile of strawberries.

The French Charentais cantaloupe, *Cucumis melo* var. *cantalupensis* is highly prized for its rich, aromatic flavour (Aubert & Bourger, 2004). The volatile profile of a ripe melon obtained from an organic solvent extraction with subsequent analysis by gas chromatography detected 28 compounds: 17 esters, 8 alcohols, and 3 carbonyl compounds (Aubert & Bourger, 2004), indicating that alcohol acyltransferases are likely to play a major role in aroma and flavour production. By using degenerate oligonucleotides based on a conserved BAHD motif (DFGWG) followed by 3'- and 5'-

RACE, 4 BAHD alcohol acyltransferases were isolated and characterized from Charentais cantaloupe in a series of publications (Aggelis, John, Karvouni, & Grierson, 1997; El-Sharkawy et al., 2005; Lucchetta et al., 2007; Yahyaoui, 2002). As with other alcohol acyltransferases, the expression level of these genes (*CmAAT1, CmAAT2, CmAAT3,* and *CmAAT4*) was fruit-specific, and increased during ripening to peak at maturity, correlating with increased enzymatic activity and production of esters (El-Sharkawy et al., 2005). Melon is a climacteric fruit, and expression of *CmAAT1-4* correlated with ethylene production as well. In fact, in ethylene-suppressed fruit (either by an antisense *ACC oxidase* mRNA (AS) being expressed or by treatment of wild-type fruit by 1-MCP, an ethylene antagonist), expression of *CmAAT1-4* was strongly reduced or completely absent. Treatment of AS fruit with ethylene one and 3 days before harvest was able to restore the expression of these genes (El-Sharkawy et al., 2005). These data indicate that in melon, expression of alcohol acyltransferases is under tight control of ethylene.

The recombinant CmAAT2, CmAAT3, and CmAAT4 were 86%, 58%, and 22% identical to CmAAT1 at the amino acid level. Although enzymatic activity could be detected for 3 of the enzymes (El-Sharkawy et al., 2005), CmAAT2 was inactive with any substrate combination or condition tested (El-Sharkawy et al., 2005; Yahyaoui, 2002). The three functional enzymes displayed some overlapping activities as well as some exclusive activities as to the substrates tested, which totaled 29 combinations of aliphatic and aromatic alcohols with aliphatic C2, C3, C4, and C6 acyl-CoA donors. In total, 26 of 29 substrate combinations yielded ester products (El-Sharkawy et al., 2005), a large majority of esters reported to occur in ripe melon (Beaulieu & Grimm, 2001).

Briefly, CmAAT1 was most active producing a wide range of short and medium chain acyl esters, CmAAT3 had a strong preference for producing benzyl acetate, and CmAAT4 almost exclusively produced acetates. In trying to determine the cause of CmAAT2's failure to show any activity, an alignment of the 4 melon acyltransferase amino acid sequences with 6 other floral and fruit scent related acyltransferases identified a conserved threonine residue that had been substituted with alanine at position 268 in CmAAT2 (El-Sharkawy et al., 2005). Site-directed mutagenesis proved that this residue is critical for enzyme activity, since mutated CmAAT2 A268T restored acyltransferase activity to CmAAT2 similar to the substrate specificity of CmAAT1, its closest homolog (84% identical). Conversely, when CmAAT1 was mutated in a reverse fashion (T268A), the substitution of its native threonine residue to alanine almost completely abolished its enzymatic activity, as only trace amounts of product could be seen for only a few compounds (El-Sharkawy et al., 2005). Whether or not CmAAT2 is a naturally inactive enzyme, or its *in vivo* substrate preference has just not yet been determined remains to be seen.

Melon contains many sulfur-containing alcohols and esters that are an important part of its volatile profile (Aubert & Bourger, 2004), and cell-free protein extracts from melon showed the production of the ester 3-(methylthio) propyl acetate by alcohol acyltransferase(s) (Shalit et al., 2001); however the question of whether the specific alcohol acyltransferases CmAAT1-4 are active with these compounds had yet to be tested. In an extension of the study published in 2005 (El-Sharkawy et al., 2005), the authors found that CmAAT1, 3, and 4 were all active to some degree in producing the thioether esters 3-(methylthio) propyl acetate and 2-(methylthio) ethyl acetate (Lucchetta

et al., 2007). The potential ability of CmAAT2 to be active with sulfur-containing alcohol substrates was either untested or not reported in this publication. Further amino acid alignment analyses followed by site-directed mutagenesis experiments identified 4 more positions in CmAAT1, CmAAT3, and CmAAT4 that were important in determining substrate specificity of the enzyme, in addition to the one already reported for CmAAT2. Two novel findings with respect to BAHD acyltransferases were also reported in this study. Firstly, when both the recombinant enzymes and the native AAT were submitted to gel filtration chromatography, the protein behaved as a 200 kDa tetramer based on detection of enzyme activity of its elution profile, and its 51 kDa subunit molecular weight was established by denaturing SDS-PAGE (Lucchetta et al., 2007). Thus the recombinant and native enzymes appeared to function as tetramers in melon, the first time a BAHD acyltransferase was reported to function as a multimer. Secondly, it was shown that free Coenzyme A (CoA-SH), a product of the acyltransferase reaction, could both stimulate and inhibit enzyme activity depending on its concentration. Activity of the enzyme increased with concentrations as low as 0.5 μM CoA-SH and up to 50 μM CoA-SH, with maximum stimulation at 2.5 μM CoA-SH which increased activity by 400%. Above 50 μM CoA-SH, activity was diminished by 20% at 500 μM and 80% at 5000 μM. (Lucchetta et al., 2007). To measure these effects in a different way, enzyme activity assays were supplemented with phospho-transacetylase and phosphoacetate, which acetylates free CoA-SH to form acetyl-CoA and phosphate. These assays were performed with one of the mutated AATs, which is incapable of utilizing acetyl-CoA as a co-substrate with ethanol but instead uses butanoyl-CoA. It was found that using high concentrations of the phosphotransacetylase (i.e. clearing all the

free CoA-SH produced from the AAT reaction) completely abolished the AAT activity, showing that some free CoA-SH is required for activity (Lucchetta et al., 2007). It has been shown that BAHD acyltransferases can also perform the reverse reaction; when supplied with CoA-SH and the appropriate ester or amide the enzyme will catalyze the conversion into the acyl-CoA and hydroxyl or amine substrates (Hoffmann, Maury, Martz, Geoffroy, & Legrand, 2003; Luo et al., 2009), thus it is not surprising that CoA-SH can affect the kinetics of the acyltransferase reaction. The kinetic and substrate specificity studies on *Cucumis melo* alcohol acyltransferases greatly increased our knowledge about BAHD alcohol acyltransferase activities as well as confirmed previous findings. Although these enzymes show remarkable versatility in the reactions they catalyze, it may be necessary for small gene families of BAHD members to be present in a single species to produce the complex volatile ester profiles exhibited by some fruit and floral species.

One of the first BAHD alcohol acyltransferases biochemically characterized from fruit was anthraniloyl-CoA:methanol anthraniloyltransferase, isolated from *Vitis labrusca* (Concord) berries (VlAMAT) (Wang & De Luca, 2005). This enzyme is responsible for the production of methyl anthranilate, thought to contribute to the characteristic "foxy" aroma of Concord berries, jams, jellies, and juices. The ecological role of methyl anthranilate is likely to deter herbivory, since it is a strong avian repellent. In fact, products containing methyl anthranilate are used industrially in areas where bird populations are considered pests, such as on golf courses. Developmental studies with *Vitis labrusca* berries demonstrated that *VlAMAT* gene expression increased during ripening, concomitant with VlAMAT enzyme activity and methyl anthranilate

accumulation. Expression of the gene was localized to the mesocarp (flesh) of the berries. VlAMAT had highest activity with anthraniloyl-CoA as the acyl donor, showed comparable affinity towards benzoyl-CoA, and displayed weak activity with acetyl-CoA. Interestingly, *in vitro* studies on substrate specificity of the enzyme showed that the least preferred substrate of VlAMAT was methanol, but instead preferred benzyl alcohol followed by octanol and other aliphatic alcohols, with generally decreasing affinity as the alcohol chain-length shortened. Once again, the *in vivo* situation favours the formation of methyl anthranilate since the fruits make large amounts of VlAMAT and accumulate methanol substrate and anthranilic acid precursor substrates rather than other metabolites that might be used by this enzyme. Remarkably, corn (*Zea mays*) also accumulates methyl anthranilate at certain stages of fruit development through an S-adenosyl-methionine (SAM) based methylation of anthranilic acid (Köllner, 2010) rather than through the AMAT-like reaction of Concord grape.

Overall, these studies of alcohol acyltransferases in fruit and flowers show that sequence similarity is not a reliable predictor of substrate specificity, since enzymes having high sequence identity can have different specificities, but also highly divergent enzymes can have similar specificities. Also, alcohol acyltransferases tend to have an expression profile and activity that correlates with the accumulation of esters during the ripening of the fruit. Lastly, BAHD alcohol acyltransferases can be very versatile, and show a remarkably broad spectrum of activities when supplied with many substrates.

1.6 The genome of *Vitis vinifera* predicts the presence of at least 50 BAHD-like acyltransferase genes.

Recently, the genome of *Vitis vinifera* was published based on the sequencing of a highly homozygous line of the cultivar Pinot Noir (Jaillon et al., 2007). In the analysis, the authors describe the current *V. vinifera* genome as containing information from three different ancestors combined in the past to produce what they termed a "paleo-hexaploid", and determined that this paleo-hexaploidy is present in all Eurosids, including Poplar and *Arabidopsis thaliana*. They also noted large expansions in gene families related to aroma properties and wine characteristics. For example, over 43 stilbene synthases (involved in the antioxidant resveratrol's biosynthesis) were found (over 20 of which have been confirmed for function), as well as 89 functional and 27 pseudogenes of the terpene synthase (TPS) family (compared to *Arabidopsis'* 30-40 TPSs) (Jaillon et al., 2007).

A search of the *Vitis vinifera* genome for putative BAHD acyltransferase genes described in the present study (see Section 3.1) identified at least 50 candidates. A phylogenetic analysis of these protein sequences with other BAHD acyltransferases placed 26 of them into Clades II and III (5 and 21 sequences, respectively), many of which aligned with alcohol acyltransferases with functions in floral and fruit scent production. In fact, a group of 5 putative BAHD acyltransferases in *V. vinifera* showed high homology (at least 84% identical at the amino acid level) to *VlAMAT*, with one candidate being 95% identical. Thus, it seems *V. vinifera* has a small family of putative alcohol acyltransferases which may be involved in the production of volatile esters that may be important for aroma production and formation of grape flavour profiles.

1.7 Conclusions

The acyl-CoA dependant BAHD acyltransferases are a versatile family of enzymes involved in the modification of many classes of plant secondary metabolites. Eighty-eight members have been biochemically characterized thus far, and they fall phylogenetically into about 5 groups or clades. They are involved in the acylation of various compounds such as anthocyanins, phenylpropanoids, alkaloids, and plant volatiles. In particular, alcohol acyltransferases acylate various alcohols to form volatile esters, important in fruit and floral scent production. These alcohol acyltransferases are versatile enzymes, and typically can utilize many different substrates to form an array of ester products *in vitro*. The final profile of volatile esters produced in the plants is probably due to the available precursors *in vivo*. The expression and activity of alcohol acyltransferases involved in fruit and floral scent is normally specific to those organs, and increases during ripening to peak at maturity. In fruit where the production of many different esters is important in their aroma profiles, small gene families of alcohol acyltransferases may be involved that increase the plants ability to produce an array of compounds. Trying to predict substrate specificity of alcohol acyltransferases based on sequence homology to known acyltransferases is difficult, since enzymes having high sequence similarity to each other can have different substrate specificities, while two divergent sequences can perform the same reactions. However, progress is being made through crystal structures, homology modelling, and site-directed mutagenesis to identify certain residues that are important in determining substrate specificity. For now, biochemical characterization remains the *de facto* method for describing the function of BAHD acyltransferases.

For wines produced from the many cultivars of *Vitis vinifera*, a major differentiating factor in the final product is the germplasm of the grapes from which they are produced. The grape berries contain many compounds that can affect the final sensory quality of the wine, either directly or indirectly through modification by the fermentation process (Dunlevy et al., 2009) such as terpenoids, norisoprenoids, and volatile aromatic and aliphatic compounds, including esters. In many different fruit species, including *Vitis labrusca* Concord grapes, the accumulation of volatile esters is due to the action of alcohol acyltransferases from the BAHD family of acyltransferases. The published genome of *V. vinifera* predicts the presence of at least 50 BAHD acyltransferase-like genes, including 5 that show high homology to *VlAMAT*, responsible for the production of methyl anthranilate which contributes to the characteristic "foxy" aroma of the berries, yet *V. vinifera* is not known to accumulate this compound. This could be due to a number of reasons. Firstly, these *VlAMAT*-like genes in *V. vinifera* may not be expressed or may be pseudogenes. Secondly, if they are being expressed and are active, either the availability of the necessary substrates may be limiting *in vivo* (Wang & De Luca, 2005), or it is also possible that the *V. vinifera VlAMAT*-like gene products have an altered substrate specificity compared to VlAMAT. Thus, this study was initiated as an effort to understand what role these *VlAMAT*-like alcohol acyltransferases might play in the development of aroma in different varieties of the wine grape berry. An understanding of biochemical function and developmental regulation of *VlAMAT*-like genes in *V. vinifera* could potentially assist in determining optimum harvest time in relation to accumulation of certain desirable (or undesirable) compounds, and could be used as genetic markers in breeding programs to select for these compounds.

Chapter 2. Materials and Methods

2.1 Source of Plant Materials

Ripe grape berries from 18 cultivars of *Vitis vinifera* were harvested in late September and October in Niagara-on-the-Lake, Ontario, 2009 (see Results Table 3.1). While in the field, berries were stored in a cooler with ice packs until they were weighed and flash frozen in liquid nitrogen in the laboratory, and subsequently stored at -80°C until further analysis. Mature *Vitis labrusca* berries that had been collected and frozen in 2004 were also used.

2.2 Chemicals

Most of the substrates used were purchased from Sigma. Radiolabeled acetyl-Coenzyme A ([acetyl-1-^{14}C], Figure 2.1 A) was purchased from PerkinElmer (Boston, MA). Radiolabeled anthranilic acid ([ring-UL-^{14}C], Figure 2.1 B) was purchased from Sigma (Oakville, ON) and benzoic acid ([ring-^{14}C (U)], Figure 2.1 C) from Moravek Biochemicals (Brea, CA).

2.3 Bioinformatic analysis

Protein sequences of all known biochemically characterized BAHD acyltransferases were obtained from Genbank (NCBI). Putative BAHD acyltransferases from the genome of *V. vinifera* Pinot Noir PN40024 were identified based on a previous method (Yu, Gou, & Liu, 2009). A short amino acid sequence (positions 319-411 from VvsbAAT1, this study) containing the conserved DFGWG motif of BAHD acyltransferases was subjected to a BLASTP search of the UniProtKB-viridiplantae database with expectation threshold value set to 100, BLOSUM62 matrix, filtering of low complexity regions, gapped search,

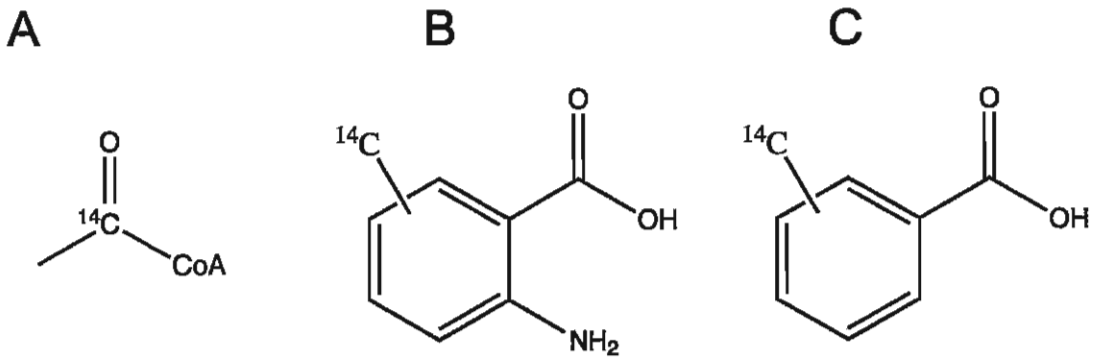

Figure 2.1: Structures and labeling pattern of (A) [acetyl-1-^{14}C]-Coenzyme A, (B) ring-^{14}C-anthranilic acid (12.5 mCi/mmol) and (C) ring-^{14}C-benzoic acid (60mCi/mmol).

and 1000 hits. These "loose" search settings were chosen to maximize the possibility of detecting even the weakest protein similarities. The search results were filtered to *V. vinifera* predicted proteins, and then specifically to those sequences published only by Jaillon *et al.* (Jaillon et al., 2007) in order to avoid redundancy with a second published genome of the same *V. vinifera* variety (Velasco et al., 2007). Protein sequences were aligned with the MUSCLE program (Edgar, 2004), and manually screened for sequences containing at least 80% (i.e. 4 out of 5) amino acids identical to the conserved DFGWG motif. The resultant 18 sequences were each subjected to a second BLASTP search of the same database with the same settings as above except the expectation threshold was lowered to 10^{-5}. This second round of searching had its duplicate results removed and sequences were aligned as above before screening for typical BAHD acyltransferase motifs (at least 80% match to HXXXD and DFGWG) allowing for possible pseudo- and truncated forms. The resultant BAHD acyltransferase predicted protein sequences from *V. vinifera* Pinot Noir were aligned with MUSCLE (Edgar, 2004), and the phylogenetic tree was constructed by neighbour joining and bootstrapping (1000 replicates) using the PHYLIP software package (Felsenstein, 1989), and visualized using FigTree version 1.3.1 software.

2.4 Detection of *VlAMAT*-like gene products by RT-PCR

Frozen berry mesocarp tissues were ground to a fine powder in liquid nitrogen using a mortar and pestle. Total RNA was extracted using Plant RNA Isolation reagent (Invitrogen), according to the manufacturers' protocols with some modifications. Briefly, around 100 mg of powdered frozen mesocarp was added to a pre-weighed, pre-frozen 1.5 mL microfuge tube. Plant RNA isolation reagent (500 µL) was mixed with the

powdered tissue and after incubation for 5 min at room temperature, extracts were centrifuged for 2 minutes at 12,000*g* to harvest the supernatants that were transferred to fresh 1.5 mL tubes. The supernatants were treated with 100 µL of 5 M sodium chloride (prepared in 0.1% DEPC-treated Milli-Q water) and 300 µL of chloroform that were thoroughly mixed by repetitive inversion for 30 sec and immediate centrifugation for 10 min at 12,000*g* at 4°C separated the mixture into 2 phases. Each aqueous upper 500 µL phase was transferred by pipette to fresh 1.5 mL tubes with an equal amount of isopropanol mixed in for overnight incubation at minus 20°C to precipitate the RNA. Precipitates were collected by centrifugation for 10 minutes at 12,000*g* at 4°C and after decanting the supernatant, pellets were washed with 1 mL of 75% ethanol in 0.1% DEPC-treated Milli-Q water, and subsequently pelleted again by centrifugation at 12,000*g* for 1 minute at room temperature. Each supernatant was removed by pipette, and the pellets were air-dried on ice for 1 minute before dissolving in 20 µL of 0.1% DEPC-treated Milli-Q water to give the final RNA preparation. Quantification and quality control of the final RNA preparation was performed by measuring its UV absorbance at 260 nm (quantification) and comparing it to the absorbance at 280 nm (for quality/purity measurement). Finally, 5 µL of RNA was visualized on a 1% agarose gel containing ethidium bromide to confirm the presence of ribosomal RNA and a lower molecular weight mRNA smear.

First strand synthesis of cDNA from RNA was performed with the Takara RNA PCR Kit version 3.0. In a final volume of 10 µL, 1 mM each dNTP mix, 5 mM $MgCl_2$, 1 unit RNase inhibitor, 125 nM oligo dT-Adaptor primer, 1 unit AMV reverse transcriptase, and

4.25 µL of the prepared RNA was mixed and incubated at 52°C for one hour, then 70°C for 10 min to inactivate the AMV reverse transcriptase.

Polymerase chain reaction (PCR) was used to amplify a 330 bp region near the 3' end of the cDNA to confirm the presence of *VlAMAT*-like transcript(s) using primers 5'-CCAGGATACTATGGAAATGC-3' (forward) and 5'-CTTCTTCTCCTTTGCTGTTC-3' (reverse) derived from an alignment of 5 genomic *V. vinifera* DNA sequences most similar to *VlAMAT* and subsequent selection of oligonucleotides that would anneal to all 5 putative transcripts. The PCR conditions used were as follows: Initial denaturation at 94°C for 2 minutes, followed by 30 cycles of a) 94°C for 30 seconds (denaturation), b) 55°C for 30 seconds (primer annealing), c) 72°C for 25 seconds (extension) and d) a final extension period of 72°C for 10 minutes. PCR products were separated by agarose (1%) gel electrophoresis and visualized by staining with ethidium bromide (Sambrook & Russell, 2001). RT-PCR performed with a second primer set [5'-CTTGGTTCCCCTCTTATCTT-3' (forward) and 5'-TTGGTGTTGGTTACCTTCTC-3' (reverse)] designed to flank the intron of *F6HBX5* (the accession number of the predicted mRNA sequence with highest identity to *VlAMAT*) was performed essentially as described above, except that the extension time was increased to 1 minute.

2.5 Sequencing of PCR products

PCR products that were cloned using Promega's pGEM-T Easy vector as described by the manufacturer were transformed into *E. coli* XL-10 Gold cells (Invitrogen). Colonies positive for vectors harboring inserts (by blue/white screening and colony PCR) were grown overnight in 3 mL Luria-Bertani (LB) liquid medium containing 50 µg/mL ampicillin. Bacterial culture pellets that were harvested by centrifugation for 10 minutes

at 5400*g* were extracted to release plasmid that were purified using Qiagen's QIAPrep Spin Column according to their protocols (http://www.qiagen.com/literature/render.aspx?id=370). The resulting pure plasmid was sent to Bio Basic Inc. (Markham, ON) for Sanger sequencing.

2.6 Isolation of protein from berries

An ammonium sulfate precipitation protocol was employed to extract protein from the mesocarp of ripe berries for enzyme assays and Western blot analysis. Berries (50-100 g) were partially thawed from storage at -80°C and the skins were carefully removed with forceps. The frozen mesocarps were then ground in liquid nitrogen using a mortar and pestle at which time the seeds were removed. Frozen powdered mesocarp tissue was further homogenized in the presence of solid 10% polyvinylpolypyrrolidone (PVPP) (w/w) before slowly stirring in 3x (w/v) ice-cold extraction buffer (250 mM Tris, pH 8.0 / 5 mM sodium metabisulfite / 10 % glycerol / 1 mM dithiothreitol (DTT) / 1 mM phenylmethylsulfonylfluoride (PMSF)). This slurry was further homogenized on ice using a Polytron equipped with a 12 mm dispersing aggregate at full power for 4 minutes (Polytron PT 1200 E, Kinematica, AG, Switzerland). The homogenate was clarified from bulk debris by filtration through 1 layer of Miracloth in a Buchner funnel under vacuum, before centrifugation at 7 250*g* for 15 min at 4°C. The filtrate was treated with ammonium sulfate 30% (w/v) that was slowly added over a period of 10 min, the homogenate was stirred gently for 30 min on ice and then centrifuged at 12 000*g* for 15 min. at 4°C. The supernatant was harvested and the procedure was repeated to obtain proteins precipitated with 70 % ammonium sulfate as described above. The 30% and 70% ammonium sulfate protein pellets were each resuspended in 5 mL buffer A (50 mM

Tris, pH 8.0 / 10% glycerol / 1 mM DTT), and desalted using Sephadex G-25 resin (PD-10 column, GE Healthcare), to a final volume of 7 mL each. The protein concentrations of each fraction were determined using a protein assay kit (Bio-Rad, Mississauga, ON) (Bradford, 1976) via the microplate assay method (http://www.bio-rad.com/LifeScience/pdf/Bulletin_9004.pdf) using 4 concentrations of bovine serum albumin (BSA) to generate a linear standard curve.

2.7 Detection of native and recombinant protein by Western blot

Grape mesocarp and/or recombinant proteins were denatured for separation by sodium dodecyl sulfate-polyacrylamide gel electrophoresis (SDS-PAGE) and then transferred to a polyvinylidene fluoride (PVDF) membrane for immunological detection of VvsbAAT1 with antibodies raised against benzoyl-CoA:benzyl alcohol benzoyltransferase (D'Auria, Chen, & Pichersky, 2002). Protein solutions were diluted 1:1 in 2x SDS-PAGE sample buffer (100 mM Tris, pH 6.8 / 4% (w/v) SDS / 0.2% (w/v) bromophenol blue / 20% (v/v) glycerol / 200 mM DTT) (Sambrook & Russell, 2001) and heated to 95°C in a heat block for 5 min to denature the protein, then centrifuged at 10 000*g* for 2 min at room temperature to pellet any insoluble material. Samples and prestained protein standards (New England Biolabs, Pickering, ON) were loaded onto SDS-PAGE gels (4% stacking gel, 12% resolving gel) and electrophoresed at 80 V for 30 minutes followed by 120 V for 90 minutes. Gel casting and electrophoresis units were used according to the manufacturer's instructions (Tetra Cell, Bio-Rad, Mississauga, ON). Following electrophoresis, gels (along with PVDF membrane and filter paper) were equilibrated in transfer buffer (24 mM Tris base / 192 mM glycine / 15% methanol) for 20 minutes before assembly into the semi-dry transfer apparatus (Trans-Blot SD, Bio-

Rad, Mississauga, ON) according to manufacturer's instructions. The transfer conditions were 25 V, 100 mA, for one hour. After transfer, PVDF membranes were carefully tucked into 50-mL centrifuge tubes with their blotted surface exposed, and rinsed in 5 mL phosphate-buffered saline solution / 0.1% Tween-20 (PBS-T) (Sambrook & Russell, 2001) for 10 min. by rotating the centrifuge tubes (Roto-Torque, Cole-Parmer). The rinse solution was discarded and the membranes were exposed to blocking solution (PBS-T / 5% skim milk powder) for one hour. Blocking solution was discarded and membranes were rinsed with PBS-T for 3-x 10 minutes as above. Membranes were probed with either a rabbit:anti-BEBT primary antibody (raised against the benzoyl-CoA:benzyl alcohol benzoyltransferase protein from *Clarkia breweri*, previously shown to react with AMAT (Wang & De Luca, 2005)), used at a dilution of 1:500 for detection of native VvsbAAT1, or a rabbit:anti-His tag primary antibody (Santa Cruz Biotechnology Inc., Santa Cruz, CA, USA), used at a dilution of 1:2000 for detection of recombinant protein. Primary antibodies were diluted in PBS-T / 5% skim milk as described and incubated with rotation overnight at 4°C. After conjugation of VvsbAAT1 with primary antibody, solutions were discarded and again rinsed 3 times as above. Membranes were then incubated with rotation in a solution of secondary antibody (goat:anti-rabbit IRDye800, Rockland Immunochemicals Inc., Gilbertsville, PA, USA; 1:5000 in PBS-T / 5% skim milk) for one hour at room temperature. The secondary antibody solution was discarded, and the membrane was rinsed 2 x 8 min with PBS-T followed by 2 x 8 min with PBS. Proteins reacting to both primary and secondary antibody were detected using a fluorescence scanner (Odyssey® Infrared Imaging System, LI-COR, Lincoln, NB, USA) using the 800 channel.

2.8 Cloning of the full-length *VlAMAT*-like open reading frame for expression in *E. coli*

Based on the published *V. vinifera* genome sequence, two oligonucleotide primers were generated to amplify the full length open reading frame (ORF) of the *VlAMAT*-like gene *F6HBX5* from cDNA. These oligonucleotides also had restriction site adapters designed into them (5'-NcoI and 3'-XhoI) so the ORF could be ligated into the pET30b(+) vector expression system. The sequences of the primers were 5'-TTTCCATGGCATCATCGTCGT-3' (forward) and 5'-TTTCTCGAGGGGCATGGATGTAATT-3' (reverse). The PCR conditions used to amplify the full-length gene sequence from cDNA were as follows:

1. Initial denaturation at 94°C for 2 minutes,
2. then 5 cycles of
    a. 94°C for 30 seconds (denaturation)
    b. 50°C for 30 seconds (primer annealing)
    c. 72°C for 90 seconds (extension)
3. followed by 25 cycles of
    a. 94°C for 30 seconds (denaturation)
    b. 60°C for 30 seconds (primer annealing)
    c. 72°C for 90 seconds (extension)
4. and a final extension period of 72°C for 10 minutes

PCR products were cloned into the pGEM-T Easy vector system, transformed into *E. coli* XL-10 Gold cells, and sequenced (as above).

2.9 Mobilization of DNA fragments encoding ORFs into the expression vector

Using the alkaline lysis method, a midi-prep from a 50 mL culture volume was used to harvest plasmid from the XL-10 Gold strain (Maniatis, Fritsch, Sambrook, & Cold Spring Harbor Laboratory, 1982). Since sequence analysis revealed an internal NcoI restriction site in the ORF of the gene sequence, the full insert was released by partial restriction digestion (described below) from the pGEM-T Easy vector. Initial mobilization of the insert, ligation into pET30(b)+ vector, and sequencing indicated that 25 base pairs of contaminating pGEM-T Easy vector sequence had been carried over to the expression constructs, which necessitated a different mobilization strategy. PCR amplification of the ORFs by the high-fidelity Pfu polymerase (Fermentas), using cDNA as template was performed using the same oligonucleotides and thermal cycling conditions described above in Section 2.8. PCR products were purified using the QIAquick purification kit (QIAgen) according to the manufacturer's protocols. Purified PCR products containing full-length ORFs of *F6HBX5*-like gene products were then subjected to a partial restriction digest. Restriction enzymes (New England Biolabs, Pickering, ON) were used according to the manufacturer's protocols with slight modifications. Initial digestion with XhoI was performed for one hour to digest the PCR product at the 3'-end of the gene. Then, a 1 in 100 dilution (final concentration 200 U/mL) of NcoI restriction enzyme was added to the digestion and aliquots were left to incubate for 10, 20, or 30 minutes. Digests were inactivated by adding an appropriate amount of 10x DNA loading dye and placing the samples on ice. The entire volume of the digest was electrophoresed in 0.6% low-melting agarose (Sigma), and bands corresponding to the appropriate size of the full-length insert (1360 bp) were excised with

a scalpel for gel extraction (QIAgen gel extraction kit). Similarly, purified pET30b(+) vector was fully digested with NcoI and XhoI restriction enzymes, and the vector backbone was gel extracted. The purified insert and vector backbone were ligated using T4 DNA ligase according to the manufacturers protocol (Fermentas, http://www.fermentas.com/templates/files/tiny_mce/coa_pdf/coa_el0011.pdf), and transformed into XL-10 Gold *E. coli* competent cells. Positive colonies (selected by blue/white screening and colony PCR) were used to prepare a midi-prep of plasmid (as above) that was used to transform the *E. coli* expression strain BL21 (DE3).

2.10 Expression and purification of recombinant VvsbAAT1 protein in *E. coli*

Optimal culture conditions to produce soluble recombinant protein had to be determined empirically. A single colony from a streak plate was inoculated into 3 mL LB media containing 50 μg/mL kanamycin, and grown overnight (12-16 hours) at 37°C, 250 rpm. This culture was used to inoculate 500 mL of fresh media and was grown at 37°C, 250 rpm until an OD_{600} of 0.4 to 0.6 was reached. At this time, protein expression was induced with 0.4 mM of isopropyl β-D-1-thiogalactopyranoside (IPTG) by growing the cultures at 20°C, 200 rpm for 20 h. Bacteria harvested by centrifugation at 7250*g* for 10 minutes at 4°C were either lysed immediately to purify protein or were stored at -20°C until needed.

His6-tagged protein purification was accomplished by immobilized metal-ion affinity chromatography (IMAC) using Ni-NTA resin (QIAgen). Bacterial pellets were resuspended in 12 mL lysis/wash buffer (50 mM Tris, pH 8.0 / 500 mM NaCl / 20 mM imidazole) and sonicated on full power (Fisher Sonic Dismembrator Model 100) in bursts of 5 seconds with 5 second cooling periods in between, for a total of 10 cycles.

Following centrifugation of insoluble material (7250*g* for 10 minutes at 4°C), 1 mL of Ni-NTA resin was added to the supernatant in a 15-mL centrifuge tube and rotated (Roto-Torque, Cole-Parmer) for 1 hour at 8°C to bind His6-tagged proteins. The supernatant ("flow-through") was aspirated by pipette after allowing the Ni-NTA resin to settle on ice, and then washed 5 times with 1 mL of lysis/wash buffer. Bound proteins were eluted from the resin with 2.5 mL elution buffer (50 mM Tris, pH 8.0 / 500 mM NaCl / 500 mM imidazole) on the Roto-torque for 15 min at 8°C. The eluate containing His6-tagged VvsbAAT1 protein was immediately desalted using Sephadex G-25 (PD-10 column, GE Healthcare) pre-equilibrated with 50 mM Tris, pH 8.0 / 1 mM DTT, 10% glycerol to give a final volume of 3.5 mL. Production of the recombinant protein and its purification was monitored by analyzing fractions by Western blotting with anti-His-probe antibody (Santa Cruz Biotechnology, Santa Cruz, CA).

2.11 Enzymatic synthesis of radiolabeled coenzyme-A substrates

Radiolabeled Coenzyme A substrates were enzymatically synthesized using benzoyl-CoA ligase (BZL) from *Rhodopseudomonas palustris* (T. Beuerle & Pichersky, 2002; Egland, Gibson, & Harwood, 1995). The recombinant enzyme is C-terminally His6-tagged, and was purified as described above in section 2.9 for the recombinant VvsbAAT1. In a 1.5 mL microfuge tube, the enzymatic reaction conditions for synthesis of the Coenzyme A thioesters were 100 mM Tris, pH 8.5, 6.7 mM ATP, 6.1 mM coenzyme A, 10 μCi of either [ring-^{14}C] benzoic acid or [ring-^{14}C] anthranilic acid, and 100 μg of purified BZL in a final volume of 500 μL. The reaction was initiated by the addition of enzyme and allowed to proceed for 4 h at room temperature, monitored by hourly sampling, and was stopped by the addition of 75 μL 6 N HCl. Contents of the

microfuge tube were extracted 3 times with 350 µL of diethyl ether to remove unreacted radiolabeled acids, and the aqueous phase was subjected to solid phase extraction using a Sep-Pak C18 cartridge as described by the manufacturer (Waters, Mississauga, ON). The time course of radiolabeled CoA substrates was monitored by liquid scintillation counting of the aqueous layer and by thin-layer chromatography (TLC). TLC samples were applied to Polygram Sil G/UV silica gel sheets (Macherey-Nagel, Germany) and developed with the solvent system 1-butanol / water / glacial acetic acid (65:35:25) (Beuerle & Pichersky, 2002). After an overnight exposure to a storage phosphor screen (GE Healthcare), radioactive products were visualized using a Fuji FLA3000 phosphorimager.

2.12 Enzyme assays

Acyltransferase activity was tested using radiolabeled acetyl-CoA, benzoyl-CoA, and anthraniloyl-CoA substrates and alcohols using radioactive enzyme assays. Successful detection of radioactive products led to the development of unlabelled enzyme assays whose products were detected by gas chromatography-mass spectrometry (GC-MS).

2.12.1 Assays using radiolabeled substrates

In a 1.5 mL microfuge tube, 10 µL of 100 mM of an alcohol to be tested, 10 µL of radiolabeled acyl-coenzyme A substrate, 60 µg protein, 20 µL 5x assay buffer (250 mM Tris, pH 7.5), and Milli-Q water up to 100 µL were mixed. The reaction was started by addition of the protein, and incubated at room temperature for 2 hours. Reactions were terminated by adding 5 µL 6 M HCl followed by extraction with 350 µL ethyl acetate.

Tubes were briefly vortexed and centrifuged for 2 minutes at 10 000*g* to separate the organic and aqueous layers, and 300 µL of the top, organic (ethyl acetate) layer was transferred to a fresh tube, of which 50 µL was then mixed with 5 mL scintillation cocktail (ScintiSafe™ Econo 2, Fisher Scientific, Ottawa, ON) for counting using a scintillation counter (LS6500, Beckman Coulter). The remaining 250 µL was dried down in a Speedvac (Thermo-Fisher) to a dry residue that was dissolved in 10 µL methanol and applied to silica gel sheets (Polygram Sil G/UV, Macherey-Nagel, Germany) for thin layer chromatography. For assays utilizing [^{14}C]acetyl-CoA as substrate, TLC plates were developed in benzene until the solvent front was approximately 1 cm from the top edge of the plate, and for assays utilizing either [ring-^{14}C]benzoyl-CoA or [ring-^{14}C]anthraniloyl-CoA TLC plates were developed using 2:1 petroleum ether:ether as the solvent system in a similar manner as described above. After developing and drying the plates (in a fume hood at room temperature), they were exposed overnight (or longer as necessary) to phosphorscreens and radioactive spots were visualized using the phosphorimager (Fuji FLA3000).

2.12.2 Assays using non-radiolabeled substrates

Enzyme assays using non-radiolabeled substrates (aliphatic CoA thioesters such as acetyl-CoA, butyryl-CoA, hexanoyl-CoA and octanoyl-CoA) were measured using gas chromatography-mass spectrometry to detect reaction products, based on a method used to measure acetyl-CoA:benzylalcohol acetyltransferase (BEAT) activity (Dudareva, D'Auria, Nam, Raguso, & Pichersky, 1998). Assays contained 200 µL of 5x assay buffer (250 mM Tris, pH 7.5 / 15 mM β-mercaptoethanol), 5 µL of 100 mM acyl-coenzyme A, 10 µL of 1 M alcohol, 150 µL protein, and Milli-Q water was added to make a 1000 µL

reaction volume. The reaction was initiated by the addition of protein and allowed to proceed for one hour at room temperature. The assay mixture was then extracted with an equal volume of hexane by brief vortexing followed by centrifugation at 10 000*g* for 2 min at room temperature to separate the phases. The top, organic layer (about 800 µL) was removed by pipette to a fresh 1.5 mL centrifuge tube, of which 200 µL was removed to a 2-mL glass GC vial containing a 250-µL vial insert (Agilent Technologies Canada Inc., Mississauga, ON), then immediately capped and crimped to seal the vial. The GC-MS system (Perkin Elmer AutoSystem XL gas chromatograph with TurboMass Gold mass spectrometer), equipped with an autosampler, was programmed to inject 2 µL of sample into the injection port held at 220°C. The column (VF-WAX ms, Varian Inc.) was heated according to the following oven program: hold at 50°C for 1 min, then ramp at 7.0°C/min to 245°C, and hold for 10 min. The mass spectrometer acquired data under the following conditions: after a 2 min solvent delay, total ion scans were initiated in EI+ ionization mode, from $m/z = 30$ to $m/z = 350$ at 2.5 scans per second. Total ion counts and masses were called by the software according to the NIST databases (NIST 98) installed in the system, and retention times were compared to authentic standards when available. Once the *cis*-3-hexenyl acetate product was confirmed by authentic standard, the mass spectrometer was programmed to acquire data in selected ion recording (SIR) mode, monitoring the ions $m/z = 41$, 43, 67, and 82.

2.13 Developmental expression analysis of *VvsbAAT1*

To create a profile of *VvsbAAT1* gene and protein expression over the growing season, plant samples were harvested at regular intervals that included flowers as well as grapes collected at different stages of development. Samples were subjected to RT-PCR

analysis as described above in section 2.3 with the *VvsbAAT1* gene-specific primer set 5'-CCAGGATACTATGGAAATGC-3' (forward) and 5'-GGATGTAATTAACAGC TCTGC-3' (reverse), along with the *Actin* primer set 5'-CTGAGAGGGGTTACA TGTTC-3' (forward) and 5'-CAGGCAGCTCATAGTTCTTC-3' (reverse).

2.14 Site-directed mutagenesis of VvsbAAT1

Site-directed mutagenesis was performed based on Agilent's Quikchange II method. Primers were initially designed using the Quikchange Primer Design Tool (www.genomics.agilent.com), then trimmed to 25 base pairs manually. The sequence of the sense primer was 5'-CTAAACCACACAATGTCTGATGCAG-3', and the antisense was the reverse complement, 5'-CTGCATCAGACATTGTGTGGTTTAG-3'. The reaction was set up as follows: 5 µL 10x PCR buffer (Fermentas 10x Pfu buffer +$MgSO_4$), 1 µL 10 mM dNTP's (Takara), 1 µL of each primer (125 ng/µL each), 1 µL Pfu polymerase (Fermentas), 1 µL of 300 ng/µL plasmid (VvsbAAT1 in pET30b) and 40 µL Milli-Q water. The thermocycler was programmed for initial denaturation at 94°C for 30 s, followed by 12 cycles of: [94°C for 30 s, 55°C for 60 s, 68°C for 420 s].

PCR products were subjected to restriction enzyme digestion with DpnI for 2 hours at 37°C, which digests methylated, parental plasmid but not the newly synthesized, mutated plasmid. Two µL of the mutagenized plasmid was transformed into competent *E. coli* XL-10 Gold cells by heat shock transformation, plated onto selective media (LB plus 50 µg/mL kanamycin) and incubated overnight at 37°C. Six colonies were selected from this plate, cultured overnight, and plasmids were purified using Qiagen's QIAPrep Spin Column according to their protocols. The resulting pure plasmid was sent to Bio Basic Inc. (Markham, ON) for Sanger sequencing to confirm successful mutagenesis.

Chapter 3. Results

3.1 The *Vitis vinifera* genome encodes 51 putative BAHD-like acyltransferases.

Bioinformatic analysis (see Materials and Methods 2.3) of the *Vitis vinifera* predicted proteome revealed the presence of at least 51 putative BAHD-like acyltransferase sequences. Phylogenetic analysis of *Vitis* BAHD-like sequences compared with 5 representative biochemically characterized BAHD acyltransferases showed their organization into at least 5 clades (Figure 3.1) that make up this family of genes. Remarkably, 26 out of 51 *V. vinifera* candidate acyltransferases align in clades predominantly involved in the biosynthesis of volatile esters (Figure 3.1). Of these 26, 5 occurred in clade II, and 21 occurred in clade III. The remaining 25 candidates fell into clade I (6 members) and clade IV (5 members), while the 14 remaining members were not grouped into any previously described clade. A set of 5 putative alcohol acyltransferases (AATs) (F6HBX5, D7U3X7, F6I088, D7U3X1, F6I087) in clade III aligned closely with VlAMAT (Figure 3.2), where they shared 86 to 95% amino acid sequence identity.

3.2 RT-PCR based identification of *VlAMAT*-like transcripts in *V. vinifera*

To determine whether or not any of the 5 highly similar *VlAMAT*-like genes were being expressed in *V. vinifera*, their extensive nucleotide sequence similarities (Figure 3.3) were used to design a single set of primers that would potentially identify any of these gene products in different varieties of *V. vinifera* (Table 3.1). Ripe berries were selected for analysis since *VlAMAT* transcript levels and enzyme activity rose throughout fruit ripening and peaked when the fruit was ripe in *V. labrusca* (Wang & De Luca, 2005)

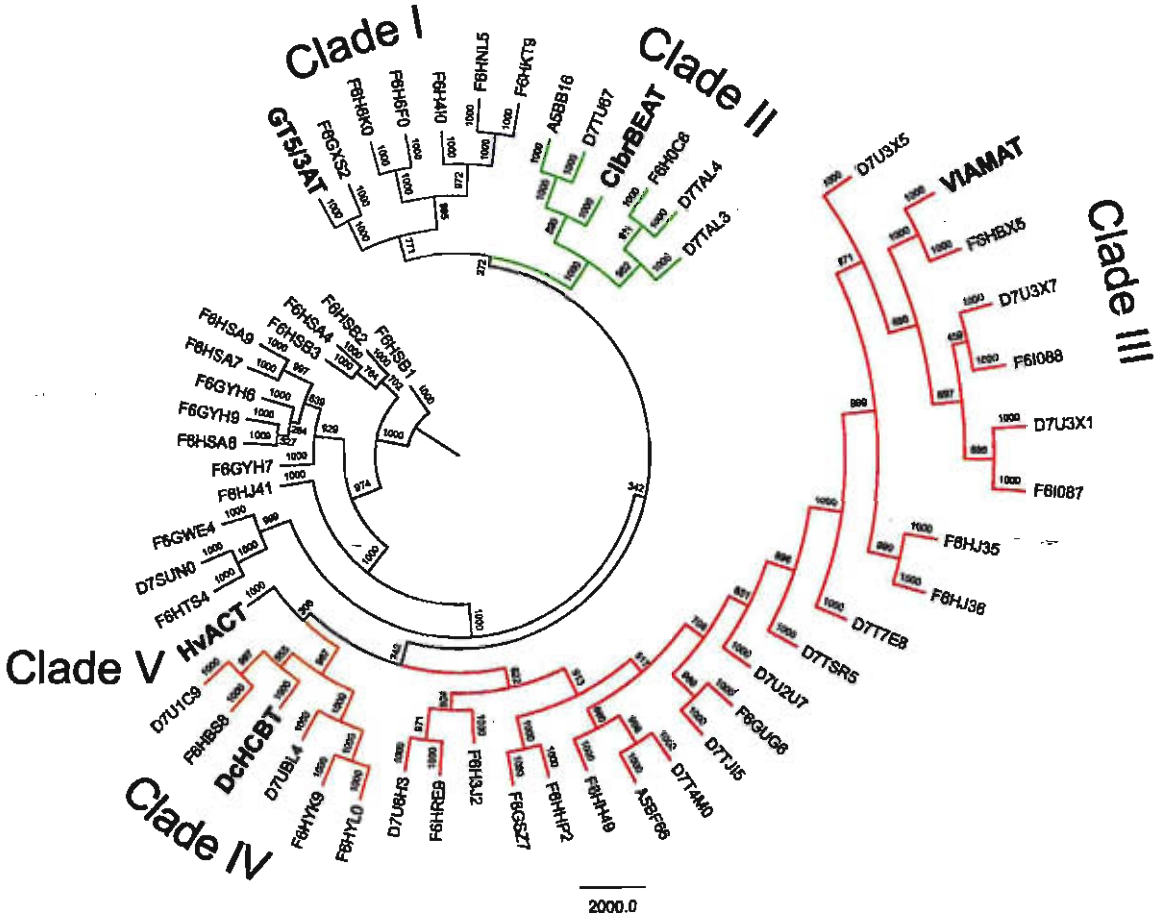

Figure 3.1: Unrooted phylogenetic tree of 51 putative BAHD-like acyltransferases from *V. vinifera*. A search of the *V. vinifera* Pinot Noir genome database for BAHD-like acyltransferases (see Materials and Methods, section 2.14) yielded 51 putative candidates. Included are 5 biochemically characterized BAHD acyltransferases (in bold with large font, Gt5/3'AT (*Gentiana triflora* anthocyanin 5/3' aromatic acyltransferase, Q9ZWR8) from clade I, ClbrBEAT (*Clarkia breweri* acetyl-CoA: benzyl alcohol acetyltransferase, AAC18062) from clade II, VlAMAT (*Vitis labrusca* anthraniloyl-CoA: methanol anthraniloyltransferase, AAW22989) from clade III, DcHCBT (*Dianthus caryophyllus* *N*-hydroxycinnamoyl/benzoyl-CoA: anthranilate *N*-hydroxycinnamoyl/benzoyltransferase, CAB11466) from clade IV, and HvACT (*Hordeum vulgare* agmatine coumaroyltransferase, AAO73071) from clade V) representing each of the 5 clades as described in Figure 1.3. The numbers at each branch indicate confidence levels from 1000 bootstrap replicates.

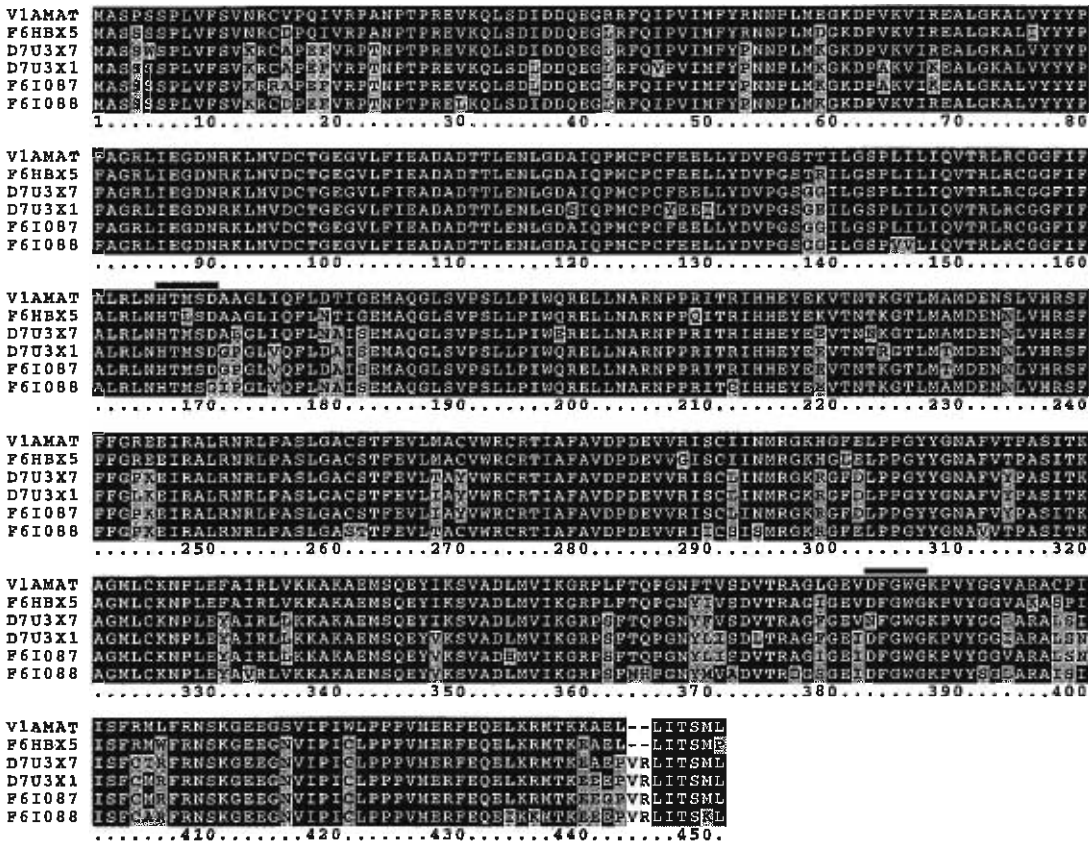

Figure 3.2: Multiple sequence alignment of VlAMAT amino acid sequence with 5 predicted VlAMAT-like amino acid sequences from *V. vinifera*. Black bars above the sequences denote the HXXXD and DFGWG motifs, conserved among the BAHD acyltransferases.

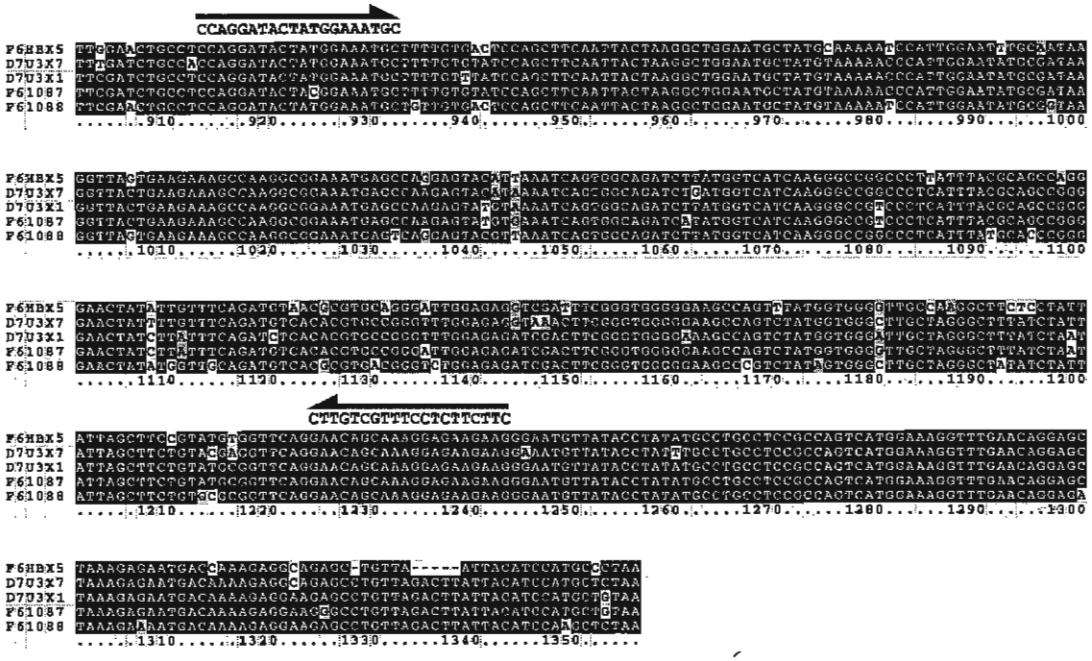

Figure 3.3: Multiple sequence alignment of a fragment of 5 predicted *VlAMAT*-like gene sequences. Arrows pointing to the right and left above the sequence data indicate conserved regions that were used to design forward and reverse oligonucleotides (also indicated by text) to identify any of the 5 most conserved putative *VvAATs* (*F6HBX5, D7U3X7, D7U3X1, F61087, F61088*).

Table 3.1: *V. vinifera* berry varieties were harvested from Chateau des Charmes Winery (1), Vineland Research and Innovation Center (2) and from Five Rows Craft Winery (3), respectively.

#	Variety	Location	#	Variety	Location
1	Chardonnay Musqué	1	**10**	Chardonnay (cultivar 2)	1
2	Aligoté	1	**11**	Vidal	1
3	Cabernet Franc	1	**12**	Gewürztraminer	1
4	Shiraz (cultivar 1)	3	**13**	Cabernet Sauvignon	1
5	Grand Noir	1	**14**	Muscat du Moulin	2
6	Chardonnay (cultivar 1)	1	**15**	Muscat Blanc	2
7	Auxerrois	1	**16**	Pinot Noir	3
8	Shiraz (cultivar 2)	3	**17**	Riesling	1
9	Sauvignon Blanc	1	**18**	Viognier	3
			19	Merlot	1

as well as for other AATs in other fruit species (González et al., 2009; Ban, Oyama-Okubo, Honda, Nakayama, & Moriguchi, 2010; El-Sharkawy et al., 2005). The RT-PCR analyses suggested that most *V. vinifera* varieties tested express one or more *VlAMAT*-like AATs (Figure 3.4).

Successful detection of *VlAMAT*-like transcripts in *V. vinifera* led to the development of another primer set that was designed to detect a properly processed *F6HBX5* transcript (the accession number of the predicted mRNA sequence with highest identity to *VlAMAT*, see Figure 3.2) by flanking the region of the intron, so that a 250 base pair (bp) PCR product would be amplified from cDNA transcribed from processed mRNA, whereas a 941 bp PCR product would be amplified from any non-spliced transcripts or genomic DNA contamination present in the RNA preparation. RT-PCR performed with this primer set confirmed the presence of processed *VlAMAT*-like transcripts in other varieties of *V. vinifera* (Figure 3.4 B). Interestingly, a slightly larger PCR product (approximately 300 bp) could be seen either exclusively in one variety (Figure 3.4 B, Muscat du Moulin) or in combination with the 250 bp product (Figure 3.4 B, Muscat Blanc and Riesling) with this primer set. An *in silico* screening of the predicted mRNA sequences of all the putative alcohol acyltransferases in *V. vinifera* (i.e. 21 sequences in clade III plus 5 sequences in clade II, see Figure 3.1) for motifs that showed 75% or higher sequence similarity to the primer set yielded no potential sources for this PCR product (data not shown). It is possible that the source is one of the remaining 25 predicted BAHD-like acyltransferases, but this PCR product would need to be sequenced to confirm this hypothesis.

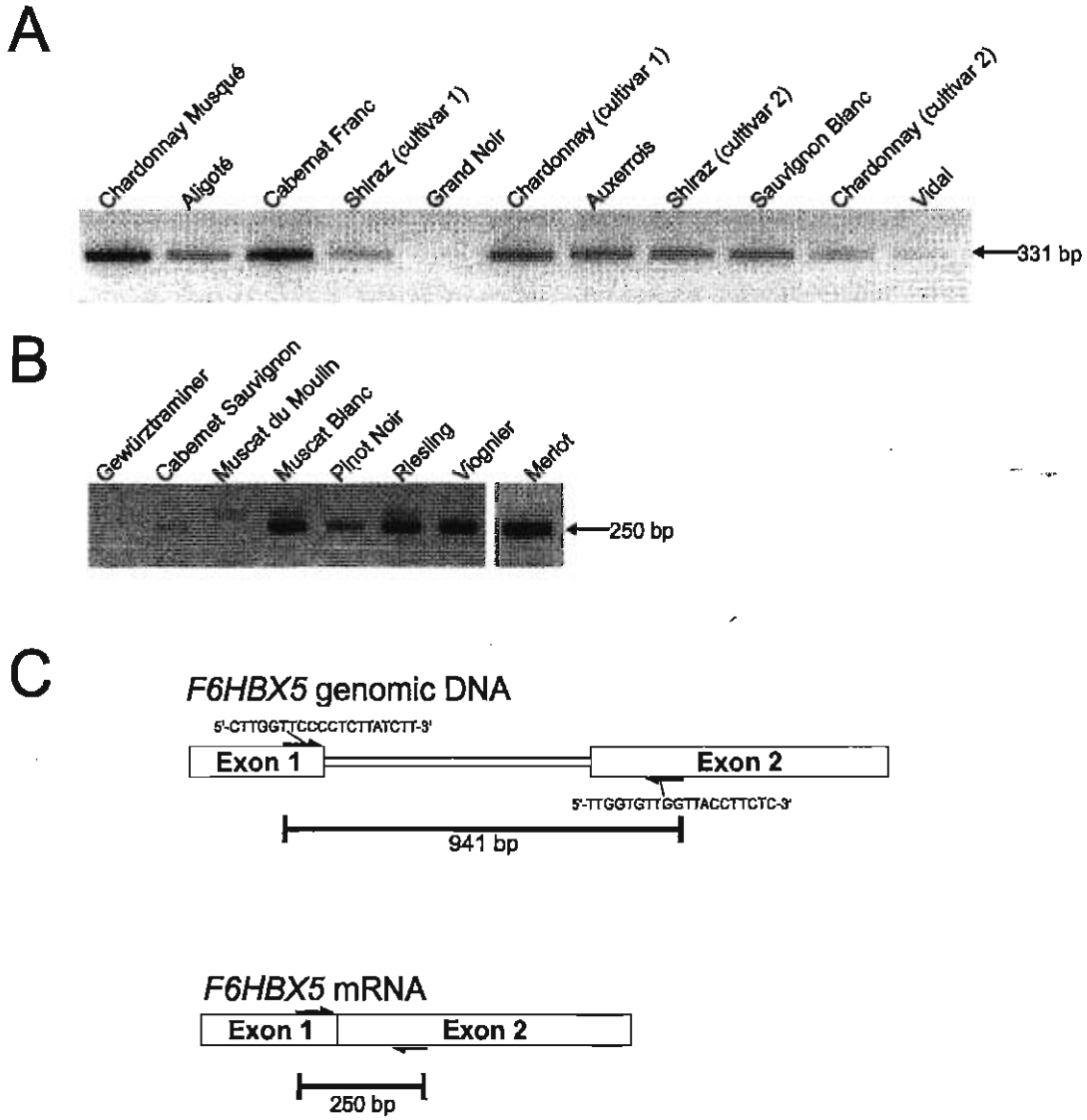

Figure 3.4: RT-PCR based identification of *VlAMAT*-like transcripts in *V. vinifera*. A: A primer set designed to amplify a 331 bp fragment from a conserved region of any of 5 *VlAMAT*-like transcripts in *V. vinifera* (described in Figure 3.2) suggest many varieties express putative alcohol acyltransferases. B: A primer set flanking the intron of the *F6HBX5* gene sequence (the putative alcohol acyltransferase most identical to *VlAMAT*) produced RT-PCR products whose size is consistent with a processed transcript. C: Cartoon of *F6HBX5* genetic sequences illustrating the primer set (arrows) used in B.

The 331 bp PCR products from the varieties Chardonnay Musqué, Cabernet Franc, Shiraz, and Sauvignon Blanc (Figure 3.4 A) were (randomly) selected for sequencing (Materials and Methods, Section 2.5), and the results indicate that multiple alcohol acyltransferases are being expressed in these varieties (Figure 3.5). The sequence of the *VlAMAT*-like RT-PCR product obtained from Chardonnay Musqué was 99% identical to *F6HBX5* (Figure 3.5 B). The sequence from Cabernet Franc was 97% identical to *VvD7U3X7*, while the sequence obtained from Sauvignon Blanc was 100% identical to *VvD7U3X1*. The sequencing reaction for the PCR product cloned from Shiraz failed, and this clone was not further characterized.

These varieties (Chardonnay Musqué, Cabernet Franç, Shiraz, and Sauvignon Blanc) were then selected to clone each respective full-length cDNA of the putative alcohol acyltransferases being expressed.

3.3 Isolation of *VlAMAT*-like cDNAs from *V. vinifera* varieties Chardonnay Musqué, Cabernet Franc, Shiraz, and Sauvignon Blanc.

In order to characterize the putative VlAMAT-like protein of *V. vinifera*, a primer set was developed to clone the full-length open reading frame of *F6HBX5* from cDNA for heterologous expression in *E. coli*. The primers were designed to incorporate an NcoI restriction site at the 5'-end and an XhoI restriction site at the 3'-end for subcloning into the pET-30(b)+ expression vector system (EMD) (Figure 3.6 A). This strategy produced PCR products of the appropriate size expected for the full length open reading frames (1361 bp, see Figure 3.6 B) using cDNA prepared from Chardonnay Musqué, Cabernet Franc, Shiraz, and Sauvignon Blanc berries. The PCR products were ligated into the TA-

A

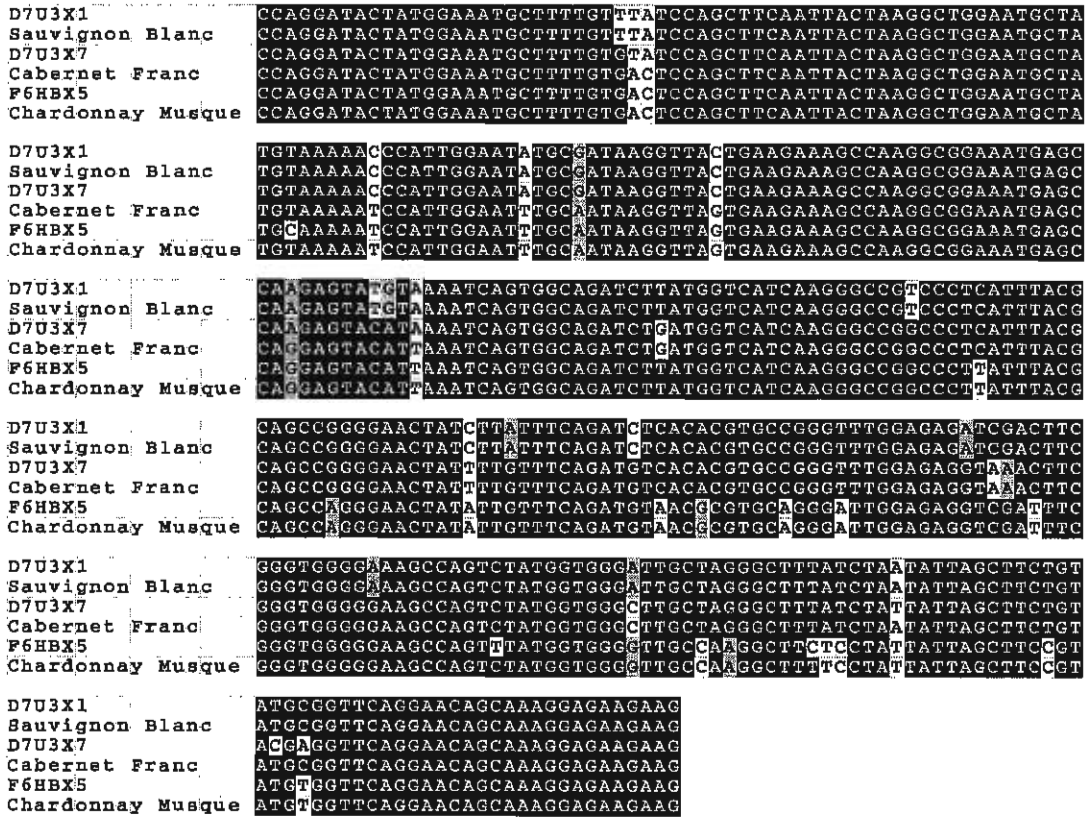

B

	F6HBX5	Chardonnay Musqué	Cabernet Franc	D7U3X1	Sauvignon Blanc	D7U3X7
F6HBX5	----					
Chardonnay Musqué	99.1	----				
Cabernet Franc	93.4	94.3	----			
D7U3X1	89.4	90.3	93.7	----		
Sauvignon Blanc	89.4	90.3	93.7	100.0	----	
D7U3X7	90.9	91.8	96.7	95.2	95.2	----

Figure 3.5: Sequence analysis of RT-PCR derived 331 bp *VIAMAT*-like transcripts in *V. vinifera*. Multiple sequence alignment (A) and computed identity matrix (B) of RT-PCR products obtained from ripe berries of Chardonnay Musqué, Cabernet Franc, and Sauvignon Blanc (Figure 3.4 A) along with predicted *VIAMAT*-like sequences from the Pinot Noir genome database (*F6HBX5*, *D7U3X1*, *D7U3X7*).

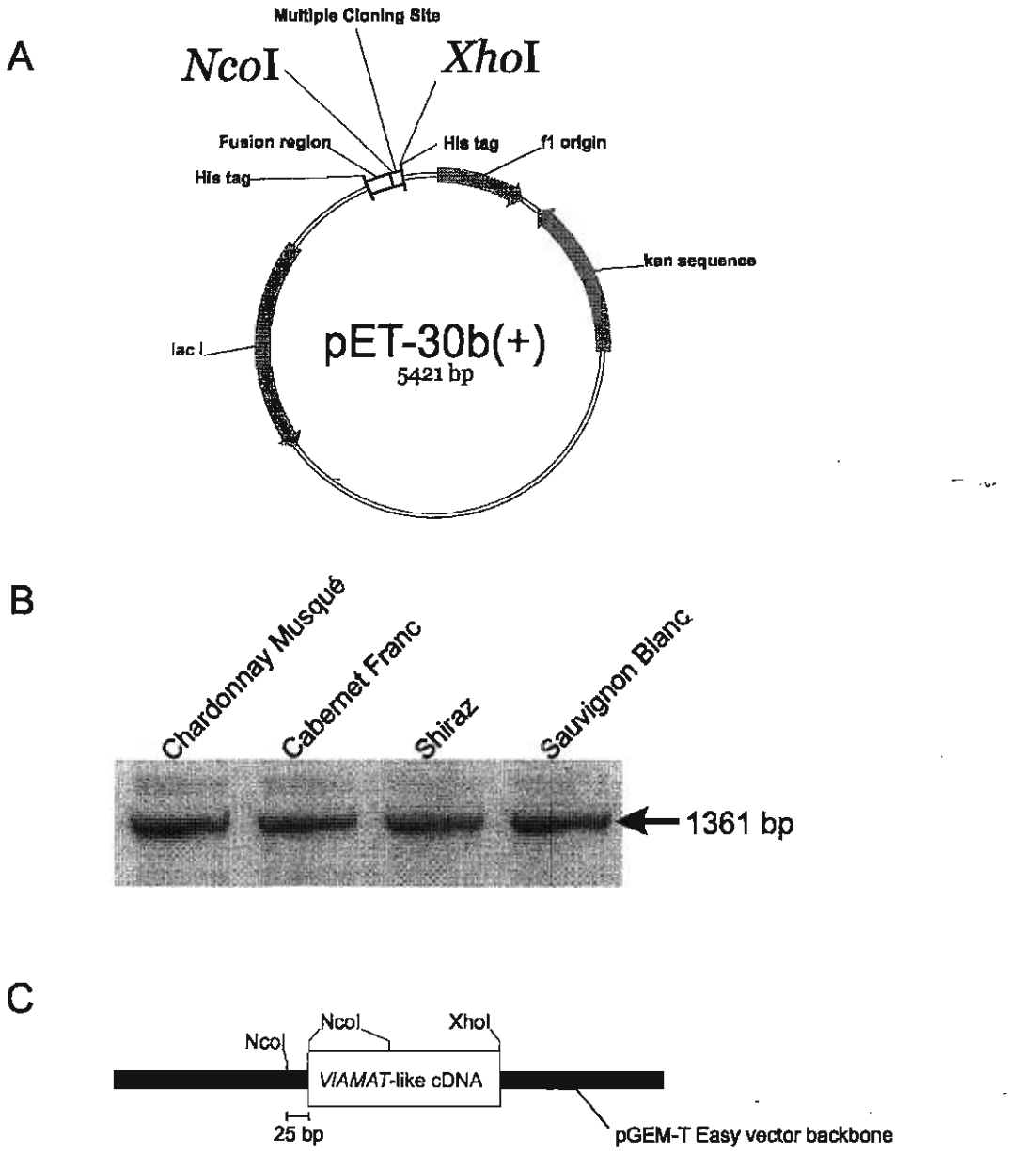

Figure 3.6: Cloning of *VlAMAT*-like cDNAs from different *Vitis vinifera* cultivars (Chardonnay Musqué, Cabernet Franc, Shiraz, and Sauvignon Blanc). The primers (5'-TTTCCATGGCATCATCGTCGT-3', forward & 5'-TTTCTCGAGGGGCATGGATGTAATT-3', reverse) derived from *F6HBX5* found in the Pinot Noir genome database were used to perform RT-PCR using RNA extracted from whole mature berries (minus seeds) of different grape cultivars. A: Diagram of the pET-30(b)+ expression vector. B: 1361 bp full-length cDNAs including 5'-NcoI and 3'-XhoI restriction sites at each end. C: Cartoon of *VlAMAT*-like cDNA in the pGEM-T Easy TA cloning vector (not to scale), indicating 25 bp of vector sequence that carried over to the pET-30(b)+ expression construct rendering it unusable.

cloning vector pGEM-T Easy (Promega) to harbour the full length *AAT* coding sequences for sequencing and subcloning purposes. However, mobilization of the full-length cDNAs via restriction digestion was unsuccessful due to the presence of a 25 bp upstream endogenous (pGEM-T Easy vector-based) NcoI restriction site (Figure 3.6 C), which seemed to be preferentially digested compared to the 5'-NcoI restriction site at the start of the *VlAMAT*-like coding sequence. This resulted in the carryover of contaminating vector sequence upstream of the *VlAMAT*-like coding sequence in the final expression construct in pET-30(b)+ (data not shown), rendering it useless for expression of functional protein. To solve this problem, proper coding sequences were produced by direct digestion of the PCR products produced by a high-fidelity Pfu polymerase amplification from each pGEM-T Easy clone. Since the predicted full length sequence of *F6HBX5* also has an internal NcoI restriction site (see Figure 3.6 C), a partial restriction digest of the PCR product was needed to create a population of intact coding sequences that were not digested internally as well. Appropriate digestion conditions were determined by modification of the concentration of restriction enzyme and time of digestion, and the full length digested product was purified via agarose gel electrophoresis (Figure 3.7). The purified full length *F6HBX5* coding sequence was then ligated into a similarly prepared pET-30(b)+ backbone and transformed into *E. coli* for protein expression.

3.4 Heterologous expression of Chardonnay Musqué, Cabernet Franc, Shiraz, and Sauvignon Blanc putative alcohol acyltransferases (*AAT*s) in *E. coli*

The cDNAs encoding the open reading frames for putative alcohol acyltransferases from Chardonnay Musqué, Cabernet Franc, Shiraz, and Sauvignon Blanc were each

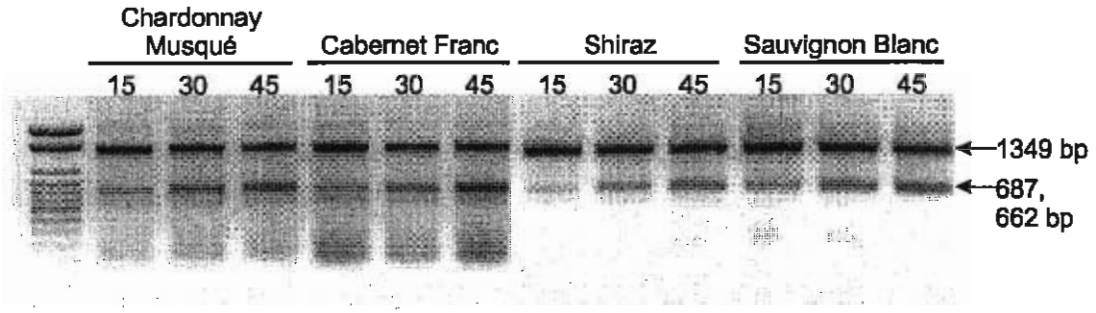

Figure 3.7: Agarose gel electrophoresis of a time course (min) partial digestion of *VlAMAT*-like PCR products with catalytic levels of *Nco*I. The presence of a common *Nco*I restriction site in the 4 PCR products of the 4 varieties of *V. vinifera* required partial restriction digestion in order to isolate sufficient amounts of the 1349 bp fragment for cloning into NcoI-XhoI restriction sites of pET30(b)+ expression vector. After digestion for 45 min, fragments (1349 bp) representing the ORF of each gene were excised from the agarose gel and purified for ligation into the expression vector. Numbers under the variety names indicate the length of the partial digest treatment, in minutes.

mobilized into a pET30(b)+ expression vector and expressed in *E. coli.* Recombinant protein from each *E. coli* extract expressing each protein were submitted to SDS-PAGE analysis and only the clone from Sauvignon Blanc appeared to expressed a full length 56 kDa fusion protein (Figure 3.8 A), while the Cabernet Franc, Chardonnay Musqué, and Shiraz clones all expressed an unexpectedly smaller 21 kDa fusion protein (Figure 3.8 B, C, and D). These results prompted a re-investigation of the sequences obtained from each variety. Sequencing of the 4 clones showed that in contrast to the Sauvignon Blanc clone, the deletion of a thymine residue in the Chardonnay Musqué, Cabernet Franc, and Shiraz clones caused a frameshift mutation that introduced an early stop codon (Figure 3.9) that should produce a putative truncated 21 kDa protein that was observed on the SDS-PAGE gels (Figure 3.8). The full-length open reading frame sequences isolated from Chardonnay Musqué, Cabernet Franc, and Shiraz were 100% identical to each other. These three sequences shared 99.6% identity compared to the one isolated from Sauvignon Blanc, and together the 4 clones isolated from Chardonnay Musqué, Cabernet Franc, Shiraz, and Sauvignon Blanc shared 99.0% identity to the *F6HBX5* sequence recorded in the Pinot Noir genome. While these truncated products were not considered further, the Sauvignon Blanc *VlAMAT*-like gene product, designated *Vitis vinifera* Sauvignon Blanc alcohol acyltransferase 1 (*VvsbAAT1*) was used for further analysis. Initial expression analysis of the recombinant protein by SDS-PAGE suggested that most if not all of VvsbAAT1 was retained in the insoluble fraction (Figure 3.10 A). By lowering the temperature of the expression cultures to 20 °C and reducing the concentration of IPTG to 200 or 400 μM, it was possible to produce some

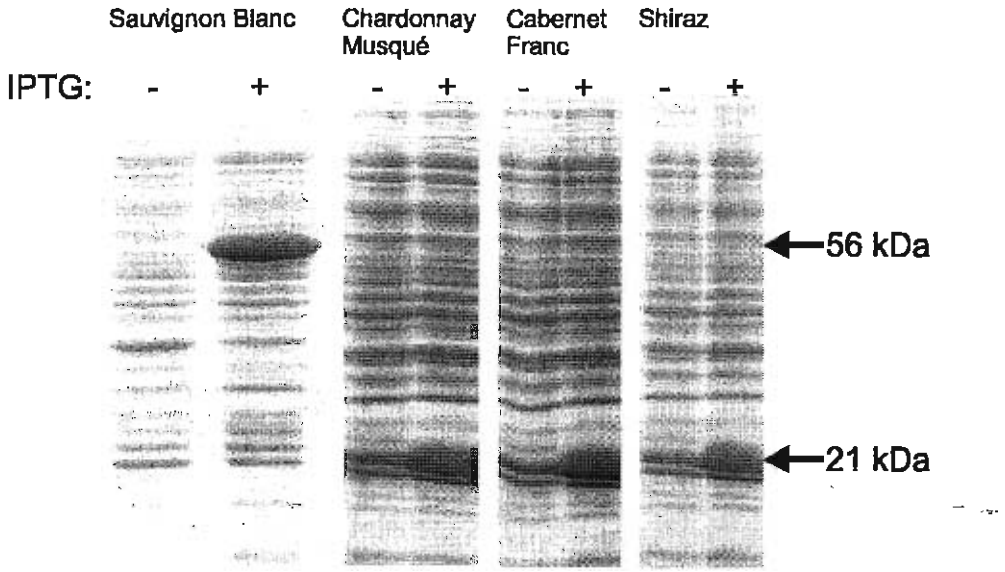

Figure 3.8: Expression of Sauvignon Blanc, Cabernet Franc, Chardonnay Musqué and Shiraz VlAMAT-like genes in *E. coli.* Protein extracts from each expression culture (minus (-) or plus (+) IPTG) were submitted to SDS-PAGE and proteins were visualized by commassie staining.

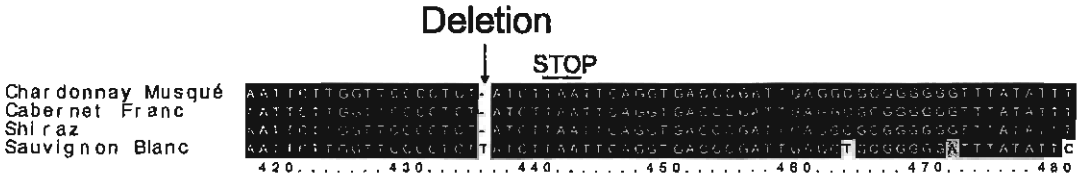

Figure 3.9: Identification of a stop codon in Chardonnay Musqué, Cabernet Franc, and Shiraz. Sequencing the *AMAT*-like expression constructs shows that the deletion of a thymine at position 435 in the gene sequences of Chardonnay Musqué, Cabernet Franc, and Shiraz introduced an early stop codon 5 bases later at position 440 (bar above TAA), resulting in the truncated protein products described in Figure 3.8.

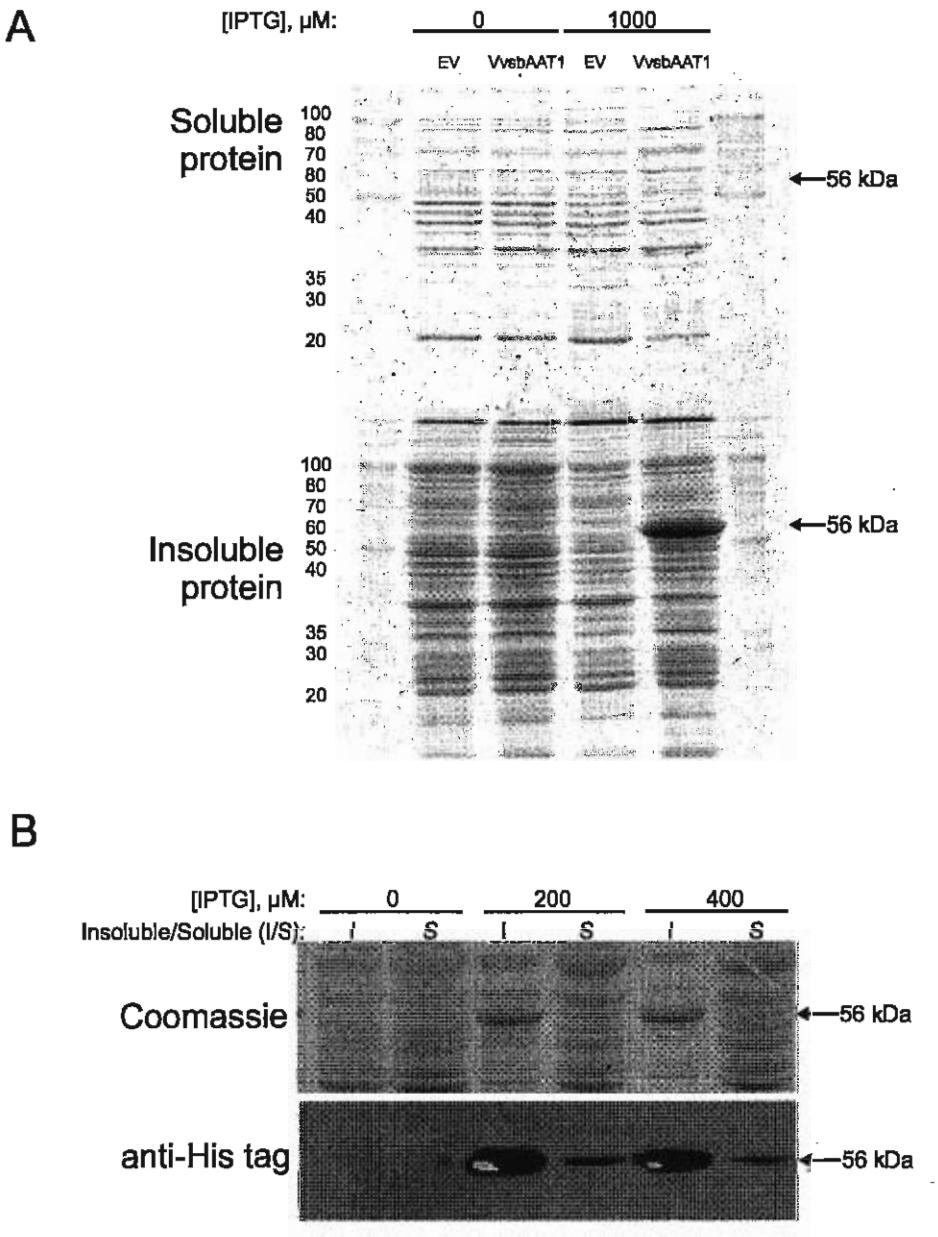

Figure 3.10: Expression of His-tagged Sauvignon blanc VIAMAT-like protein (VvsbAAT1, 56 kDa) in *E. coli* appears mostly as insoluble inclusion bodies. A: Each expression culture (± IPTG) and cultures with empty pET-30(b)+ vector (EV) were grown at 37 °C, extracted for soluble and insoluble protein, submitted to SDS-PAGE and gels were stained with Coomassie blue. B: His-tagged VvsbAAT1 was expressed in *E. coli* (+ 0, 200, or 400 µM IPTG) at lower temperature (20°C) and each expression culture was extracted for soluble and insoluble protein. Protein extracts were submitted to SDS-PAGE followed either by Coomassie staining or electrophoretic transfer of proteins to PVDF membranes and immunoblotting using an anti-His-tag antibody.

soluble protein (Figure 3.10 B), although the bulk of the recombinant protein remained in the insoluble fraction.

3.5 Partial purification of His6-tagged recombinant VvsbAAT1

Once established (Figure 3.10B), the conditions to produce soluble recombinant VvsbAAT1 in *E. coli* expression cultures were scaled up in order to produce enough soluble protein for enzyme assays. Lysates from expression culture pellets harbouring either a pET30(b)+ empty vector (as a negative control) or the pET30(b)+-*VvsbAAT1* expression construct were applied to immobilized metal-ion affinity chromatography (IMAC) columns to purify the His6-tagged proteins. Analysis in duplicate by SDS-PAGE followed by either Coomassie staining (Figure 3.11 A) or by electrophoretic transfer of proteins to PVDF membrane followed by detection with anti-His antibody (Figure 3.11 B) showed that the recombinant His6-tagged VvsbAAT1 protein (56 kDa) could be partially purified by the immobilized metal-ion affinity column, along with a few other non-specific *E. coli* proteins (Figure 3.11 A), which has been observed with this method (Müller, Arndt, Bauer, & Plückthun, 1998). While more intense bands of the recombinant His6-tagged VvsbAAT1 protein can be seen throughout successive steps of the purification procedure, no such bands reacting with the anti-His antibody can be seen in *E. coli* extracts expressing empty vector (Figure 3.11 B).

3.6 Gas chromatographic profile of ripe Sauvignou Blanc berries

Ripe Sauvignon Blanc berries accumulate a variety of alcohols and volatile esters (Chaudhary, Kepner, & Webb, 1964) (Figure 3.12). The 2- to 6-carbon aliphatic alcohols such as ethanol, isoamyl alcohol, 2-methyl-1-butanol and hexanol as well as

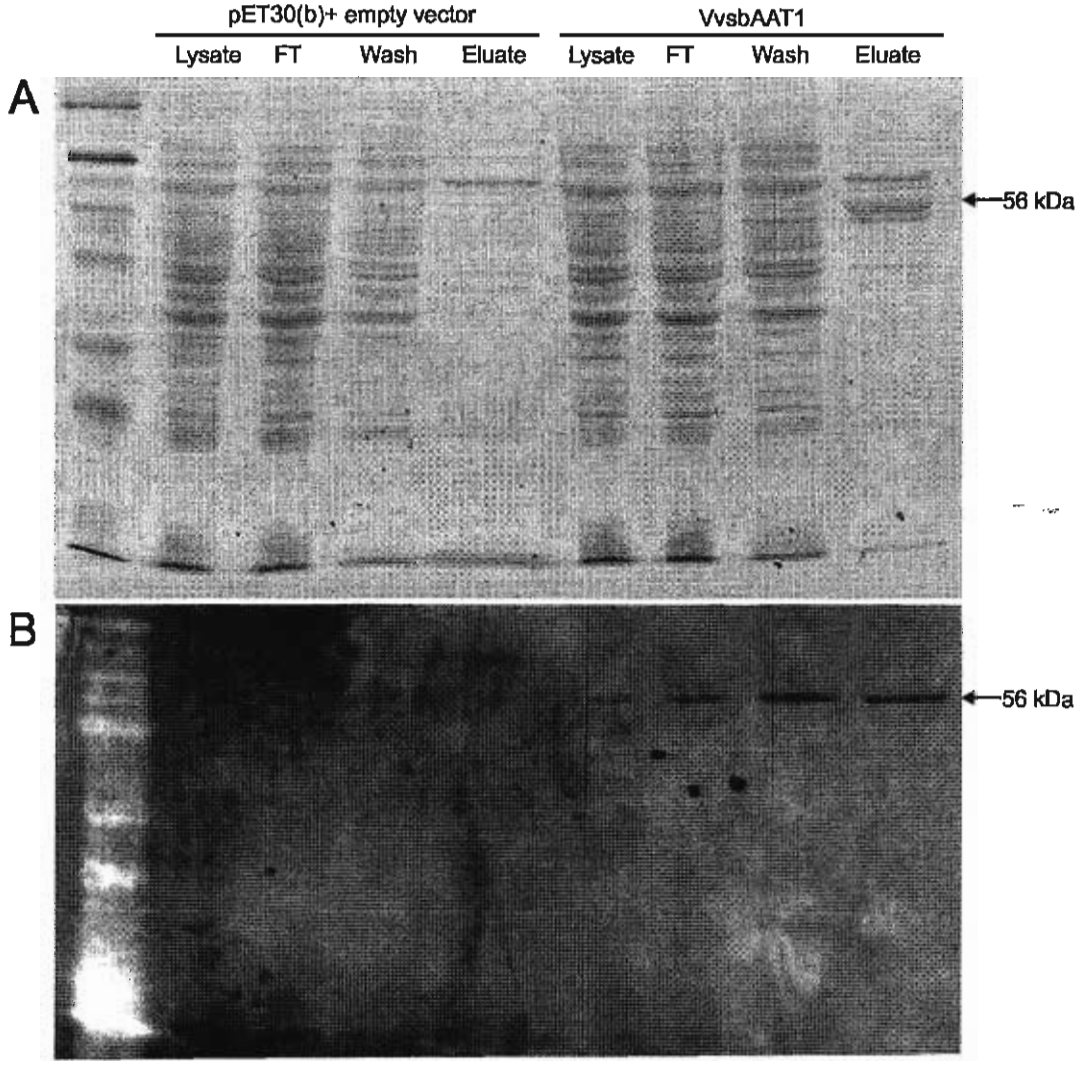

Figure 3.11: Expression and purification of His6-tagged VvsbAAT1 (56 kDa) from the soluble fraction of *E. coli* extracts by immobilized metal-ion affinity chromatography. Lysates from empty pET-30(b)+ vector or VvsbAAT1 expression cultures were subjected to immobilized metal-ion affinity chromatography and the fractions obtained (flowthrough (FT), wash, and eluate) were analyzed by SDS-PAGE. Protein was visualized by Coomassie staining (A) or anti-His-tag antibody after electrophoretic transfer to a PVDF membrane and immunoblotting (B).

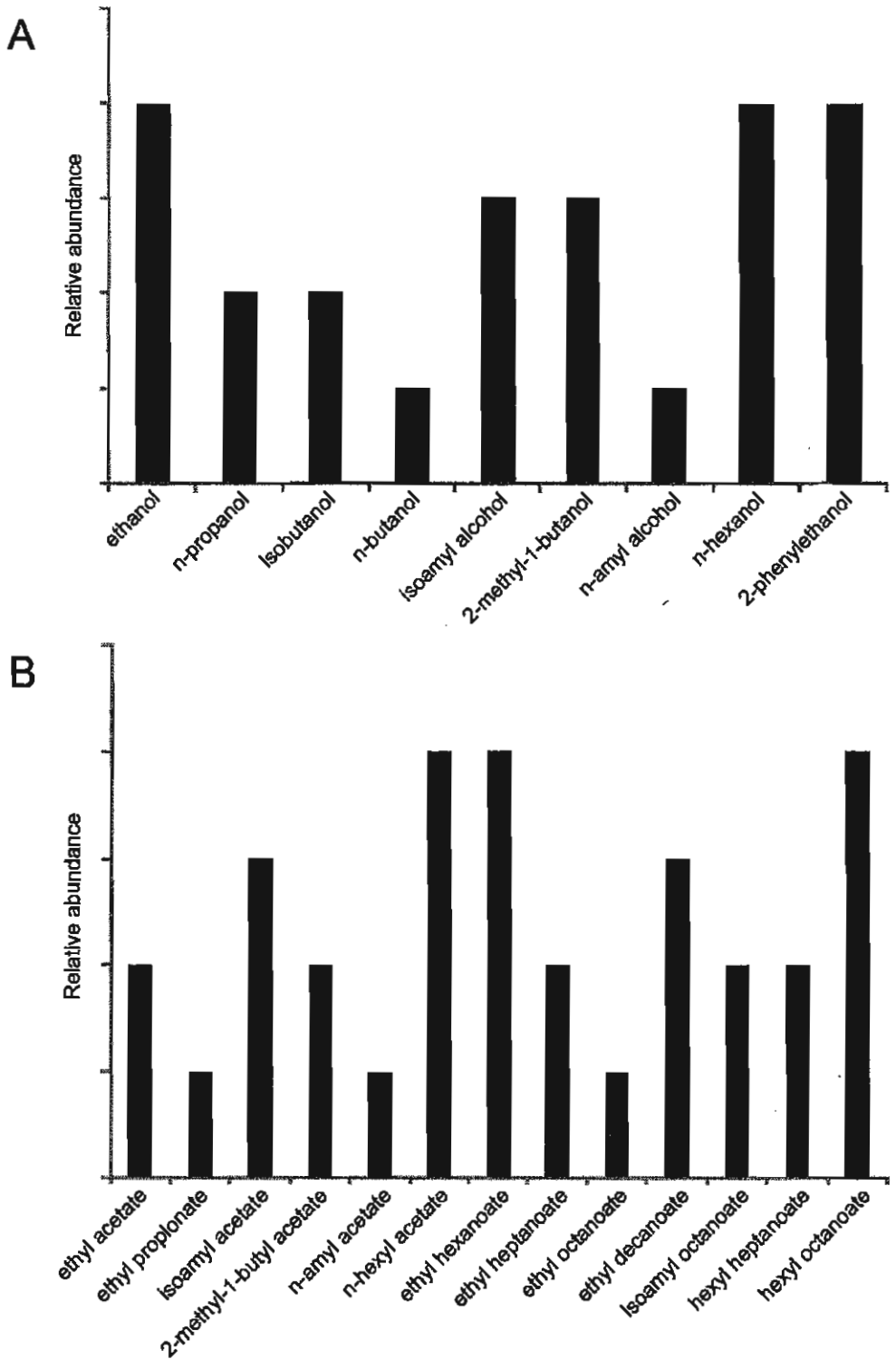

Figure 3.12: Detection of volatile alcohols (A) and alcohol esters (B) by gas chromatography as described in Chaudhary *et al.*, 1964.

2-phenylethanol are important berry constituents (Figure 3.12 A). Interestingly, the major volatile esters found also have short- to medium-chain length aliphatic carbon moieties (Figure 3.12 B), and are mostly ethyl, amyl, isoamyl and hexyl esters of acetates, hexanoates, octanoates, and other straight-chain carboxylic acid derivatives. The presence of these esters in Sauvignon Blanc grapes as in other fruits (Aharoni et al., 2000; Balbontín et al., 2010; Beekwilder et al., 2004; El-Sharkawy et al., 2005; Günther, Chervin, Marsh, Newcomb, & Souleyre, 2011; Wang & De Luca, 2005) raise the possibility that they are formed from alcohol precursors in an acyl-CoA dependant manner by alcohol acyltransferases, where alcohol molecules are acyl acceptors and various coenzyme A-activated carboxylic acids (acetyl-CoA, hexanoyl-CoA, and octanoyl-CoA) are acyl donors.

3.7 Enzymatic synthesis and purification of anthraniloyl- and benzoyl-coenzyme A thioester substrates

3.7.1 Expression of recombinant benzoate-coenzyme A ligase and purification using immobilized metal-ion affinity chromatography.

In order to test the activity of the recombinant VvsbAAT1 enzyme, aromatic acyl-CoA thioesters ([ring-^{14}C] anthraniloyl-CoA and [ring-^{14}C] benzoyl-CoA) that are not commercially available were produced using a benzoate-CoA ligase (BZL) clone from *Rhodopseudomonas palustris* (Beuerle & Pichersky, 2002). The BZL clone harboured a hexahistidine tag (His6-tag), and was purified to near homogeneity from *E. coli* cultures using immobilized metal ion chromatography (Figure 3.13).

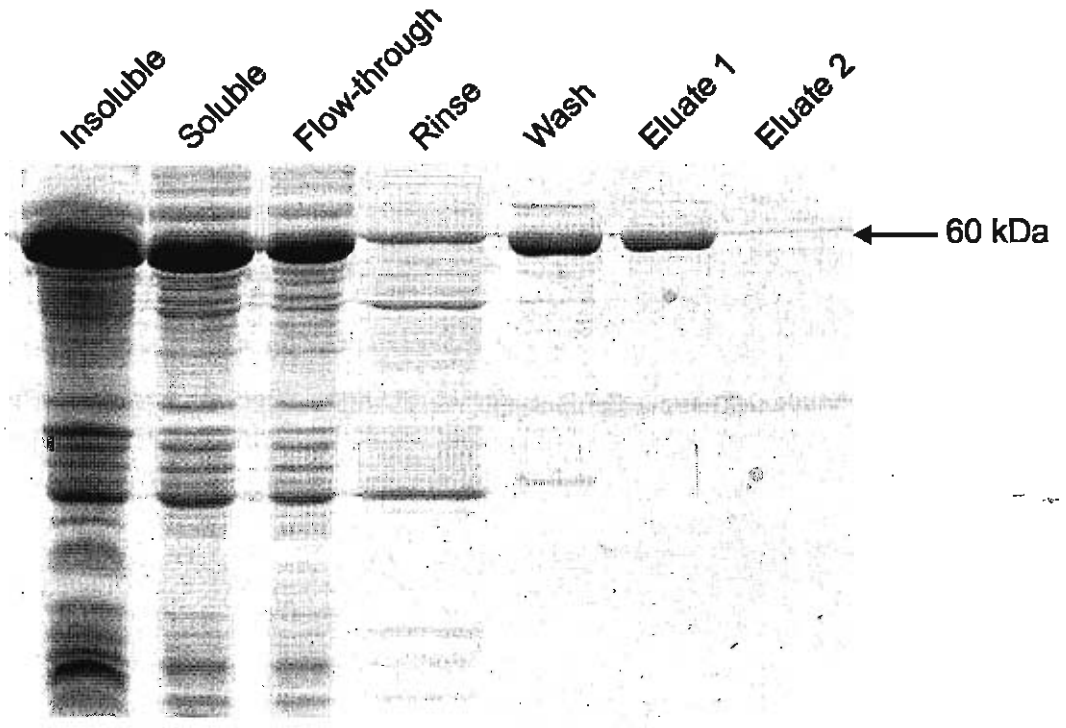

Figure 3.13: Expression and purification of recombinant benzoate:CoA ligase (60 kDa) from *E. coli* cultures by nickel-affinity chromatography. His-tagged benzoate:CoA ligase was expressed in *E. coli* (+ IPTG) followed by extraction for soluble and insoluble protein. Soluble protein was subjected to nickel-affinity chromatography and after rinsing the column with buffer, the benzoate:CoA ligase was eluted with imidazole (Wash & Eluate 1).

3.7.2 Enzymatic synthesis and purification of [ring-^{14}C] anthraniloyl-CoA and [ring-^{14}C] benzoyl-CoA.

The BZL-mediated synthesis of [ring-^{14}C] anthraniloyl-CoA and [ring-^{14}C] benzoyl-CoA involved a 4 hour incubation, stopping the reaction by acidification, and extraction with ethyl acetate to remove unincorporated acid substrate (Beuerle & Pichersky, 2002), as described in Materials and Methods 2.11. Each remaining aqueous phase was treated with ammonium acetate (4% w/v) to facilitate solid-phase extraction on C18 cartridges (Waters, Mississauga ON) for purification of the newly synthesized [ring-^{14}C] anthraniloyl-CoA and [ring-^{14}C] benzoyl-CoA thioesters. The high amounts of radioactivity in the flowthrough and wash fractions (washed with 4% ammonium acetate) for each synthesis can be attributed mostly to unincorporated substrate [[ring-^{14}C] anthranilic acid (R_f = 0.9, Figure 3.14 A) and [ring-^{14}C] benzoic acid (R_f = 0.9, Figure 3.14 B)], and perhaps some unbound [ring-^{14}C] anthraniloyl-CoA (R_f = 0.5, Figure 3.14 A) and [ring-^{14}C] benzoyl-CoA (R_f = 0.5, Figure 3.14 B). Each CoA ester was released from the SPE cartridge by washing with water and radioactive fractions were collected for analysis by thin layer chromatography (insets in Figure 3.14 A and B). Fractions corresponding to each product were collected to recover 30% more [ring-^{14}C] benzoyl-CoA (radioactivity) than [ring-^{14}C] anthraniloyl-CoA (radioactivity), reflecting the preferred substrate specificity of BZL for benzoic acid (Beuerle & Pichersky, 2002).

3.7.3 Enzymatic synthesis and purification of anthraniloyl-CoA and benzoyl-CoA (non-radiolabeled)

Enzymatic synthesis and purification of non-radiolabeled anthraniloyl-CoA and benzoyl-CoA substrates was performed in a similar manner, except for some aspects of

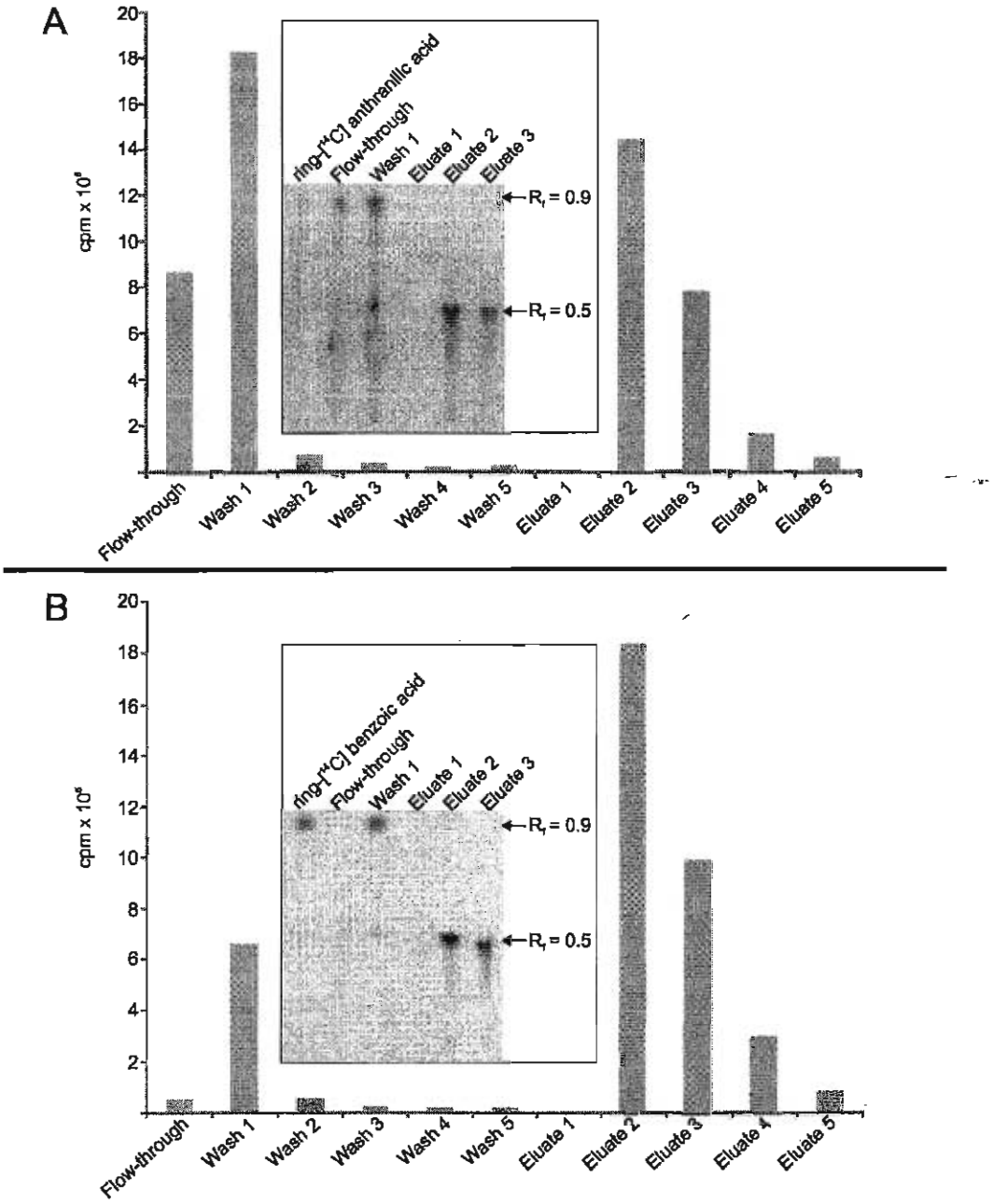

Figure 3.14: Purification of radiolabeled anthraniloyl-CoA (A) and benzoyl-CoA (B) produced with benzoate:CoA ligase (Materials and Methods 2.11). After application to a solid-phase extraction (SPE) cartridge, fractions were collected including the flow through, the washes with 5 x 1 mL of 4% ammonium acetate and the water eluates (eluate 1 = 200 µL fraction, eluates 2-5 = 1 mL fractions). Purified radiolabeled products were detected by liquid scintillation counting (in counts per minute, cpm) as well as visualized with autoradiographic detection of anthraniloyl- and benzoyl-CoAs (R_f = 0.5) on silica gel TLC plates (insets in A and B).

the purification and analysis of products (see Materials and Methods 2.11). The CoA esters eluted from the C18 cartridge (in 500 µL water) were lyophilized, resuspended in 25 µL of water, and 1 µL was subjected to TLC analysis (Figure 3.15 A). Photos of the TLC plates visualized under UV_{254} light show spots co-migrating with Coenzyme A standards at an R_f of 0.23 in the water eluates 2 and 3 off the C18 cartridge in the anthraniloyl-CoA synthesis (Figure 3.15 A). Ninhydrin treatment of the TLC plate from the anthraniloyl-CoA synthesis gives a positive result for a primary amine product at an R_f value of 0.53 (Figure 3.15 A). Although the Coenzyme A moiety also contains a primary amine group, it did not react as strongly or at all with ninhydrin, as no spot with an Rf = 0.23 was detected (Figure 3.15 A). Since eluates 2 and 3 (Figure 3.15 A) contained anthraniloyl-CoA as well as some contaminating free Coenzyme A, anthraniloyl-CoA was further purified by applying the eluate 2 fraction to silica gel column chromatography (Materials and Methods 2.11) and eluting with the same solvent system used for developing the TLC plates (butanol:water:acetic acid in a ratio of 65:35:25). The rapid mobility of anthranilic acid compared to anthraniloyl-CoA and the slower mobility of free Coenzyme A (Figure 3.15A and B) permitted complete separation and purification of anthraniloyl-CoA from these potential contaminants (Figure 3.15 B). Comparison of UV_{254} visualization and ninhydrin treatment of the TLC plate (Figure 3.15 B) shows spots positive for a primary amine reaction (anthraniloyl-CoA) in fractions 5 and 6, and the free Coenzyme A eluting later in fractions 8, 9, and 10. Fractions 5 and 6 were pooled, lyophilized, and resuspended in pure water to use in subsequent alcohol acyltransferase activity assays.

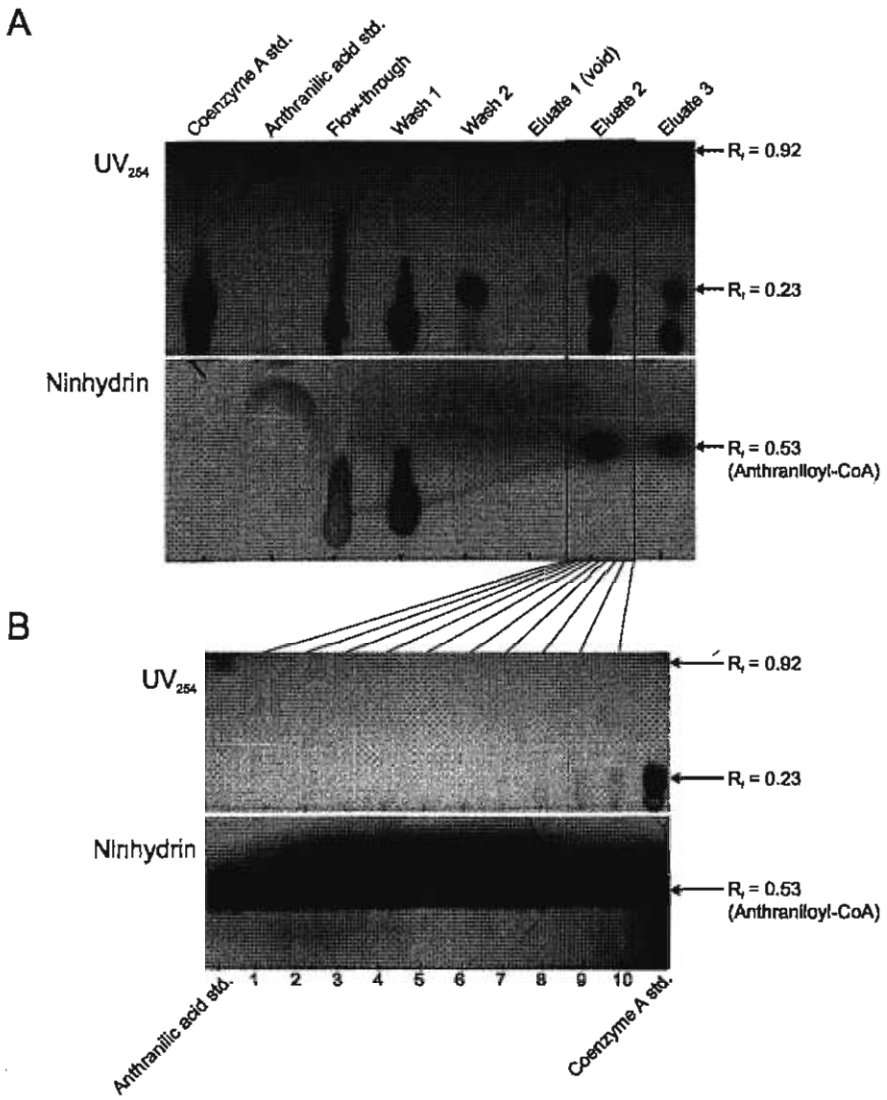

Figure 3.15: Purification of anthraniloyl-CoA produced with benzoate-CoA ligase (Materials and Methods 2.11). Samples of fractions from the SPE purification (A) of enzymatically synthesized anthraniloyl-CoA were applied to a silica gel plate, subjected to TLC (in the solvent system 1-butanol:water:acetic acid 65:35:25) and visualized under UV light (UV_{254}) and treatment with ninhydrin to identify synthesized anthraniloyl-CoA (R_f = 0.53, eluates 2 and 3). Synthesized anthraniloyl-CoA (eluate 2, boxed area in A) was further purified by fractionation (B) on a silica gel column into 10 x 500 µL fractions (1-10, again subjected to TLC and visualization under UV light and treatment with nihydrin) to separate the contaminating coenzyme A substrate (fractions 8-10) from the synthesized anthraniloyl-CoA (fractions 5 and 6).

Since benzoyl-CoA does not contain a primary amine group for detection by ninhydrin treatment, a similar analysis by TLC was not possible with this synthesized product, however the same protocol was used to purify this substrate (data not shown).

3.8 Enzyme activity assays with [^{14}C] acetyl-CoA, [ring-^{14}C] benzoyl-CoA, and [ring-^{14}C] anthraniloyl-CoA

Alcohol acyltransferase activity assays were performed with ripe grape berry protein extracts from both *V. labrusca* (Concord) and *V. vinifera* (Sauvignon Blanc). As previously reported (Wang & De Luca, 2005), assays using radiolabeled substrates ([^{14}C] acetyl-CoA, [ring-^{14}C] anthraniloyl-CoA, and [ring-^{14}C] benzoyl-CoA) produced varying amounts of radiolabeled products with berry protein from *V. labrusca*, namely benzyl-, and octyl acetates (Figure 3.16 A), ethyl-, benzyl- and octyl anthranilates (Figure 3.16 B), and ethyl-, benzyl- and octyl benzoates (Figure 3.16 C) compared to control assays containing no alcohol acceptor (Figure 3.16 A, B and C, lane 5 for *V. labrusca*). *V. labrusca* berry protein was also able to utilize *cis*-3-hexenol as an acyl acceptor with all three radiolabeled Coenzyme A substrates (Figure 3.16 A, B, and C lanes 3, respectively), which had not been tested previously (Wang & De Luca, 2005). However, no radiolabeled products could be detected using berry protein extracted from 0-30% and 30-70% ammonium sulfate precipitates from Sauvignon Blanc grapes (Figure 3.16 A, B and C). Radioactive spots at the origin were detected in almost all assays, corresponding to unreacted acyl-CoA substrate (Figure 3.16 A, B, and C; compare to lane R_C acyl-CoA standards).

Similarly, enzyme assays using recombinant protein from *E. coli* cultures expressing *VlAMAT* and *VvsbAAT1* demonstrated that VlAMAT was active towards these

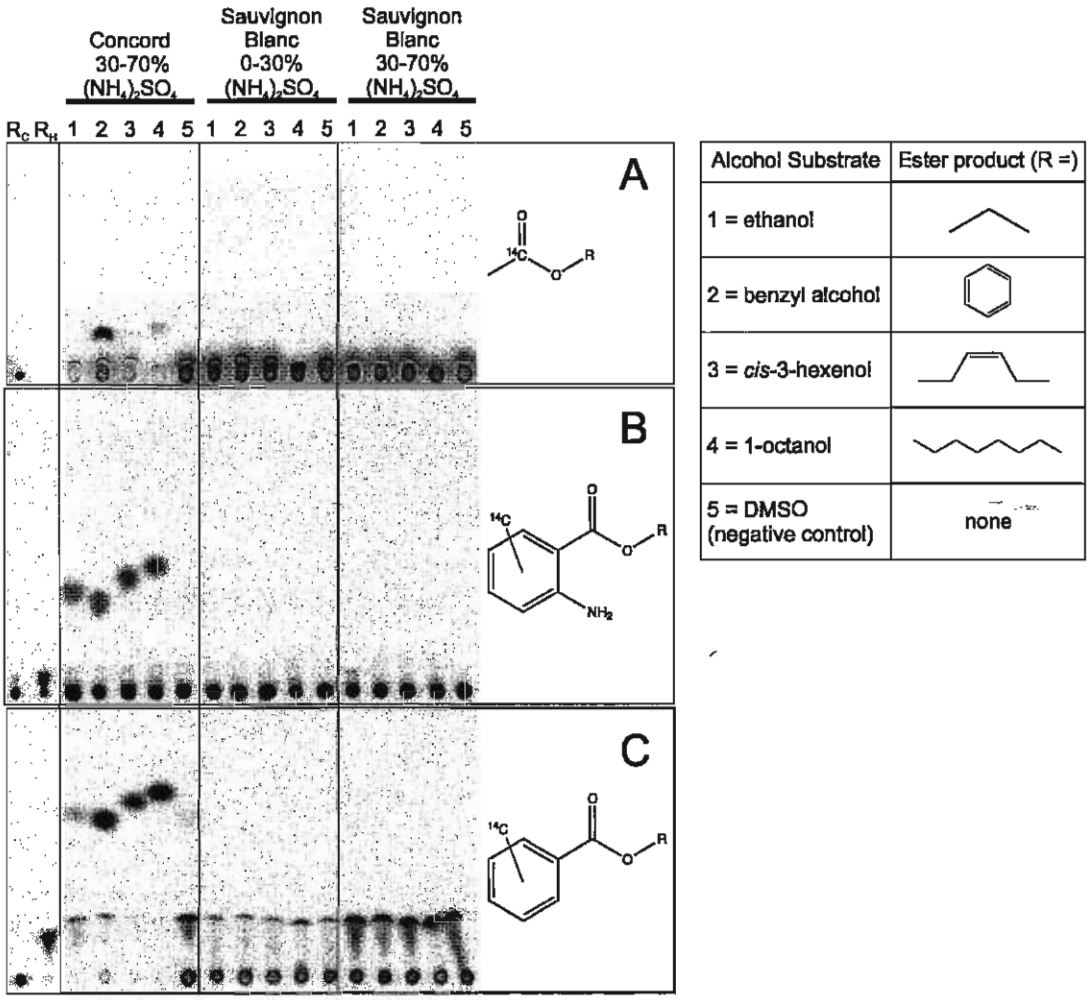

Figure 3.16: VlAMAT-like enzyme activities in *Vitis labrusca* (Concord) and Sauvignon Blanc mature berry extracts. Desalted protein extracts from Concord and Sauvignon Blanc grapes [$(NH_4)_2SO4$ precipitations] were assayed for VlAMAT-like activity using [acetyl-1-^{14}C]-CoA (A), [ring-^{14}C-anthraniloyl]-CoA (B) or [ring-^{14}C-benzoyl]-CoA (C) thioesters together with ethanol, benzyl alcohol, cis-3-hexenol, 1-octanol, or DMSO (negative control) as substrates. Reaction mixtures were processed and submitted to Silica Gel G TLC (See Materials and Methods 2.11.1) and radioactive reaction products were detected by autoradiography. Alcohol substrates with molecular structures for corresponding reaction products are listed as R groups in the table. R_C is the radiolabeled CoA substrate for each TLC plate, R_H is the radiolabeled acid standard for each TLC plate except for [acetic acid-1-^{14}C] in (A) which was not available.

radiolabeled substrates, but VvsbAAT1 was not (data not shown). This raised the possibility that VvsbAAT1 has a different substrate specificity compared with VlAMAT, even though their amino acid sequences are 95% identical (Appendix I, Figure S3).

3.9 Detection of acetyl-CoA:*cis*-3-hexenol acetyltransferase (CHAT) activity in Sauvignon Blanc berries by Gas Chromatography-Mass Spectrometry (GC-MS)

The failure to detect any enzymatic activity using the radiolabeled acetyl-CoA, benzoyl-CoA, and anthraniloyl-CoA substrates suggested that recombinant VvsbAAT1 might not be active or that it might have an altered substrate specificity compared to VlAMAT. In order to perform enzyme assays with some commercially available (non-radiolabeled) aliphatic acyl-CoA donors (such as butyryl-CoA, hexanoyl-CoA, and octanoyl-CoA), the reaction products were detected by GC-MS (Materials and Methods 2.12.2). The assay was developed using crude protein extracts from *A. thaliana* leaves that are well known for their acetyl-CoA:*cis*-3-hexenol acetyltransferase (CHAT) activity (Auria, Pichersky, Schaub, Hansel, & Gershenzon, 2007) to produce *cis*-3-hexenyl acetate from *cis*-3-hexenol and acetyl-CoA. *Arabidopsis* leaf extracts were positive for CHAT activity (Figure 3.17 A) producing a new peak (R_t = 7.23 min) corresponding to *cis*-3-hexenyl acetate with the correct mass spectrum (Figure 3.17 E) while negative controls did not show any product formation (Figure 3.17 B, C, and D). With the GC-MS system established for CHAT assays, Sauvignon Blanc berries were re-assayed for this activity. Surprisingly, ammonium sulfate precipitated (30-70%) protein displayed CHAT activity (Figure 3.18 B) while the buffer control did not (Figure 3.18 C). The appearance of CHAT activity in GC-MS assays (Figure 3.18 B) compared to the lack of activity

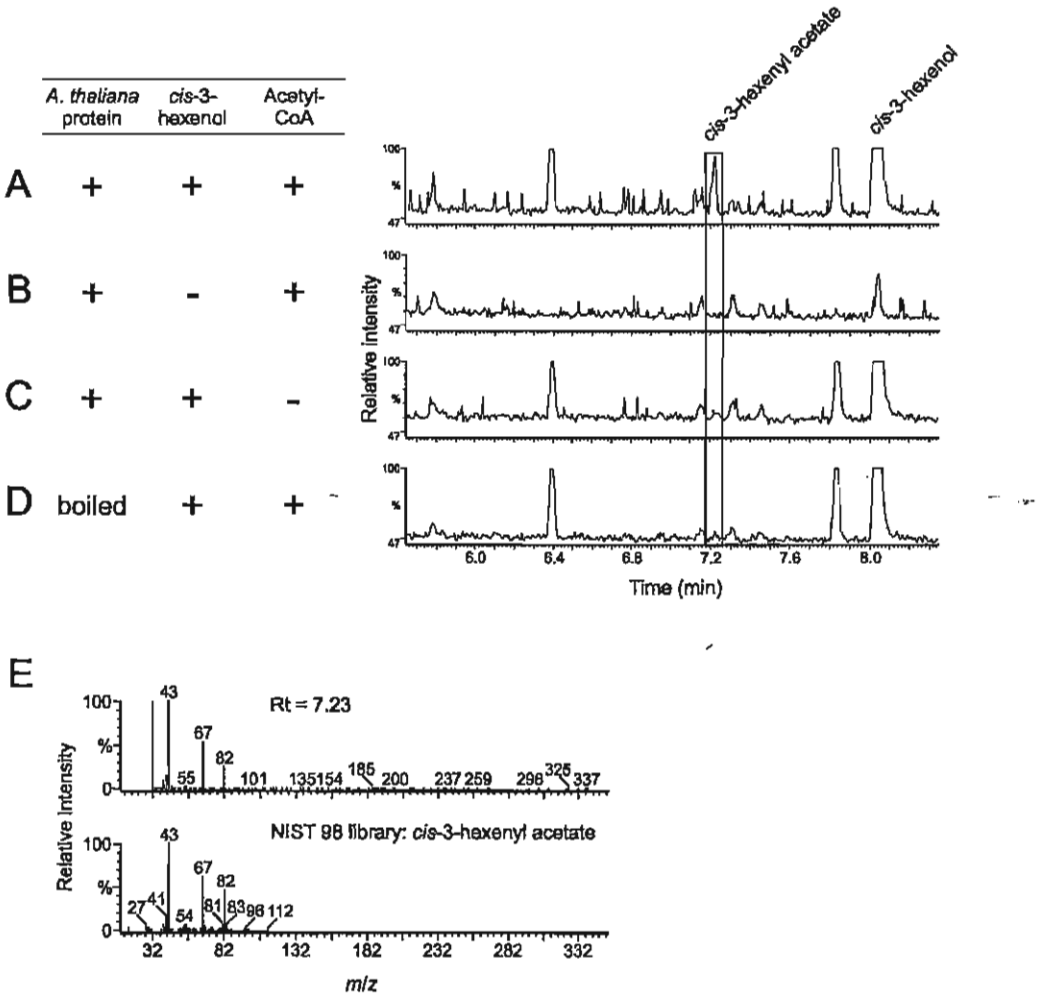

Figure 3.17: Description of Acetyl CoA: *cis*-3-hexenol acetyltransferase (CHAT) assay in *Arabidopsis thaliana* protein extracts using Gas Chromatography-Mass Spectrometry. Crude desalted protein extracts were assayed for CHAT activity with (A) *cis*-3-hexenol + acetyl-CoA; (B) + acetyl-CoA; (C) + *cis*-3-hexenol and (D) boiled leaf extract + *cis*-3-hexenol + acetyl-CoA. The mass spec profile of peak at Rt = 7.23 compared to mass spec profile of pure *cis*-3-hexenyl acetate from NIST/EPA/NIH 98 Mass Spectral Library (E). Peak at Rt = 8.04 min is *cis*-3-hexenol, and peaks at Rt = 6.39 min and Rt = 7.84 min are impurities from the alcohol substrate.

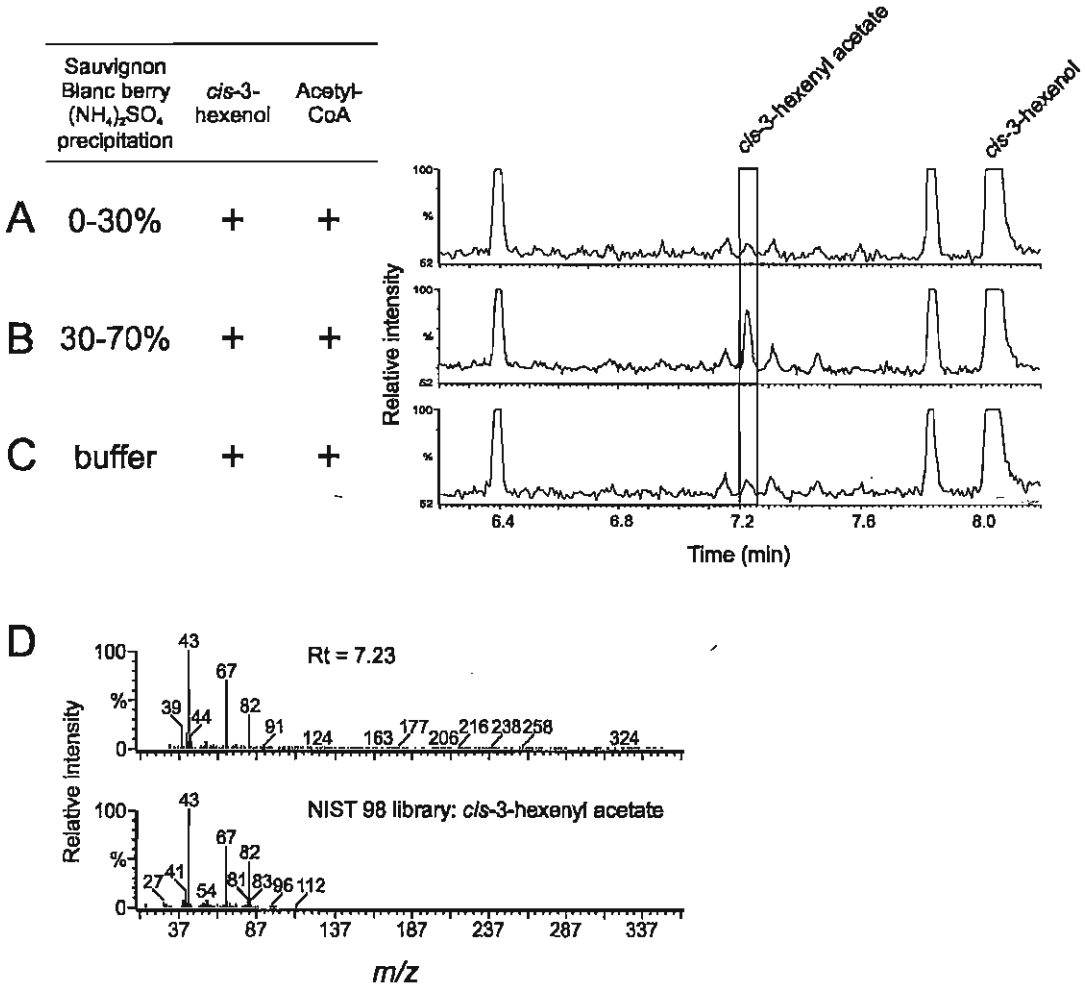

Figure 3.18: Description of Acetyl CoA: *cis*-3-hexenol acetyltransferase (CHAT) assay in *V. vinifera* Sauvignon Blanc mature berry protein extracts using Gas Chromatography-Mass Spectrometry. Enzyme assays performed with (A) 0-30% $(NH_4)_2SO_4$ precipitated protein, (B) 30-70% $(NH_4)_2SO_4$ precipitated protein or (C) Tris buffer only. (D) The mass spec profile of peak at Rt = 7.23 min in (B) compared to mass spec profile of *cis*-3-hexenyl acetate obtained from NIST/EPA/NIH 98 Mass Spectral Library. Peak at Rt = 8.04 min is *cis*-3-hexenol, and peaks at Rt = 6.40 min and Rt = 7.83 min are impurities from the alcohol substrate.

observed in radiolabeled assays (Figure 3.16 A) might be explained by the difference in the final concentration of [^{14}C] acetyl-CoA (3.33 µM) compared to the non-radiolabeled acetyl-CoA (500 µM) used in each assay (see Materials and Methods 2.12.1 vs. 2.12.2). Also, the methodology of measuring radiolabeled product by thin-layer chromatography requires concentration of the organic extraction phase by vacuum centrifugation, which may result in the loss of volatile compounds, whereas analysis by GC-MS permits the organic phase to be analyzed directly, without the need for vacuum centrifugation and possible evaporation of the product.

3.10 Acetyl-CoA:*cis*-3-hexenol acetyltransferase (CHAT) activity by recombinant VvsbAAT1 protein

After confirmation of CHAT activity in Sauvignon Blanc berry protein extracts (Figure 3.18), the recombinant IMAC-purified VvsbAAT1 was subjected to similar enzyme assays. GC-MS analysis showed that recombinant VvsbAAT1 produced *cis*-3-hexenyl acetate (Rt=7.32 min, Figure 3.19 A) in the presence of acetyl-CoA and *cis*-3-hexenol, while assays without substrate, with boiled protein, or with protein isolated from *E. coli* harbouring the empty vector did not (Figure 3.19 B, C, and D respectively). These results confirmed that recombinant VvsbAAT1 was biochemically active, and that it may be responsible for the CHAT activity observed with the protein extracts from ripe Sauvignon Blanc berries (Figure 3.18).

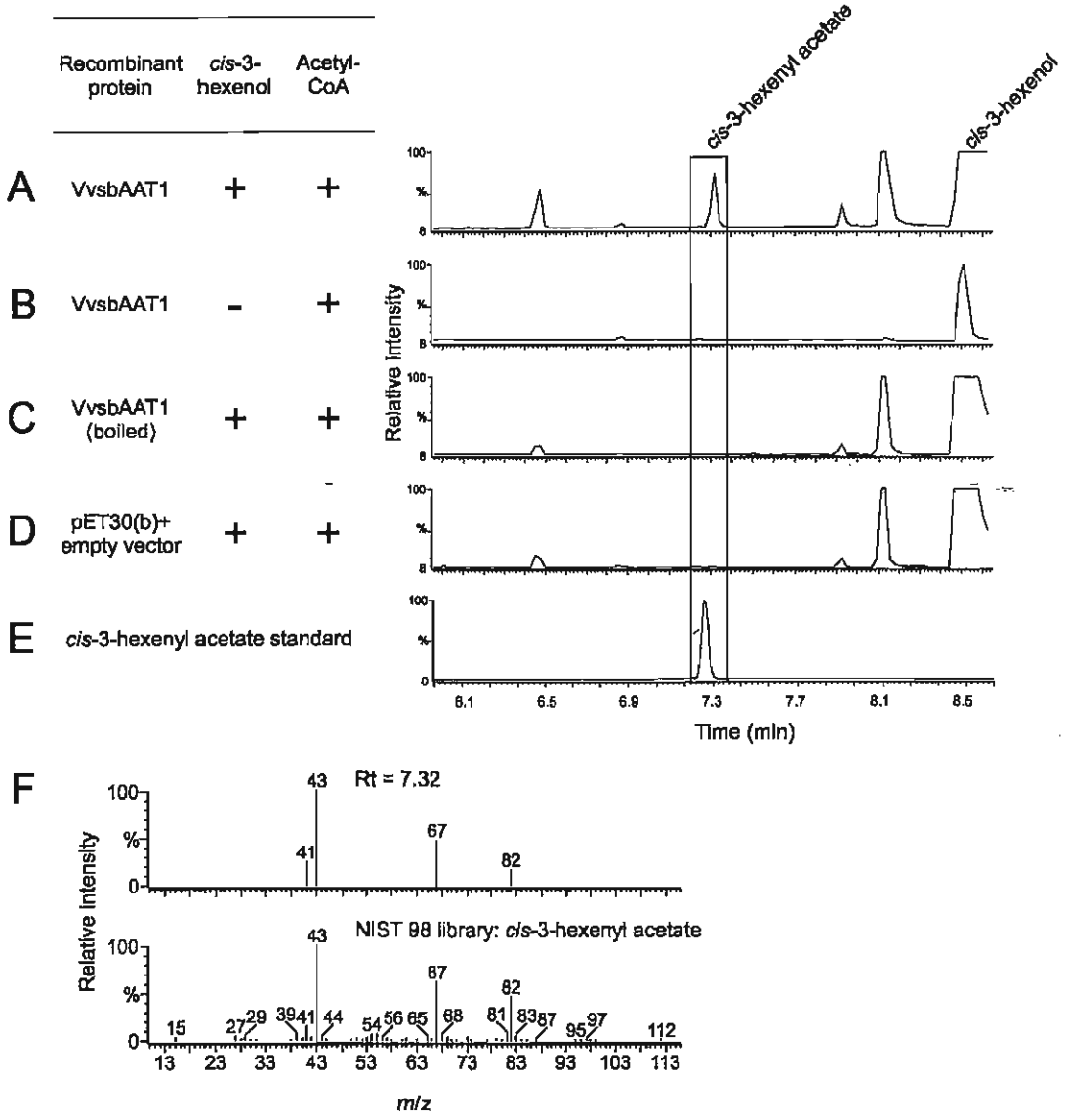

Figure 3.19: Description of Acetyl CoA: *cis*-3-hexenol acetyltransferase (CHAT) assay with recombinant VvsbAAT1 using Gas Chromatography-Mass Spectrometry. Nickel-affinity purified recombinant VvsbAAT1 protein preparations were assayed for CHAT activity with (A) *cis*-3-hexenol + acetyl-CoA; (B) + acetyl-CoA; (C) boiled recombinant VvsbAAT1 + *cis*-3-hexenol + acetyl-CoA and (D) protein from an *E. coli* expression culture harbouring an empty pET30(b)+ vector + *cis*-3-hexenol + acetyl-CoA. (E) *cis*-3-hexenyl acetate authentic standard. (F) Comparison of mass spec profile of peak at Rt = 7.32 min in (A) with *cis*-3-hexenyl acetate from NIST/EPA/NIH 98 Mass Spectral Library. Peak at Rt = 8.50 min is *cis*-3-hexenol, and peaks at Rt = 6.43 min and Rt = 8.10 min are impurities from the alcohol substrate.

3.11 Determination of pH optimum for CHAT activity in recombinant VvsbAAT1

The CHAT enzyme assays shown in Figure 3.19 were performed in Tris-HCl, pH 7.5 (Materials and Methods 2.12.2). The pH optima of recombinant VvsbAAT1 protein was determined using 3 different buffer systems (Bis-Tris, Tris, or Gly-Gly). While VvsbAAT1 was active throughout this pH range, CHAT activity was optimal at pH 8.5 in Gly-Gly buffer (Figure 3.20). These pH conditions should be used to perform substrate specificity assays in order to compare VvsbAAT1 to VlAMAT.

3.12 Developmental expression analysis

In *V. labrusca* berries, *VlAMAT* transcripts, protein levels, enzyme activity and methyl anthranilate levels begin to rise at the onset of ripening or *veraison*, starting around 10 weeks post-flowering (wpf) (Wang & De Luca, 2005). Similar results have also been observed with the appearance of other alcohol acyltransferases and metabolite accumulation during ripening of other fruits (González et al., 2009). It was also shown in *V. labrusca* that expression of *VlAMAT* was localized to the mesocarp (flesh) of the berry (Wang & De Luca, 2005). Similar preliminary analyses with *VvsbAAT1* transcripts in *V. vinifera* berries sampled throughout the growing season revealed that it is expressed rather uniformly throughout grape development but not in flowers (Figure 3.21 A). PCR products could not be detected in the 8 wpf samples for both *VvsbAAT1* and *Actin*, and also for 7 wpf for *Actin*. It is unclear whether this is due to poor quality of RNA isolated for these samples or if it is indeed an accurate reflection of transcript levels. This experiment will be repeated several times using quantitative RT-PCR (qRT-PCR) to obtain a more accurate estimate of transcript levels for these genes. Nevertheless, *VvsbAAT1* expression in the berries can be detected starting as early as 2 wpf in contrast

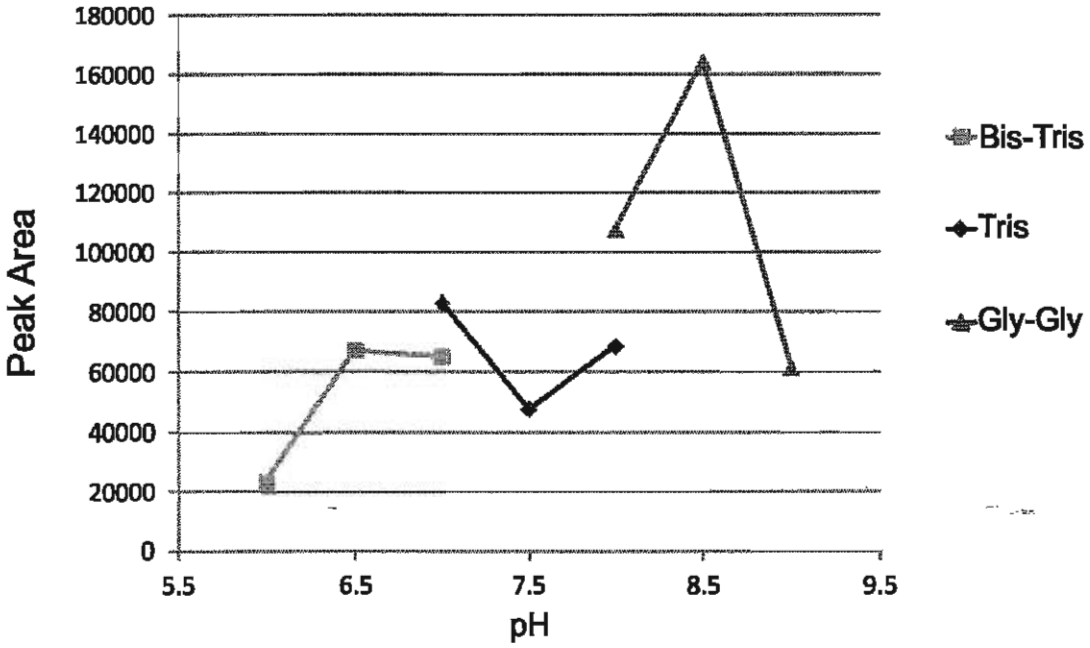

Figure 3.20: Peak area quantification of acetyl CoA: *cis*-3-hexenol acetyltransferase (CHAT) assays with recombinant VvsbAAT1 in different buffer systems by GC-MS. IMAC-purified recombinant VvsbAAT1 protein preparations were assayed for CHAT activity in Bis-Tris buffer, pH 6.0, 6.5 and 7.0; Tris buffer pH 7.0, 7.5 and 8.0; and Gly-Gly buffer pH 8.0, 8.5 and 9.0.

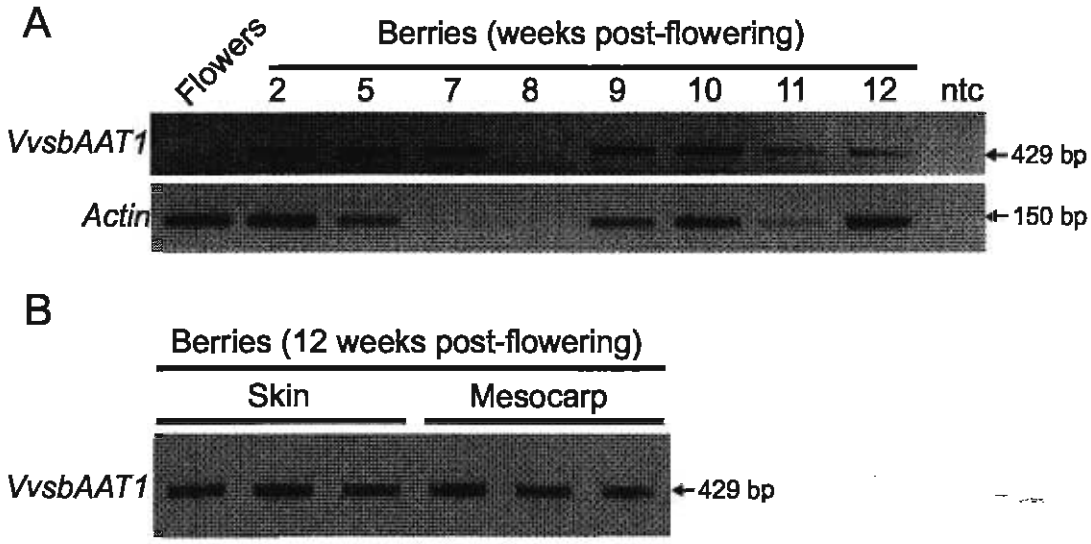

Figure 3.21: RT-PCR performed with gene-specific primers for *VvsbAAT1* in different developmental stages of the berry (A) or different tissues within a mature berry (B). (A) RNA isolated from whole flowers (0 weeks post-flowering [wpf]) or whole berries (2-12 wpf) was subjected to RT-PCR with both *VvsbAAT1* and *Actin* gene-specific primers, together with a no-template control (ntc). (B) RNA isolated from either the skin or mesocarp of mature berries (12 wpf) was subjected to RT-PCR with *VvsbAAT1* gene-specific primers in triplicate.

to *VlAMAT* which could not be detected in *V. labrusca* berries until 10 wpf (Wang & De Luca, 2005). Also, unlike the case for *V. labrusca*, *VvsbAAT1* is expressed both in the mesocarp and skin of ripe berries (Figure 3.21 B).

Chapter 4. Discussion

Plants can communicate with their environment via both physical and chemical means. One particular means of chemical communication employed by some plants is by both generating and sensing volatile molecules. Plant volatile molecules can play various ecological roles in the environment, such as to attract pollinators or seed dispersers, to deter herbivory, or even to activate defense responses in inter-plant signalling.

4.1 Some varieties of *Vitis vinifera* express genes encoding acyltransferases that produce truncated products

The present study describes the cloning, heterologous expression, and preliminary biochemical characterization of a BAHD acyltransferase involved in volatile ester biosynthesis in the wine grape, *Vitis vinifera* cv. Sauvignon Blanc. Previous studies had described a BAHD acyltransferase (VlAMAT) in the closely related *Vitis labrusca* Concord berry, responsible for the formation of the characteristic 'foxy' aroma compound, methyl anthranilate. Like most other fruit and floral scent related BAHD alcohol acyltransferases, gene expression, protein levels, enzyme activity, and accumulation of methyl anthranilate began to rise at the onset of berry ripening and peaked at maturity. The published genome of *Vitis vinifera* cv. Pinot Noir (Jaillon et al., 2007) was used to identify *VlAMAT*-like genes and resulted in 5 highly similar matches with one candidate sharing 95% amino acid sequence identity. This full-length candidate gene (*VvsbAAT1*) was cloned by RT-PCR from mRNA transcripts isolated from mature grapes *V. vinifera* cv. Sauvignon Blanc. This clone encoded a putative protein with the same molecular weight as that of VlAMAT (MW = 50 kDa). Expression of *VvsbAAT1* in

E. coli produced a recombinant protein of the expected size (MW = 50 kDa plus 6 kDa *N*-terminal fusion tag), while full-length cDNA clones from Chardonnay Musqué, Cabernet Franc, and Shiraz all produced truncated proteins approximately 22 kDa in size (16 kDa plus 6 kDa *N*-terminal fusion tag). While the significance of these results is unclear, the *Vitis vinifera* genome has at least 2 candidate genes (Uniprot accessions D7TFE0 and D7U3X5) with 89% and 53% identity to the three genes isolated from Chardonnay Musqué, Cabernet Franc, and Shiraz (data not shown). All the truncated forms of the acyltransferases produce almost identical 22 kDa proteins in their *N*-terminal regions, and are missing the DFGWG motif normally located near the *C*-terminal end of a typical BAHD acyltransferase. The putative truncated proteins (Uniprot accessions D7TFE0 and D7U3X5) described in the Pinot Noir genomic database do contain the HXXXD catalytic motif while those described here do not. It is possible that the truncated forms of Pinot Noir display some acyltransferase activity, since other studies with mutagenized BAHD acyltransferases (Bayer, Ma, & Stöckigt, 2004; Suzuki, Nakayama, & Nishino, 2003; Unno et al., 2007) have shown that the *C*-terminal DFGWG motif is important but not essential for enzyme activity. It is unlikely that the truncated forms cloned in this study have any acyltransferase activity, since they are missing the catalytic HXXXD domain ((Bayer et al., 2004; Morales-Quintana, Fuentes, Gaete-Eastman, Herrera, & Moya-Leon, 2010; Suzuki et al., 2003; Unno et al., 2007) and their possible biological roles remain to be established.

4.2 *VvsbAAT1* catalyzes the formation of *cis*-3-hexenyl acetate

Previous studies have shown that Sauvignon Blanc produce and accumulate mostly aliphatic volatile esters with minor amounts of aromatic esters (Chaudhary, Kepner, &

Webb, 1964; Sefton, Francis, & Williams, 1994). The preliminary results obtained with VvsbAAT1 suggest that it may play a role in the formation of volatile esters typical of Sauvignon Blanc, since GC-MS analyses of enzyme assays with crude protein berry extracts (Figure 3.18) and IMAC-purified recombinant protein (Figure 3.19) showed the production of the aliphatic *cis*-3-hexenyl acetate, while radioactive assays using crude protein berry extracts (Figure 3.16 B and C) or recombinant protein were unable to detect the formation of aromatic anthranilate or benzoate esters. However, these assays need to be repeated by GC-MS to determine whether or not the recombinant protein has any activity towards aromatic acyl-CoA substrates.

An alcohol acyltransferase from *A. thaliana* that also catalyzes the formation of *cis*-3-hexenyl acetate (AtCHAT) was isolated and characterized previously (D'Auria, Pichersky, Schaub, Hansel, & Gershenzon, 2007). It was shown that the production of this green-leaf volatile correlated with mechanical injury to the leaves and the upregulation of *AtCHAT* (D'Auria et al., 2007). It was suggested by the authors that a possible role of *AtCHAT* in the plant may be to prime the plant defenses for subsequent injury by producing increased amounts of *cis*-3-hexenyl acetate than normally available at basal levels, since green-leaf volatiles have been shown to have anti-fungal and anti-bacterial properties, and also may serve as an indirect defense mechanism by attracting predators of herbivores (D'Auria et al., 2007). Another possible role of *AtCHAT* postulated by the authors' was the detoxification of the C7 aldehyde (*E*)-2-hexenal, which can cause DNA damage in mammalian cells and may have a similar effect in plants (D'Auria et al., 2007). Future enzyme assays by GC-MS using many possible alcohol and acyl-CoA substrates will determine the substrate specificity of VvsbAAT1

and measurement of enzyme kinetics will elucidate its preferred substrates *in vitro* so that predictions can be made about the biological role of *VvsbAAT1 in vivo*. The uniform expression of *VvsbAAT1* throughout berry development (Figure 3.21) is unlike the profiles seen for other fruit- and floral-scent related alcohol acyltransferases (Beekwilder et al., 2004; Boatright et al., 2004; Dexter et al., 2007; El-Sharkawy et al., 2005; González et al., 2009; Wang & De Luca, 2005), which typically increase with the ripening or development of the mature fruit or flower, suggesting that the role of *VvsbAAT1 in vivo* may not be related to fruit-ripening. Further studies on expression of *VvsbAAT1* in other plant tissues such as leaves and stems and in stressed or mechanically damaged tissues my help to elucidate whether or not it also plays a role similar to *AtCHAT in vivo*.

4.3 Future studies with putative alcohol acyltransferases in *V. vinifera*

There are 4 other putative BAHD acyltransferases (D7U3X7, F6I088, D7U3X1, F6I087, see Figure 3.1) in the genome of Pinot Noir that have high similarity to *VvsbAAT1*. Whether or not these same sequences are conserved in all cultivars of *V. vinifera* is unknown. However, even between the published genomes of Pinot Noir cv.PN400024 (used in this study for phylogenetic analysis) and Pinot Noir cv. ENTAV 115 (Velasco et al., 2007) there are apparent differences in the number of *VlAMAT*-like genes and in their amino acid sequences (data not shown). Whether or not these differences are due to technical or biological variation remains to be seen. If indeed some of these putative alcohol acyltransferases contribute to the aroma and taste profiles of the mature berries, it is possible that certain genes may have been either selected for or against in the many hundreds of different cultivars developed by humans (Myles, 2011).

The conserved HXXXD motif in BAHD acyltransferases lies in the active site of the enzyme and is involved in the general base catalysis (D'Auria, 2006). In VlAMAT and 4 of the 5 putative AATs in *V. vinifera* that have high similarity to VlAMAT, this sequence is HT**M**SD, however in VvSBAAT1 this sequence is HT**L**SD. To test the possibility that the substitution of the sulfur-containing methionine residue with the aliphatic leucine residue has an effect on substrate specificity, a single base pair was mutagenized in the recombinant VvSBAAT1 to change the codon for leucine to methionine (**T**TG→**A**TG). The mutagenized enzyme (VvSBAAT1-L168M) will be expressed in *E. coli*, purified, and subjected to enzyme activity assays.

4.4 Conclusions

The genome of *Vitis vinifera* predicts that a small family of 5 alcohol acyltransferases may be involved in the formation of volatile aroma compounds. Some of these putative alcohol acyltransferases share a high degree of amino acid sequence identity with VlAMAT, which is the enzyme responsible for producing the "foxy" methyl anthranilate in *V. labrusca* Concord berries. Many varieties of *V. vinifera* express *VlAMAT*-like gene products even though methyl anthranilate does not accumulate in *V. vinifera* berries. A cDNA isolated from *V. vinifera* cv. Sauvignon Blanc (*VvsbAAT1)*, with 95% amino acid sequence identity to VlAMAT was cloned and expressed in *E. coli*. Preliminary biochemical characterization showed that VvsbAAT1 can catalyze the formation of the "green-leaf" volatile *cis*-3-hexenyl acetate. More work is needed to establish the function of this enzyme *in vivo* by demonstrating its kinetics with a full range of possible substrates, and correlating this data to tissue-specific and developmental gene expression profiling, protein analysis, and volatile metabolite profiles in Sauvignon

Blanc grapes. The use of a mutagenized VvsbAAT1 may help to elucidate if certain amino acids contribute to substrate specificity of the enzyme. The cloning and biochemical characterization of other alcohol acyltransferases in this family of enzymes could be useful as genetic markers for certain aroma or taste properties in breeding programs of *V. vinifera*.

References

Aggelis, A., John, I., Karvouni, Z., & Grierson, D. (1997). Characterization of two cDNA clones for mRNAs expressed during ripening of melon (*Cucumis melo* L.) fruits. *Plant Molecular Biology, 33*(2), 313-322.

Aharoni, A., Keizer, L. C. P., Bouwmeester, H. J., Sun, Z., Alvarez-Huerta, M., Verhoeven, H. A., et al. (2000). Identification of the SAAT gene involved in strawberry flavor biogenesis by use of DNA microarrays. *The Plant Cell Online, 12*(5), 647-661.

Aubert, C., & Bourger, N. (2004). Investigation of volatiles in Charentais cantaloupe melons (*Cucumis melo* var. *Cantalupensis*). Characterization of aroma constituents in some cultivars. *Journal of Agricultural and Food Chemistry, 52*(14), 4522-4528.

Augustyn, O., Rapp, A., & Wyk, J. (1982). Some volatile aroma components of *Vitis vinifera* L. cv. Sauvignon Blanc. *South African Journal of Enology and Viticulture, 3*(53-60), 1-12.

Balbontín, C., Gaete-Eastman, C., Fuentes, L., Figueroa, C. R., Herrera, R., Manriquez, D., et al. (2010). VpAAT1, a gene encoding an alcohol acyltransferase, is involved in ester biosynthesis during ripening of mountain papaya fruit. *Journal of Agricultural and Food Chemistry, 58*(8), 5114-5121.

Ban, Y., Oyama-Okubo, N., Honda, C., Nakayama, M., & Moriguchi, T. (2010). Emitted and endogenous volatiles in 'tsugaru' apple: The mechanism of ester and (E, E)-[alpha]-farnesene accumulation. *Food Chemistry, 118*(2), 272-277.

Bate, N. J., & Rothstein, S. J. (1998). C6-volatiles derived from the lipoxygenase pathway induce a subset of defense-related genes. *The Plant Journal, 16*(5), 561-569.

Bayer, A., Ma, X., & Stöckigt, J. (2004). Acetyltransfer in natural product biosynthesis--functional cloning and molecular analysis of vinorine synthase. *Bioorganic & Medicinal Chemistry, 12*(10), 2787-2795.

Beaulieu, J. C., & Grimm, C. C. (2001). Identification of volatile compounds in cantaloupe at various developmental stages using solid phase microextraction. *Journal of Agricultural and Food Chemistry, 49*(3), 1345-1352.

Beekwilder, J., Alvarez-Huerta, M., Neef, E., Verstappen, F. W. A., Bouwmeester, H. J., & Aharoni, A. (2004). Functional characterization of enzymes forming volatile esters from strawberry and banana. *Plant Physiology, 135*(4), 1865-1878.

Berger, A., Meinhard, J., & Petersen, M. (2006). Rosmarinic acid synthase is a new member of the superfamily of BAHD acyltransferases. *Planta, 224*(6), 1503-1510.

Besseau, S., Hoffmann, L., Geoffroy, P., Lapierre, C., Pollet, B., & Legrand, M. (2007). Flavonoid accumulation in *Arabidopsis* repressed in lignin synthesis affects auxin transport and plant growth. *The Plant Cell Online, 19*(1), 148-162.

Beuerle, T., & Pichersky, E. (2002). Enzymatic synthesis and purification of aromatic Coenzyme A esters. *Analytical Biochemistry, 302*(2), 305-312.

Bloor, S. J., & Abrahams, S. (2002). The structure of the major anthocyanin in *Arabidopsis thaliana*. *Phytochemistry, 59*(3), 343-346.

Boatright, J., Negre, F., Chen, X., Kish, C. M., Wood, B., Peel, G., et al. (2004). Understanding in vivo benzenoid metabolism in petunia petal tissue. *Plant Physiology, 135*(4), 1993-2011.

Bunsupa, S., Okada, T., Saito, K., & Yamazaki, M. (2011). An acyltransferase-like gene obtained by differential gene expression profiles of quinolizidine alkaloid-producing and nonproducing cultivars of *Lupinus angustifolius*. *Plant Biotechnology, 28*, 89-94.

Burhenne, K., Kristensen, B. K., & Rasmussen, S. K. (2003). A new class of N-hydroxycinnamoyltransferases. Purification, cloning, and expression of a barley agmatine coumaroyltransferase (EC 2.3.1.64). *J Biol Chem, 278*(16), 13919-13927.

Cabaroglu, T., Baumes, R., Canbas, A., Bayonove, C., Lepoutrre, J. P., & Gunata, Z. (1997). Aroma composition of a white wine of *Vitis vinifera* L. cv. Emir as affected by skin contact. *Journal of Food Science, 62*(4), 680-683.

Chaudhary, S. S., Kepner, R. E., & Webb, A. D. (1964). Identification of some volatile compounds in an extract of the grape, *Vitis vinifera* var. Sauvignon Blanc. *American Journal of Enology and Viticulture, 15*(4), 190-198.

Comino, C., Lanteri, S., Portis, E., Acquadro, A., Romani, A., Hehn, A., et al. (2007). Isolation and functional characterization of a cDNA coding a hydroxycinnamoyltransferase involved in phenylpropanoid biosynthesis in *Cynara cardunculus*. *BMC Plant Biology, 7*, 14-27.

Croft, K. P. C., Juttner, F., & Slusarenko, A. J. (1993). Volatile products of the lipoxygenase pathway evolved from *Phaseolus vulgaris* leaves inoculated with *Pseudomonas syringae* pv *phaseolicola*. *Plant Physiology, 101*(1), 13-24.

Crooks, G. E., Hon, G., Chandonia, J. M., & Brenner, S. E. (2004). WebLogo: A sequence logo generator. *Genome Research, 14*(6), 1188-1190.

Czernic, P., Chen Huang, H., & Marco, Y. (1996). Characterization of hsr201 and hsr515, two tobacco genes preferentially expressed during the hypersensitive reaction provoked by phytopathogenic bacteria. *Plant Molecular Biology, 31*(2), 255-265.

D'Auria, J. C. (2006). Acyltransferases in plants: A good time to be BAHD. *Current Opinion in Plant Biology, 9*(3), 331-340.

D'Auria, J. C., Pichersky, E., Schaub, A., Hansel, A., & Gershenzon, J. (2007). Characterization of a BAHD acyltransferase responsible for producing the green leaf volatile (Z)-3-hexen-1-yl acetate in *Arabidopsis thaliana. Plant Journal, 49*(2), 194-207.

D'Auria, J. C., Reichelt, M., Luck, K., Svatos, A., & Gershenzon, J. (2007). Identification and characterization of the BAHD acyltransferase malonyl CoA: Anthocyanidin 5-O-glucoside-6"-O-malonyltransferase (At5MAT) in *Arabidopsis thaliana. FEBS Letters, 581*(5), 872-878.

D'Auria, J. C., Chen, F., & Pichersky, E. (2002). Characterization of an acyltransferase capable of synthesizing benzylbenzoate and other volatile esters in flowers and damaged leaves of *Clarkia breweri. Plant Physiology, 130*(1), 466-476.

Dexter, R., Qualley, A., Kish, C., Ma, C., Koeduka, T., Nagegowda, D., et al. (2007). Characterization of a petunia acetyltransferase involved in the biosynthesis of the floral volatile isoeugenol. *Plant Journal, 49*(2), 265-275.

Dhaubhadel, S., Farhangkhoee, M., & Chapman, R. (2008). Identification and characterization of isoflavonoid specific glycosyltransferase and malonyltransferase from soybean seeds. *Journal of Experimental Botany, 59*(4), 981-994.

Dudareva, N., D'Auria, J. C., Nam, K. H., Raguso, R. A., & Pichersky, E. (1998). Acetyl-CoA: Benzylalcohol acetyltransferase–an enzyme involved in floral scent production in *Clarkia breweri. The Plant Journal, 14*(3), 297-304.

Dudareva, N., Negre, F., Nagegowda, D., & Orlova, I. (2006). Plant volatiles: Recent advances and future perspectives. *Critical Reviews in Plant Sciences, 25*(5), 417-440.

Dudareva, N., Pichersky, E., & Gershenzon, J. (2004). Biochemistry of plant volatiles. *Plant Physiology, 135*(4), 1893-1902.

Dudareva, N., Raguso, R. A., Wang, J., Ross, J. R., & Pichersky, E. (1998). Floral scent production in *Clarkia breweri* . III. Enzymatic synthesis and emission of benzenoid esters. *Plant Physiology, 116*(2), 599-604.

Dunlevy, J., Kalua, C., Keyzers, R., & Boss, P. (2009). The production of flavour & aroma compounds in grape berries. *Grapevine Molecular Physiology & Biotechnology,* , 293-340.

El-Sharkawy, I., Manriquez, D., Flores, F., Latche, A., & Pech, J. (2004). Molecular and genetic regulation of sensory quality of climacteric fruit. *V International Postharvest Symposium 682,* pp. 377-382.

El-Sharkawy, I., Manriquez, D., Flores, F. B., Regad, F., Bouzayen, M., Latche, A., et al. (2005). Functional characterization of a melon alcohol acyl-transferase gene family involved in the biosynthesis of ester volatiles. Identification of the crucial role of a threonine residue for enzyme activity. *Plant Mol Biol, 59*(2), 345-362.

Fellenberg, C., Böttcher, C., & Vogt, T. (2009). Phenylpropanoid polyamine conjugate biosynthesis in *Arabidopsis thaliana* flower buds. *Phytochemistry, 70*(11-12), 1392-1400.

Fenoll, J., Manso, A., Hellín, P., Ruiz, L., & Flores, P. (2009). Changes in the aromatic composition of the *Vitis vinifera* grape Muscat Hamburg during ripening. *Food Chemistry, 114*(2), 420-428.

Field, B., & Osbourn, A. E. (2008). Metabolic diversification--independent assembly of operon-like gene clusters in different plants. *Science, 320*(5875), 543-547.

Fridman, E., & Pichersky, E. (2005). Metabolomics, genomics, proteomics, and the identification of enzymes and their substrates and products. *Current Opinion in Plant Biology, 8*(3), 242-248.

Fujiwara, H., Tanaka, Y., Fukui, Y., Ashikari, T., Yamaguchi, M., & Kusumi, T. (1998). Purification and characterization of anthocyanin 3-aromatic acyltransferase from *Perilla frutescens*. *Plant Science, 137*(1), 87-94.

Fujiwara, H., Tanaka, Y., Fukui, Y., Nakao, M., Ashikari, T., & Kusumi, T. (1997). Anthocyanin 5-aromatic acyltransferase from *Gentiana triflora*. Purification, characterization and its role in anthocyanin biosynthesis. *European Journal of Biochemistry, 249*(1), 45-51.

Fujiwara, H., Tanaka, Y., Yonekura-Sakakibara, K., Fukuchi-Mizutani, M., Nakao, M., Fukui, Y., et al. (1998). cDNA cloning, gene expression and subcellular localization of anthocyanin 5-aromatic acyltransferase from *Gentiana triflora*. *Plant Journal, 16*(4), 421-431.

Girard, B., Fukumoto, L., Mazza, G., Delaquis, P., & Ewert, B. (2002). Volatile terpene constituents in maturing Gewürztraminer grapes from British Columbia. *American Journal of Enology and Viticulture, 53*(2), 99-109.

González, M., Gaete-Eastman, C., Valdenegro, M., Figueroa, C. R., Fuentes, L., Herrera, R., et al. (2009). Aroma development during ripening of *Fragaria chiloensis* fruit and participation of an alcohol acyltransferase (FcAAT1) gene. *Journal of Agricultural and Food Chemistry, 57*(19), 9123-9132.

Gou, J. Y., Yu, X. H., & Liu, C. J. (2009). A hydroxycinnamoyltransferase responsible for synthesizing suberin aromatics in *Arabidopsis*. *Proceedings of the National Academy of Sciences, 106*(44), 18855-18860.

Grienenberger, E., Besseau, S., Geoffroy, P., Debayle, D., Heintz, D., Lapierre, C., et al. (2009). A BAHD acyltransferase is expressed in the tapetum of *Arabidopsis* anthers and is involved in the synthesis of hydroxycinnamoyl spermidines. *Plant Journal, 58*(2), 246-259.

Grothe, T., Lenz, R., & Kutchan, T. M. (2001). Molecular characterization of the salutaridinol 7-O-acetyltransferase involved in morphine biosynthesis in opium poppy *Papaver somniferum*. *Journal of Biological Chemistry, 276*(33), 30717-30723.

Günther, C. S., Chervin, C., Marsh, K. B., Newcomb, R. D., & Souleyre, E. J. F. (2011). Characterisation of two alcohol acyltransferases from kiwifruit (*Actinidia* spp.) reveals distinct substrate preferences. *Phytochemistry, 72*(8), 700-710.

Günther, C. S., Matich, A. J., Marsh, K. B., & Nicolau, L. (2010). (Methylsulfanyl)alkanoate ester biosynthesis in *Actinidia chinensis* kiwifruit and changes during cold storage. *Phytochemistry, 71*(7), 742-750.

Hoffmann, L., Besseau, S., Geoffroy, P., Ritzenthaler, C., Meyer, D., Lapierre, C., et al. (2005). Acyltransferase-catalysed p-coumarate ester formation is a committed step of lignin biosynthesis. *Plant Biosystems, 139*(1), 50-53.

Hoffmann, L., Maury, S., Martz, F., Geoffroy, P., & Legrand, M. (2003). Purification, cloning, and properties of an acyltransferase controlling shikimate and quinate ester intermediates in phenylpropanoid metabolism. *Journal of Biological Chemistry, 278*(1), 95-103.

Hoffmann, L., Besseau, S., Geoffroy, P., Ritzenthaler, C., Meyer, D., Lapierre, C., et al. (2004). Silencing of hydroxycinnamoyl-coenzyme A shikimate/quinate hydroxycinnamoyltransferase affects phenylpropanoid biosynthesis. *Plant Cell, 16*(6), 1446-1465.

Jogl, G., & Tong, L. (2003). Crystal structure of carnitine acetyltransferase and implications for the catalytic mechanism and fatty acid transport. *Cell, 112*(1), 113-122.

Jones, A. L., Gane, A. M., Herbert, D., Willey, D. L., Rutter, A. J., Kille, P., et al. (2003). (Beta)-ketoacyl-acyl carrier protein synthase III from pea (*Pisum sativum* L.): Properties, inhibition by a novel thiolactomycin analogue and isolation of a cDNA clone encoding the enzyme. *Planta, 216*(5), 752-761.

Kaffarnik, F., Heller, W., Hertkorn, N., & Sandermann, H. (2005). Flavonol 3-O-glycoside hydroxycinnamoyltransferases from Scots pine (*Pinus sylvestris* L.). *FEBS J, 272*(6), 1415-1424.

Kalua, C. M., & Boss, P. K. (2008). Sample preparation optimization in wine and grapes: Dilution and sample/headspace volume equilibrium theory for headspace solid-phase microextraction. *Journal of Chromatography A, 1192*(1), 25-35.

Kamsteeg, J., Van Brederode, J., Hommels, C., & Van Nigtevecht, G. (1980). Identification, properties and genetic control of hydroxycinnamoyl-coenzyme A: Anthocyanidin 3-rhamnosyl (1→ 6) glucoside, 4-hydroxycinnamoyl transferase isolated from petals of *Silene dioica. Biochemie und Physiologie der Pflanzen, 175*, 403–411.

Kim, D. H., Kim, S. K., Kim, J. H., Kim, B. G., & Ahn, J. H. (2009). Molecular characterization of flavonoid malonyltransferase from *Oryza sativa. Plant Physiology and Biochemistry, 47*(11-12), 991-997.

Köllner, T. G., Lenk, C., Zhao, N., Seidl-Adams, I., Gershenzon, J., Chen, F., & Degenhardt, J. (2010). Herbivore-induced SABATH methyltransferases of maize that methylate anthranilic acid using S-adenosyl-L-methionine. *Plant Physiology, 153*(4), 1795-1807.

Kolosova, N., Gorenstein, N., Kish, C. M., & Dudareva, N. (2001). Regulation of circadian methyl benzoate emission in diurnally and nocturnally emitting plants. *The Plant Cell Online, 13*(10), 2333-2347.

Kubota, N., Yamane, Y., Toriu, K., Kawazu, K., Higuchi, T., & Nishimura, S. (1999). Identification of active substances in garlic responsible for breaking bud dormancy in grapevines. *Journal of the Japanese Society for Horticultural Science, 68*(6), 1111-1117.

Laflamme, P., St-Piérrè, B., & De Luca, V. (2001). Molecular and biochemical analysis of a Madagascar periwinkle root-specific minovincinine-19-hydroxy-O-acetyltransferase. *Plant Physiology, 125*(1), 189-198.

Lamorte, S. A., Gambuti, A., Genovese, A., Selicato, S., & Moio, L. (2008). Free and glycoconjugated volatiles of *V. vinifera* grape 'Falanghina'. *Vitis - Journal of Grapevine Research, 47*(4), 241-243.

Landmann, C., Hücherig, S., Fink, B., Hoffmann, T., Dittlein, D., Coiner, H. A., et al. (2011). Substrate promiscuity of a rosmarinic acid synthase from lavender (*Lavandula angustifolia* L.). *Planta, 234*(2), 305-320.

Lepelley, M., Cheminade, G., Tremillon, N., Simkin, A., Caillet, V., & McCarthy, J. (2007). Chlorogenic acid synthesis in coffee: An analysis of CGA content and real-time RT-PCR expression of HCT, HQT, C3H1, and CCoAOMT1 genes during grain development in *C. canephora. Plant Science, 172*(5), 978-996.

Li, D., Shen, J., Wu, T., Xu, Y., Zong, X., Li, D., et al. (2008). Overexpression of the apple alcohol acyltransferase gene alters the profile of volatile blends in transgenic tobacco leaves. *Physiologia Plantarum, 134*(3), 394-402.

Li, D., Xu, Y., Xu, G., Gu, L., Li, D., & Shu, H. (2006). Molecular cloning and expression of a gene encoding alcohol acyltransferase (MdAAT2) from apple (cv. Golden Delicious). *Phytochemistry, 67*(7), 658-667.

Lotfy, S., Javelle, F., & Negrel, J. (1996). Purification and characterization of hydroxycinnamoyl-coenzyme A: ω-hydroxypalmitic acid *O*-hydroxycinnamoyltransferase from tobacco (*Nicotiana tabacum* L.) cell-suspension cultures. *Planta, 199*(3), 475-480.

Lucchetta, L., Manriquez, D., El-Sharkawy, I., Flores, F. B., Sanchez-Bel, P., Zouine, M., et al. (2007). Biochemical and catalytic properties of three recombinant alcohol acyltransferases of melon. Sulfur-containing ester formation, regulatory role of CoA-SH in activity, and sequence elements conferring substrate preference. *Journal of Agricultural and Food Chemistry, 55*(13), 5213-5220.

Luo, J., Fuell, C., Parr, A., Hill, L., Bailey, P., Elliott, K., et al. (2009). A novel polyamine acyltransferase responsible for the accumulation of spermidine conjugates in *Arabidopsis* seed. *Plant Cell, 21*(1), 318-333.

Luo, J., Nishiyama, Y., Fuell, C., Taguchi, G., Elliott, K., Hill, L., et al. (2007). Convergent evolution in the BAHD family of acyl transferases: Identification and characterization of anthocyanin acyl transferases from *Arabidopsis thaliana. The Plant Journal, 50*(4), 678-695.

Ma, X., Koepke, J., Bayer, A., Linhard, V., Fritzsch, G., Zhang, B., et al. (2004). Vinorine synthase from *Rauvolfia*: The first example of crystallization and preliminary X-ray diffraction analysis of an enzyme of the BAHD superfamily. *Biochimica Et Biophysica Acta (BBA)-Proteins & Proteomics, 1701*(1-2), 129-132.

Ma, X., Koepke, J., Panjikar, S., Fritzsch, G., & Stockigt, J. (2005). Crystal structure of vinorine synthase, the first representative of the BAHD superfamily. *J Biol Chem, 280*(14), 13576-13583.

Martin, D. M., & Bohlmann, J. (2004). Identification of *Vitis vinifera* (-)-(α)-terpineol synthase by in silico screening of full-length cDNA ESTs and functional characterization of recombinant terpene synthase. *Phytochemistry, 65*(9), 1223-1229.

Martin, D. M., Toub, O., Chiang, A., Lo, B. C., Ohse, S., Lund, S. T., et al. (2009). The bouquet of grapevine (*Vitis vinifera* L. cv. Cabernet Sauvignon) flowers arises from the biosynthesis of sesquiterpene volatiles in pollen grains. *Proceedings of the National Academy of Sciences, 106*(17), 7245-7250.

Mattevi, A., Obmolova, G., Kalk, K. H., Westphal, A. H., de Kok, A., & Hol, W. G. J. (1993). Refined crystal structure of the catalytic domain of dihydrolipoyl transacetylase (E2p) from *Azotobacter vinelandii* at 2.6 Å resolution. *Journal of Molecular Biology, 230*(4), 1183-1199.

Molina, I., Li-Beisson, Y., Beisson, F., Ohlrogge, J. B., & Pollard, M. (2009). Identification of an *Arabidopsis* feruloyl-coenzyme A transferase required for suberin synthesis. *Plant Physiology, 151*(3), 1317-1328.

Morales-Quintana, L., Fuentes, L., Gaete-Eastman, C., Herrera, R., & Moya-Leon, M. A. (2011). Structural characterization and substrate specificity of VpAAT1 protein related to ester biosynthesis in mountain papaya fruit. *Journal of Molecular Graphics and Modelling, 29*(5), 635-642.

Mugford, S. T., Qi, X., Bakht, S., Hill, L., Wegel, E., Hughes, R. K., et al. (2009). A serine carboxypeptidase-like acyltransferase is required for synthesis of antimicrobial compounds and disease resistance in oats. *The Plant Cell, 21*(8), 2473-2484.

Muroi, A., Ishihara, A., Tanaka, C., Ishizuka, A., Takabayashi, J., Miyoshi, H., et al. (2009). Accumulation of hydroxycinnamic acid amides induced by pathogen infection and identification of agmatine coumaroyltransferase in *Arabidopsis thaliana. Planta, 230*(3), 517-527.

Nakatsuka, T., Mishiba, K., Kubota, A., Abe, Y., Yamamura, S., Nakamura, N., et al. (2010). Genetic engineering of novel flower colour by suppression of anthocyanin modification genes in gentian. *Journal of Plant Physiology, 167*(3), 231-237.

Nakayama, T., Suzuki, H., & Nishino, T. (2003). Anthocyanin acyltransferases: Specificities, mechanism, phylogenetics, and applications. *Journal of Molecular Catalysis B: Enzymatic, 23*(2-6), 117-132.

Nam, K. H., Dudareva, N., & Pichersky, E. (1999). Characterization of benzylalcohol acetyltransferases in scented and non-scented *Clarkia* species: *Plant and Cell Physiology, 40*(9), 916-923.

Nawarathne, I. N., & Walker, K. D. (2010). Point mutations (Q19P and N23K) increase the operational solubility of a 2α-O-benzoyltransferase that conveys various acyl groups from CoA to a taxane acceptor. *Journal of Natural Products, 73*(2), 151-159.

Negre-Zakharov, F., Long, M. C., & Dudareva, N. (2009). Floral scents and fruit aromas inspired by nature. *Plant-Derived Natural Products,* pp.405-431 Springer.

Negruk, V., Yang, P., Subramanian, M., McNevin, J. P., & Lemieux, B. (1996). Molecular cloning and characterization of the CER2 gene of *Arabidopsis thaliana. The Plant Journal, 9*(2), 137-145.

Nevarez, D. M., Mengistu, Y. A., Nawarathne, I. N., & Walker, K. D. (2009). An *N*-aroyltransferase of the BAHD superfamily has broad aroyl CoA specificity in vitro with analogues of *N*-dearoylpaclitaxel. *Journal of the American Chemical Society, 131*(16), 5994-6002.

Niggeweg, R., Michael, A. J., & Martin, C. (2004). Engineering plants with increased levels of the antioxidant chlorogenic acid. *Nature Biotechnology, 22*(6), 746-754.

Nogueira, J., Fernandes, P., & Nascimento, A. (2003). Composition of volatiles of banana cultivars from Madeira Island. *Phytochemical Analysis, 14*(2), 87-90.

Okada, T., Hirai, M. Y., Suzuki, H., Yamazaki, M., & Saito, K. (2005). Molecular characterization of a novel quinolizidine alkaloid O-tigloyltransferase: cDNA cloning, catalytic activity of recombinant protein and expression analysis in *Lupinus* plants. *Plant Cell Physiol, 46*(1), 233-244.

Ong, B. Y., & Nagel, C. W. (1978). High-pressure liquid chromatographyic analysis of hydroxycinnamic acid—tartaric acid esters and their glucose esters in *Vitis vinifera*. *Journal of Chromatography A, 157*, 345-355.

Panikashvili, D., Shi, J. X., Schreiber, L., & Aharoni, A. (2009). The *Arabidopsis* DCR encoding a soluble BAHD acyltransferase is required for cutin polyester formation and seed hydration properties. *Plant Physiology, 151*(4), 1773-1789.

Pichersky, E., & Gang, D. R. (2000). Genetics and biochemistry of secondary metabolites in plants: An evolutionary perspective. *Trends in Plant Science, 5*(10), 439-445.

Pichersky, E., Noel, J. P., & Dudareva, N. (2006). Biosynthesis of plant volatiles: Nature's diversity and ingenuity. *Science, 311*(5762), 808-811.

Pyysalo, T., Honkanen, E., & Hirvi, T. (1979). Volatiles of wild strawberries, *Fragaria vesca* L., compared to those of cultivated berries, *Fragaria* x *ananassa* cv senga sengana. *Journal of Agricultural and Food Chemistry, 27*(1), 19-22.

Raguso, R. A., & Pichersky, E. (1995). Floral volatiles from *Clarkia breweri* and *C. concinna* (onagraceae): Recent evolution of floral scent and moth pollination. *Plant Systematics and Evolution, 194*(1), 55-67.

Ruberto, G., Renda, A., Amico, V., & Tringali, C. (2008). Volatile components of grape pomaces from different cultivars of Sicilian *Vitis vinifera* L. *Bioresource Technology, 99*(2), 260-268.

Sander, M., & Petersen, M. (2011). Distinct substrate specificities and unusual substrate flexibilities of two hydroxycinnamoyltransferases, rosmarinic acid synthase and hydroxycinnamoyl-CoA: Shikimate hydroxycinnamoyl-transferase, from *Coleus blumei* benth. *Planta, 233*(6), 1157-1171.

Schneider, T. D., & Stephens, R. M. (1990). Sequence logos: A new way to display consensus sequences. *Nucleic Acids Research, 18*(20), 6097-6100.

Schneider, R., Razungles, A., Augier, C., & Baumes, R. (2001). Monoterpenic and norisoprenoidic glycoconjugates of *Vitis vinifera* L. cv. Melon B. as precursors of odorants in Muscadet wines. *Journal of Chromatography A, 936*(1-2), 145-157.

Sefton, M. A., Francis, I. L., & Williams, P. J. (1994). Free and bound volatile secondary metabolites of *Vitis vinifera* grape cv. Sauvignon Blanc. *Journal of Food Science, 59*(1), 142-147.

Serra, O., Hohn, C., Franke, R., Prat, S., Molinas, M., & Figueras, M. (2010). A feruloyl transferase involved in the biosynthesis of suberin and suberin-associated wax is required for maturation and sealing properties of potato periderm. *The Plant Journal, 62*(2), 277-290.

Shalit, M., Katzir, N., Tadmor, Y., Larkov, O., Burger, Y., Shalekhet, F., et al. (2001). Acetyl-CoA: Alcohol acetyltransferase activity and aroma formation in ripening melon fruits. *Journal of Agricultural and Food Chemistry, 49*(2), 794-799.

Shalit, M., Guterman, I., Volpin, H., Bar, E., Tamari, T., Menda, N., et al. (2003). Volatile ester formation in roses. Identification of an acetyl-coenzyme A. Geraniol/Citronellol acetyltransferase in developing rose petals. *Plant Physiology, 131*(4), 1868-1876.

Sharma, P. K., Sangwan, N. S., Mishra, B. N., & Sangwan, R. S. (2009). Coherent ontogenic dynamics of geraniol acetyltransferase activity and geranyl acetate concentration in flowers and leaves of aroma grass *Cymbopogon martinii* var. Motia. *Plant Growth Regulation, 57*(2), 103-108.

Shaw, W. V. (1992). Chemical anatomy of antibiotic resistance: Chloramphenicol acetyltransferase. *Science Progress, 76*(301-302), 565-580.

Shiota, H. (1993). New esteric components in the volatiles of banana fruit (*Musa sapientum* L.). *Journal of Agricultural and Food Chemistry, 41*(11), 2056-2062.

Soler, M., Serra, O., Molinas, M., Huguet, G., Fluch, S., & Figueras, M. (2007). A genomic approach to suberin biosynthesis and cork differentiation. *Plant Physiology, 144*(1), 419-431.

Sonnante, G., D'Amore, R., Blanco, E., Pierri, C. L., De Palma, M., Luo, J., et al. (2010). Novel hydroxycinnamoyl-coenzyme A quinate transferase genes from artichoke are involved in the synthesis of chlorogenic acid. *Plant Physiology, 153*(3), 1224-1238.

Souleyre, E. J. F., Greenwood, D. R., Friel, E. N., Karunairetnam, S., & Newcomb, R. D. (2005). An alcohol acyl transferase from apple (cv. Royal Gala), MpAAT1,

produces esters involved in apple fruit flavor. *The FEBS Journal, 272*(12), 3132-3144.

Stehle, F., Brandt, W., Stubbs, M. T., Milkowski, C., & Strack, D. (2009). Sinapoyltransferases in the light of molecular evolution. *Phytochemistry, 70*(15-16), 1652-1662.

Stellari, G. M., Mazourek, M., & Jahn, M. M. (2010). Contrasting modes for loss of pungency between cultivated and wild species of *Capsicum*. *Heredity, 104*(5), 460-471.

Stewart, C., Kang, B., Liu, K., Mazourek, M., Moore, S. L., Yoo, E. Y., et al. (2005). The Pun1 gene for pungency in pepper encodes a putative acyltransferase. *The Plant Journal, 42*(5), 675-688.

Stöveken, T., Kalscheuer, R., & Steinbüchel, A. (2009). Both histidine residues of the conserved HHXXXDG motif are essential for wax ester synthase/acyl-CoA: Diacylglycerol acyltransferase catalysis. *European Journal of Lipid Science and Technology, 111*(2), 112-119.

St-Pierre, B., & De Luca, V. (2000). Evolution of acyltransferase genes: Origin and diversification of the BAHD superfamily of acyltransferases involved in secondary metabolism. *Recent Advances in Phytochemistry, 34*, 285-316.

St-Pierre, B., Laflamme, P., Alarco, A. M., & De Luca, V. (1998). The terminal *O*-acetyltransferase involved in vindoline biosynthesis defines a new class of proteins responsible for coenzyme A-dependent acyl transfer. *The Plant Journal, 14*(6), 703-713.

Sullivan, M. L. (2009). A novel red clover hydroxycinnamoyl transferase has enzymatic activities consistent with a role in phaselic acid biosynthesis. *Plant Physiology, 150*(4), 1866-1879.

Sullivan, M. L., & Zarnowski, R. (2011). Red clover HCT2, a hydroxycinnamoyl-coenzyme A: Malate hydroxycinnamoyl transferase, plays a crucial role in biosynthesis of phaselic acid and other hydroxycinnamoyl-malate esters in vivo. *Plant Physiology, 155*(3), 1060-1067.

Suzuki, H., Nakayama, T., Nagae, S., Yamaguchi, M. A., Iwashita, T., Fukui, Y., et al. (2004). cDNA cloning and functional characterization of flavonol 3-O-glucoside-6''-O-malonyltransferases from flowers of *Verbena hybrida* and *Lamium purpureum*. *Journal of Molecular Catalysis B: Enzymatic, 28*(2-3), 87-93.

Suzuki, H., Nakayama, T., & Nishino, T. (2003). Proposed mechanism and functional amino acid residues of malonyl-CoA:Anthocyanin 5-*O*-glucoside-6'''-*O*-

malonyltransferase from flowers of *Salvia splendens*, a member of the versatile plant acyltransferase family. *Biochemistry, 42*(6), 1764-1771.

Suzuki, H., Nakayama, T., Yamaguchi, M., & Nishino, T. (2004). cDNA cloning and characterization of two *Dendranthema* x *morifolium* anthocyanin malonyltransferases with different functional activities. *Plant Science, 166*(1), 89-96.

Suzuki, H., Nakayama, T., Yonekura-Sakakibara, K., Fukui, Y., Nakamura, N., Nakao, M., et al. (2001). Malonyl-CoA:Anthocyanin 5-*O*-glucoside-6'''-*O*-malonyltransferase from scarlet sage (*Salvia splendens*) flowers. Enzyme purification, gene cloning, expression, and characterization. *Journal of Biological Chemistry, 276*(52), 49013-49019.

Suzuki, H., Nakayama, T., Yonekura-Sakakibara, K., Fukui, Y., Nakamura, N., Yamaguchi, M., et al. (2002). cDNA cloning, heterologous expressions, and functional characterization of malonyl-coenzyme A:Anthocyanidin 3-O-glucoside-6"-O-malonyltransferase from *Dahlia* flowers. *Plant Physiology, 130*(4), 2142-2151.

Suzuki, H., Nishino, T., & Nakayama, T. (2007). Anthocyanin acyltransferase engineered for the synthesis of a novel polyacylated anthocyanin. *Plant Biotechnology, 24*(5), 495-501.

Suzuki, H., Nishino, T., & Nakayama, T. (2007). cDNA cloning of a BAHD acyltransferase from soybean (*Glycine max*): Isoflavone 7-*O*-glucoside-6"-*O*-malonyltransferase. *Phytochemistry, 68*(15), 2035-2042.

Suzuki, H., Sawada, S., Yonekura-Sakakibara, K., Nakayama, T., Yamaguchi, M., & Nishino, T. (2003). Identification of a cDNA encoding malonyl-coenzyme A: Anthocyanidin 3-O-glucoside 6"-*O*-malonyltransferase from Cineraria (*Senecio cruentus*) flowers. *Plant Biotechnology, 20*(3), 229-234.

Suzuki, H., Sawada, S., Watanabe, K., Nagae, S., Yamaguchi, M., Nakayama, T., et al. (2004). Identification and characterization of a novel anthocyanin malonyltransferase from scarlet sage (*Salvia splendens*) flowers: An enzyme that is phylogenetically separated from other anthocyanin acyltransferases. *The Plant Journal, 38*(6), 994-1003.

Symons, G. M., & Reid, J. B. (2004). Brassinosteroids do not undergo long-distance transport in pea. Implications for the regulation of endogenous brassinosteroid levels. *Plant Physiology, 135*(4), 2196-2206.

Tacke, E., Korfhage, C., Michel, D., Maddaloni, M., Motto, M., Lanzini, S., et al. (1995). Transposon tagging of the maize Glossy2 locus with the transposable element En/Spm. *The Plant Journal, 8*(6), 907-917.

Taguchi, G., Ubukata, T., Nozue, H., Kobayashi, Y., Takahi, M., Yamamoto, H., et al. (2010). Malonylation is a key reaction in the metabolism of xenobiotic phenolic glucosides in *Arabidopsis* and tobacco. *The Plant Journal, 63*(6), 1031-1041.

Taguchi, G., Shitchi, Y., Shirasawa, S., Yamamoto, H., & Hayashida, N. (2005). Molecular cloning, characterization, and downregulation of an acyltransferase that catalyzes the malonylation of flavonoid and naphthol glucosides in tobacco cells. *The Plant Journal, 42*(4), 481-491.

Tao, Y., Li, H., Wang, H., & Zhang, L. (2008). Volatile compounds of young Cabernet Sauvignon red wine from Changli county (China). *Journal of Food Composition & Analysis, 21*(8), 689-694.

Tohge, T., Nishiyama, Y., Hirai, M. Y., Yano, M., Nakajima, J., Awazuhara, M., et al. (2005). Functional genomics by integrated analysis of metabolome and transcriptome of *Arabidopsis* plants over-expressing an MYB transcription factor. *The Plant Journal, 42*(2), 218-235.

Tominaga, T., des Gachons, C. P., & Dubourdieu, D. (1998). A new type of flavor precursors in *Vitis vinifera* L. cv. Sauvignon Blanc: S-cysteine conjugates. *Journal of Agricultural and Food Chemistry, 46*(12), 5215-5219.

Tuominen, L. K., Johnson, V. E., & Chung-Jui, T. (2011). Differential phylogenetic expansions in BAHD acyltransferases across five angiosperm taxa and evidence of divergent expression among *Populus* paralogues. *BMC Genomics, 12*(1), 236-252.

Ugliano, M., & Moio, L. (2008). Free and hydrolytically released volatile compounds of *Vitis vinifera* L. cv. Fiano grapes as odour-active constituents of Fiano wine. *Analytica Chimica Acta, 621*(1), 79-85.

Unno, H., Ichimaida, F., Suzuki, H., Takahashi, S., Tanaka, Y., Saito, A., et al. (2007). Structural and mutational studies of anthocyanin malonyltransferases establish the features of BAHD enzyme catalysis. *Journal of Biological Chemistry, 282*(21), 15812-15822.

Vacic, V., Iakoucheva, L. M., & Radivojac, P. (2006). Two sample logo: A graphical representation of the differences between two sets of sequence alignments. *Bioinformatics, 22*(12), 1536-1537.

Verdonk, J. C., Ric de Vos, C., Verhoeven, H. A., Haring, M. A., van Tunen, A. J., & Schuurink, R. C. (2003). Regulation of floral scent production in petunia revealed by targeted metabolomics. *Phytochemistry, 62*(6), 997-1008.

Walker, K., & Croteau, R. (2000). Molecular cloning of a 10-deacetylbaccatin III-10-*O*-acetyl transferase cDNA from *Taxus* and functional expression in *Escherichia coli*.

Proceedings of the National Academy of Sciences of the United States of America, 97(2), 583-587.

Walker, K., Long, R., & Croteau, R. (2002). The final acylation step in Taxol biosynthesis: Cloning of the taxoid C13-side-chain *N*-benzoyltransferase from *Taxus*. *Proceedings of the National Academy of Sciences of the United States of America, 99*(14), 9166-9171.

Walker, K., & Croteau, R. (2000). Taxol biosynthesis: Molecular cloning of a benzoyl-CoA:Taxane 2α-*O*-benzoyltransferase cDNA from *Taxus* and functional expression in *Escherichia coli*. *Proceedings of the National Academy of Sciences of the United States of America, 97*(25), 13591-13596.

Walker, K., Ketchum, R. E., Hezari, M., Gatfield, D., Goleniowski, M., Barthol, A., et al. (1999). Partial purification and characterization of acetyl coenzyme A: Taxa-4(20),11(12)-dien-5α-ol *O*-acetyl transferase that catalyzes the first acylation step of Taxol biosynthesis. *Archives of Biochemistry and Biophysics, 364*(2), 273-279.

Walker, K., Schoendorf, A., & Croteau, R. (2000). Molecular cloning of a taxa-4(20),11(12)-dien-5alpha-ol-*O*-acetyl transferase cDNA from *Taxus* and functional expression in *Escherichia coli*. *Archives of Biochemistry and Biophysics, 374*(2), 371-380.

Walker, K., Fujisaki, S., Long, R., & Croteau, R. (2002). Molecular cloning and heterologous expression of the C-13 phenylpropanoid side chain-CoA acyltransferase that functions in Taxol biosynthesis. *Proceedings of the National Academy of Sciences of the United States of America, 99*(20), 12715-12720.

Wang, J., & De Luca, V. D. (2005). The biosynthesis and regulation of biosynthesis of Concord grape fruit esters, including 'foxy' methylanthranilate. *The Plant Journal, 44*(4), 606-619.

Wang, J., & Pichersky, E. (1998). Characterization of *S*-adenosyl-l-methionine:(iso)eugenol *O*-methyltransferase involved in floral scent production in *Clarkia breweri*. *Archives of Biochemistry and Biophysics, 349*(1), 153-160.

Weitzel, C., & Petersen, M. (2011). Cloning and characterisation of rosmarinic acid synthase from *Melissa officinalis* L. *Phytochemistry, 72*(7), 572-578.

Wyllie, S. G., & Fellman, J. K. (2000). Formation of volatile branched chain esters in bananas (*Musa sapientum* L.). *Journal of Agricultural and Food Chemistry, 48*(8), 3493-3496.

Xia, Y., Nikolau, B. J., & Schnable, P. S. (1996). Cloning and characterization of CER2, an *Arabidopsis* gene that affects cuticular wax accumulation. *Plant Cell, 8*(8), 1291-1304.

Xia, Y., Nikolau, B. J., & Schnable, P. S. (1997). Developmental and hormonal regulation of the *Arabidopsis* CER2 gene that codes for a nuclear-localized protein required for the normal accumulation of cuticular waxes. *Plant Physiology, 115*(3), 925-937.

Yabuya, T., Yamaguchi, M., Fukui, Y., Katoh, K., Imayama, T., & Ino, I. (2001). Characterization of anthocyanin p-coumaroyltransferase in flowers of *Iris ensata*. *Plant Science, 160*(3), 499-503.

Yahyaoui, F.E.L.;Wongs-Aree, C., Latché, A., Hackett, R., Grierson, D., Pech, J. (2002). Molecular and biochemical characteristics of a gene encoding an alcohol acyl-transferase involved in the generation of aroma volatile esters during melon ripening. *European Journal of Biochemistry, 269*(9), 2359-2366.

Yamaguchi, M. A., Kawanobu, S., Maki, T., & Ino, I. (1996). Cyanidin 3-malonylglucoside and malonyl-coenzyme A: Anthocyanidin malonyltransferase in *Lactuca sativa* leaves. *Phytochemistry, 42*(3), 661-663.

Yan, Y., & Liao, J. C. (2009). Engineering metabolic systems for production of advanced fuels. *Journal of Industrial Microbiology and Biotechnology, 36*(4), 471-479.

Yang, D. S., Balandrán-Quintana, R. R., Ruiz, C. F., Toledo, R. T., & Kays, S. J. (2009). Effect of hyperbaric, controlled atmosphere, and UV treatments on peach volatiles. *Postharvest Biology and Technology, 51*(3), 334-341.

Yang, Q., Xuan Trinh, H., Imai, S., Ishihara, A., Zhang, L., Nakayashiki, H., et al. (2004). Analysis of the involvement of hydroxyanthranilate hydroxycinnamoyltransferase and caffeoyl-CoA 3-*O*-methyltransferase in phytoalexin biosynthesis in oat. *Molecular Plant-Microbe Interactions, 17*(1), 81-89.

Yang, C., Wang, Y., Liang, Z., Fan, P., Wu, B., Yang, L., et al. (2009). Volatiles of grape berries evaluated at the germplasm level by headspace-SPME with GC–MS. *Food Chemistry, 114*(3), 1106-1114.

Yang, Q., Reinhard, K., Schiltz, E., & Matern, U. (1997). Characterization and heterologous expression of hydroxycinnamoyl/benzoyl-CoA:Anthranilate *N*-hydroxycinnamoyl/benzoyltransferase from elicited cell cultures of carnation, *Dianthus caryophyllus* L. *Plant Molecular Biology, 35*(6), 777-789.

Yonekura-Sakakibara, K., Nakayama, T., Yamazaki, M., & Saito, K. (2009). Modification and stabilization of anthocyanins. *Anthocyanins* (pp. 169-190) Springer.

Yonekura-Sakakibara, K., Tanaka, Y., Fukuchi-Mizutani, M., Fujiwara, H., Fukui, Y., Ashikari, T., et al. (2000). Molecular and biochemical characterization of a novel hydroxycinnamoyl-CoA: Anthocyanin 3-*O*-glucoside-6"-*O*-acyltransferase from *Perilla frutescens*. *Plant and Cell Physiology, 41*(4), 495-502.

Yoshihara, N., Imayama, T., Matsuo, Y., Fukuchi-Mizutani, M., Tanaka, Y., Ino, I., et al. (2006). Characterization of cDNA clones encoding anthocyanin 3-*p*-coumaroyltransferase from *Iris hollandica*. *Plant Science, 171*(5), 632-639.

Yu, X. H., Gou, J. Y., & Liu, C. J. (2009). BAHD superfamily of acyl-CoA dependent acyltransferases in *Populus* and *Arabidopsis*: Bioinformatics and gene expression. *Plant Molecular Biology, 70*(4), 421-442.

Yu, X., Chen, M., & Liu, C. (2008). Nucleocytoplasmic-localized acyltransferases catalyze the malonylation of 7-*O*-glycosidic (iso)flavones in *Medicago truncatula*. *The Plant Journal, 55*(3), 382-396.

Yu, M., & Facchini, P. J. (1999). Purification, characterization, and immunolocalization of hydroxycinnamoyl-CoA: Tyramine *N*-(hydroxycinnamoyl)transferase from opium poppy. *Planta, 209*(1), 33-44.

Zheng, Z., Qualley, A., Fan, B., Dudareva, N., & Chen, Z. (2009). An important role of a BAHD acyl transferase-like protein in plant innate immunity. *Plant Journal, 57*(6), 1040-1053.

Zhu, Y., Rudell, D. R., & Mattheis, J. P. (2008). Characterization of cultivar differences in alcohol acyltransferase and 1-aminocyclopropane-1-carboxylate synthase gene expression and volatile ester emission during apple fruit maturation and ripening. *Postharvest Biology and Technology, 49*(3), 330-339.

Appendix I: Supplementary Figures

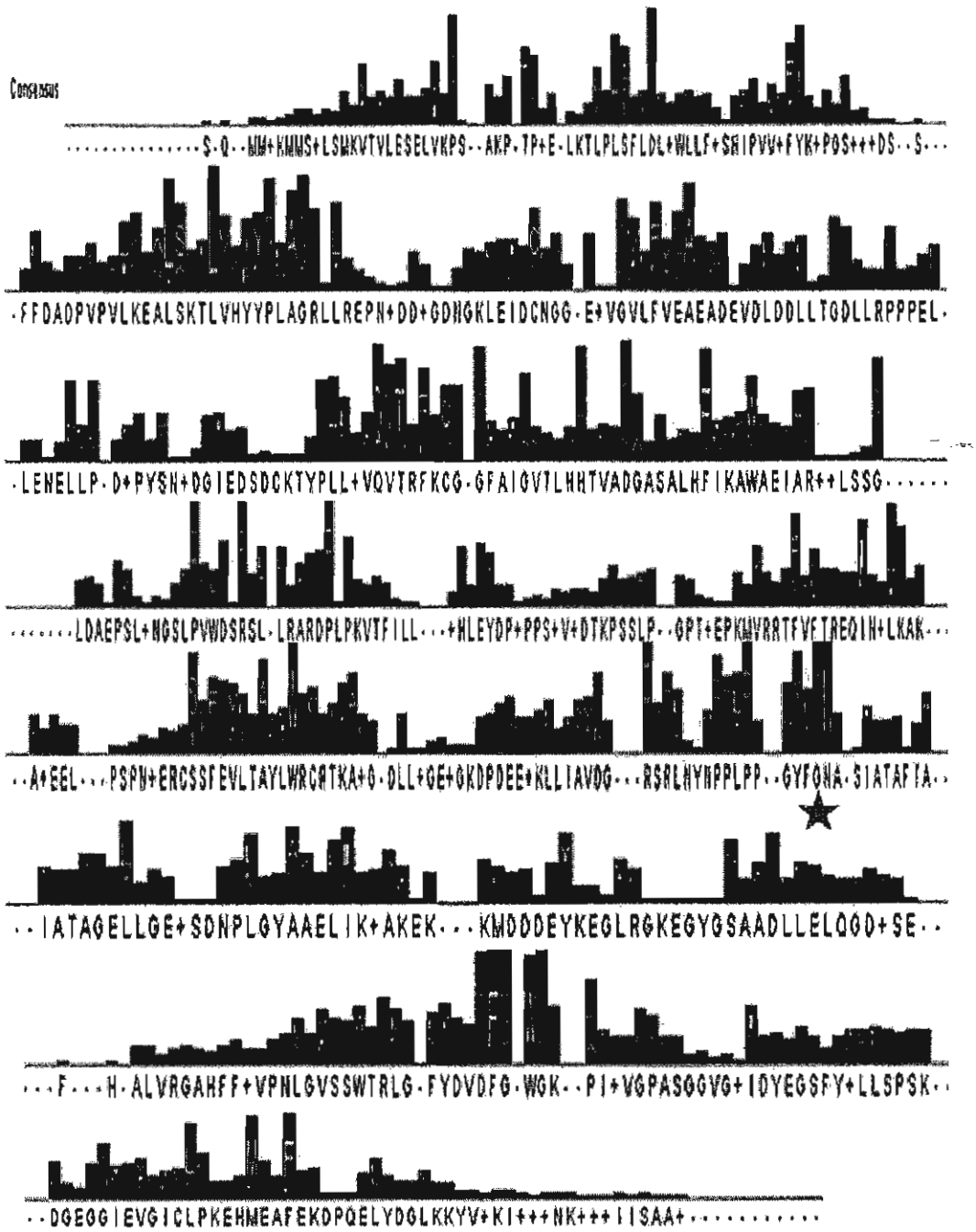

Figure S1: Consensus sequence of 88 biochemically characterized BAHD acyltransferases visualized using sequence logos (Crooks, Hon, Chandonia, & Brenner, 2004; Schneider & Stephens, 1990). Each position in the alignment is represented by a stack: the overall height of the stack indicates the conservation at that position, and the heights of the symbols within the stack indicate the relative frequency of that particular amino acid. The highly conserved glycine (G) of the YFGNC motif is marked with a star.

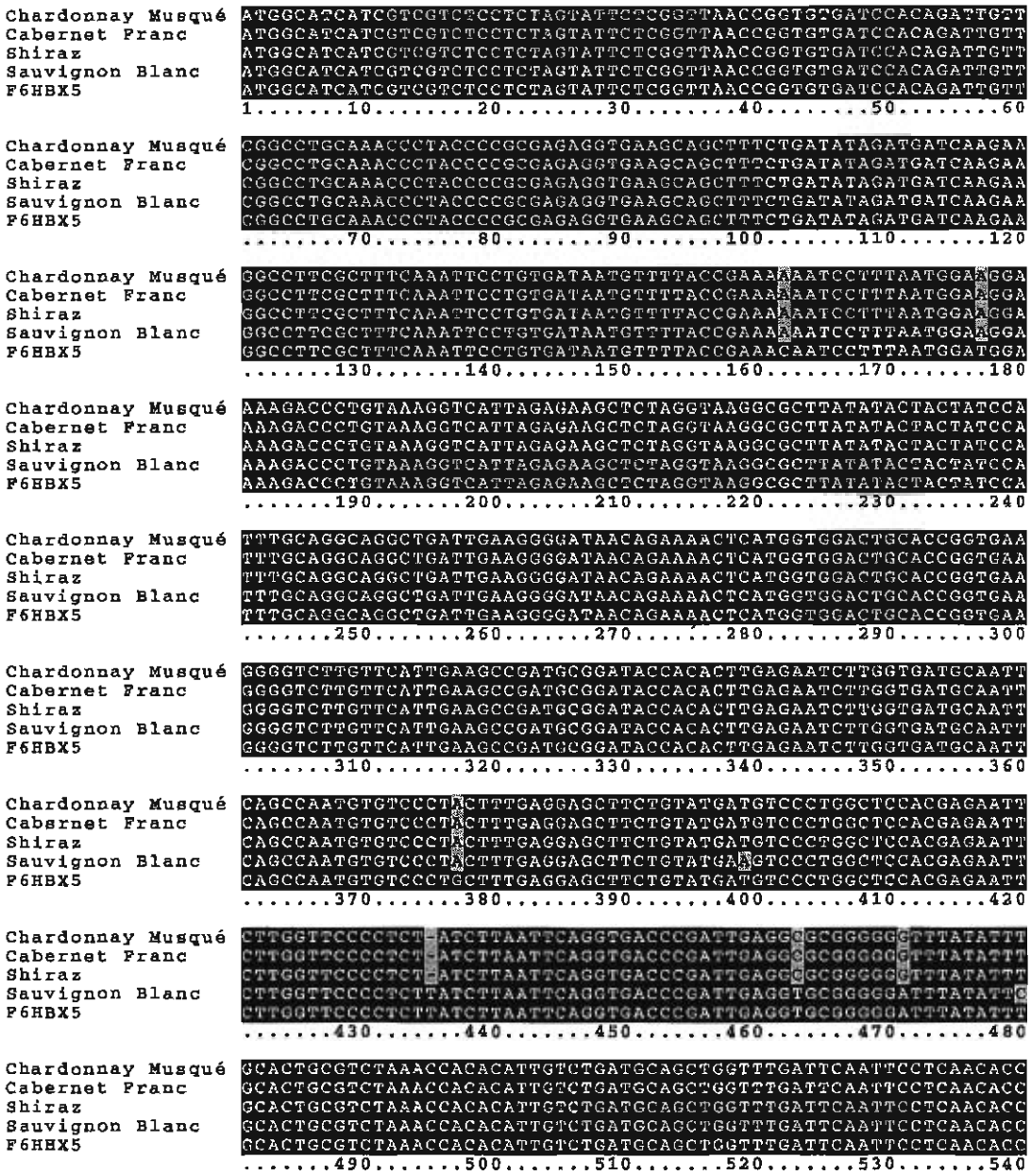

Figure S2: Multiple sequence alignment of full-length *VIAMAT*-like sequences isolated from Chardonnay Musqué, Cabernet Franc, Shiraz, and Sauvignon Blanc with *F6HBX5* from the genome of *V. vinifera* cv. Pinot Noir. The sequences from Chardonnay Musqué, Cabernet Franc, Shiraz, and Sauvignon Blanc include the pET30(b)+ vector-derived C-terminal His-tag coding sequence at the 3'-end.

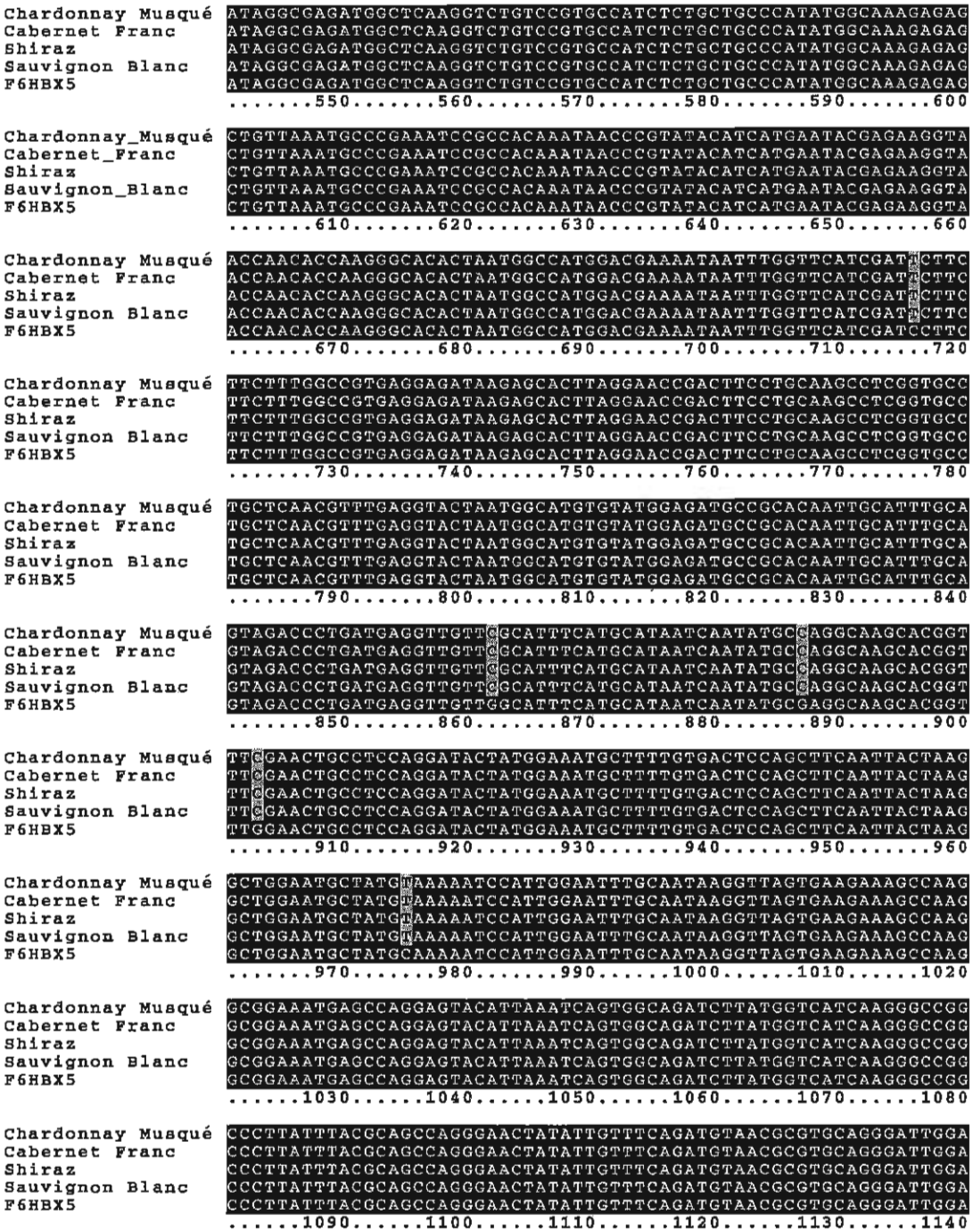
Chardonnay Musqué
Cabernet Franc
Shiraz
Sauvignon Blanc
F6HBX5
.....550.....560.....570.....580.....590.....600
Chardonnay_Musqué
Cabernet_Franc
Shiraz
Sauvignon_Blanc
F6HBX5
.....610.....620.....630.....640.....650.....660
.....670.....680.....690.....700.....710.....720
.....730.....740.....750.....760.....770.....780
.....790.....800.....810.....820.....830.....840
.....850.....860.....870.....880.....890.....900
.....910.....920.....930.....940.....950.....960
.....970.....980.....990.....1000.....1010.....1020
.....1030.....1040.....1050.....1060.....1070.....1080
.....1090.....1100.....1110.....1120.....1130.....1140

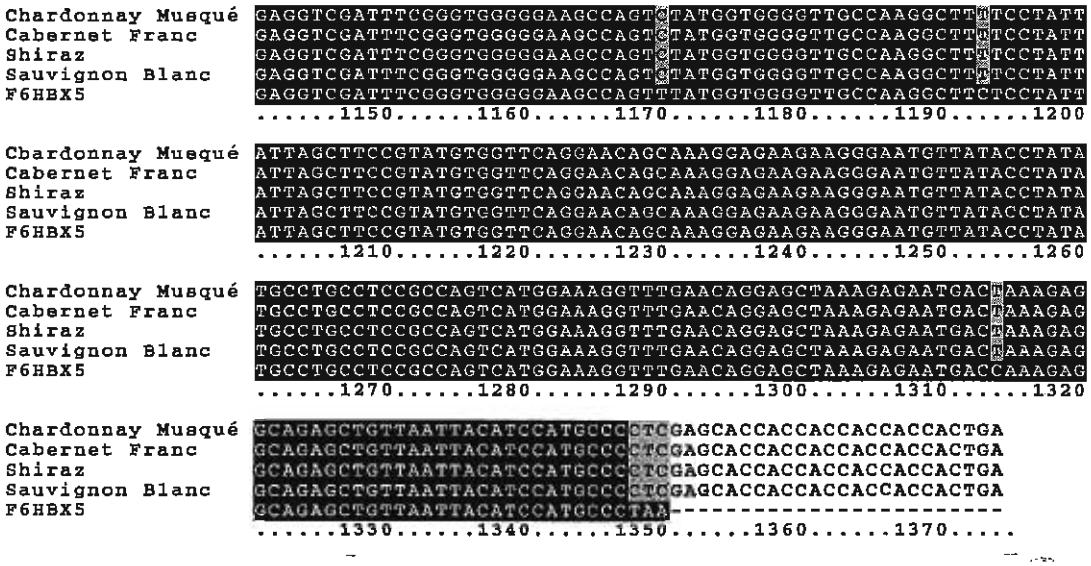
Chardonnay Musqué
Cabernet Franc
Shiraz
Sauvignon Blanc
F6HBX5
.....1150.....1160.....1170.....1180.....1190.....1200
Chardonnay Musqué
Cabernet Franc
Shiraz
Sauvignon Blanc
F6HBX5
.....1210.....1220.....1230.....1240.....1250.....1260
Chardonnay Musqué
Cabernet Franc
Shiraz
Sauvignon Blanc
F6HBX5
.....1270.....1280.....1290.....1300.....1310.....1320
Chardonnay Musqué
Cabernet Franc
Shiraz
Sauvignon Blanc
F6HBX5
.....1330.....1340.....1350.....1360.....1370.....

```
VlAMAT    MASPSSPLVFSVNRCVPQIVRPANPTPREVKQLSDIDDQEGRRFQIPVIMFYRNNPLMEG
VvsbAAT1  MASSSSPLVFSVNRCDPQIVRPANPTPREVKQLSDIDDQEGLRFQIPVIMFYRKNPLMEG
          1.......10........20........30........40........50........60

VlAMAT    KDPVKVIREALGKALVYYYPFAGRLIEGDNRKLMVDCTGEGVLFIEADADTTLENLGDAI
VvsbAAT1  KDPVKVIREALGKALIYYYPFAGRLIEGDNRKLMVDCTGEGVLFIEADADTTLENLGDAI
          ........70........80........90.......100.......110.......120

VlAMAT    QPMCPCFEELLYDVPGSTTILGSPLILIQVTRLRCGGFIFALRLNHTMSDAAGLIQFLDT
VvsbAAT1  QPMCPYFEELLYEVPGSTRILGSPLILIQVTRLRCGGFIFALRLNHTLSDAAGLIQFLNT
          .......130.......140.......150.......160.......170.......180

VlAMAT    IGEMAQGLSVPSLLPIWQRELLNARNPPRITRIHHEYEKVTNTKGTLMAMDENSLVHRSF
VvsbAAT1  IGEMAQGLSVPSLLPIWQRELLNARNPEQITRIHHEYEKVTNTKGTLMAMDENNLVHRFF
          .......190.......200.......210.......220.......230.......240

VlAMAT    FFGREEIRALRNRLPASLGACSTFEVLMACVWRCRTIAFAVDPDEVVRISCIINMRGKHG
VvsbAAT1  FFGREEIRALRNRLPASLGACSTFEVLMACVWRCRTIAFAVDPDEVVRISCIINMPGKHG
          .......250.......260.......270.......280.......290.......300

VlAMAT    FELPPGYYGNAFVTPASITKAGMLCKNPLEFAIRLVKKAKAEMSQEYIKSVADLMVIKGR
VvsbAAT1  FELPPGYYGNAFVTPASITKAGMLCKNPLEFAIRLVKKAKAEMSQEYIKSVADLMVIKGR
          .......310.......320.......330.......340.......350.......360

VlAMAT    PLFTQPGNFTVSDVTRAGLGEVDFGWGKPVYGGVARACPIISFRMLFRNSKGEEGSVIPI
VvsbAAT1  PLFTQPGNYIVSDVTRAGFGEVDFGWGKPVYGGVAKAFPIISFRMWFRNSKGEEGNVIPI
          .......370.......380.......390.......400.......410.......420

VlAMAT    WLPPPVMERFEQELKRMTKKAELLITSML--
VvsbAAT1  CLPPPVMERFEQELKRMTKEAELLITSMPLE
          .......430.......440.......450.
```

Figure S3: Multiple sequence alignment of VlAMAT (Wang & De Luca, 2005) and VvsbAAT1 amino acid sequences (this work).